Raman spectroscopy in Earth Sciences

Dr. Simona Ferrando

Outline

- Basics:
  - Basics in Raman spectroscopy
  - A typical μ-Raman spectrometer
- Applications:
  - Minerals
  - Fluid inclusions
  - Glasses & melt inclusions

Basics

Basics on Raman spectroscopy

Chandrasekhara Venkata Raman
Nobel Prize in Physics (1930)

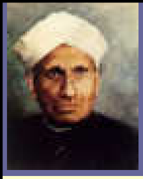

A BIT OF HISTORY

1871 – Elastic light scattering theory is published by J.W. Strutt (Lord Rayleigh, 1904 Nobel prize in Physics for the discovery of argon)

1923 – Inelastic light scattering is predicted by A. Smekel

1928 – Landsberg and Mandelstam see unexpected frequency shifts in scattering from quartz

1928 –

Indian J. Phys. 2 387–398 (1928)

A new radiation*

C V RAMAN, F.R.S.

1930 – C.V. Raman wins Nobel Prize in Physics

1961 – Invention of laser makes Raman experiments reasonable

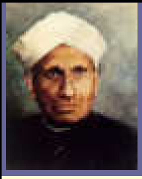

DIFFUSION

When an electromagnetic radiation hits a medium, light can be:
- reflected
- transmitted after refraction and, in some cases, absorption
- re-emitted (fluorescence)
- **scattered (diffusion)**

Diffusion largely occur when light interacts with objects smaller than its wavelength (e.g. molecules illuminated with visible light)

Monochromatic light (e.g. laser) amplify the effect

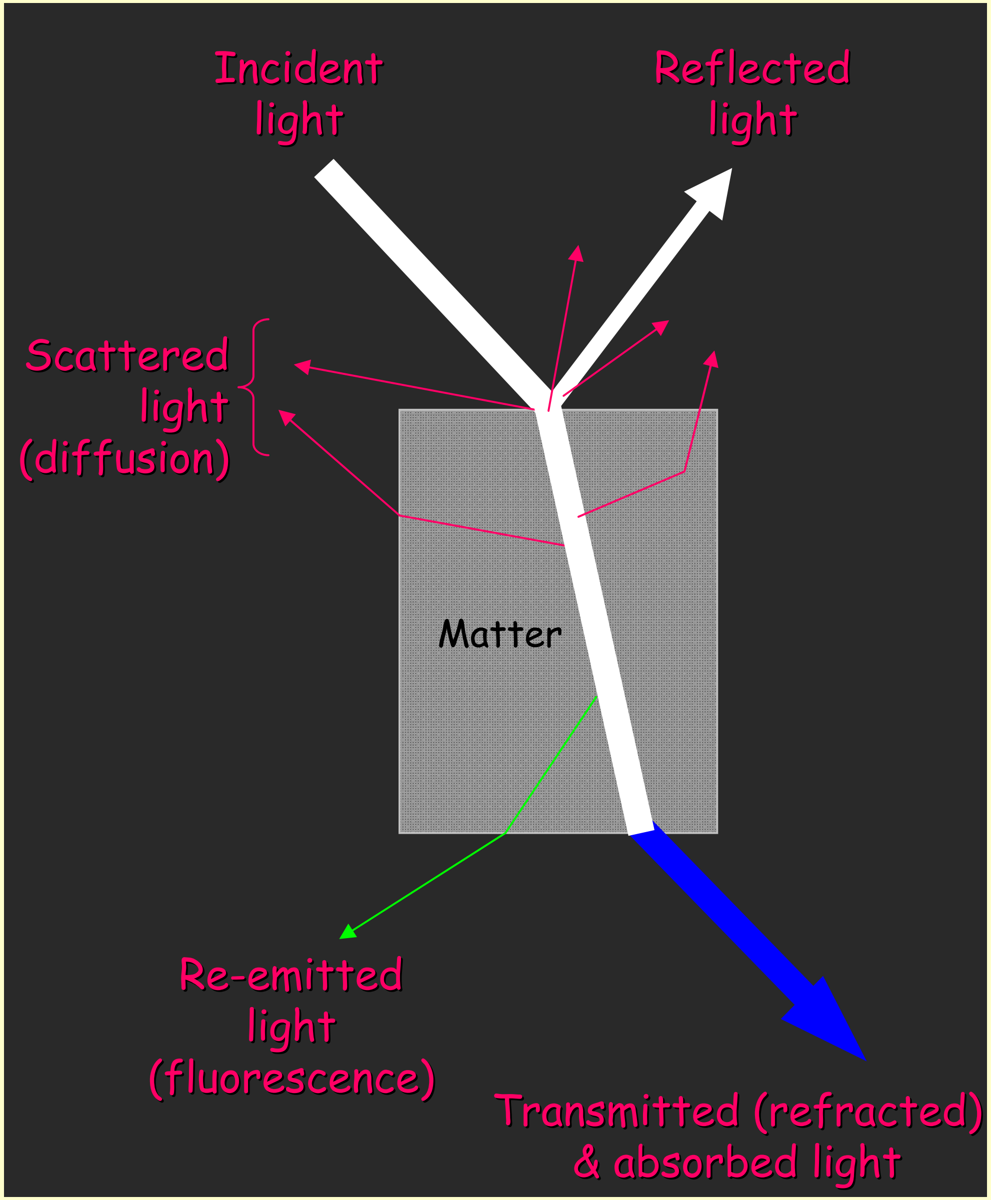

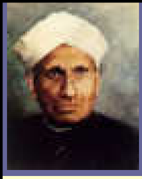

ELASTIC & INELASTIC SCATTERING

Monochromatic light is scattered by matter (solid, liquid, gas) mainly in radiations maintaining incident frequency ν_i(→ the molecule remains in the same energetic/quantum state; **elastic scattering or "Rayleigh scattering"**).

Rare radiations have frequencies $\nu_{Raman} = \nu_i \pm \nu_{molecular}$ higher or lower than incident light **(**the molecule is left in a different energetic/quantum state → **inelastic scattering or "Raman effect"**).

$\nu_{molecular}$ is a frequency due to vibrational, rotational, or electronic transitions within a molecule.

The Raman effect due to **vibrational frequency** ν_v is the most important.

Only a very small portion (~10^{-7}) of the incident electromagnetic field is scattered inelastically.

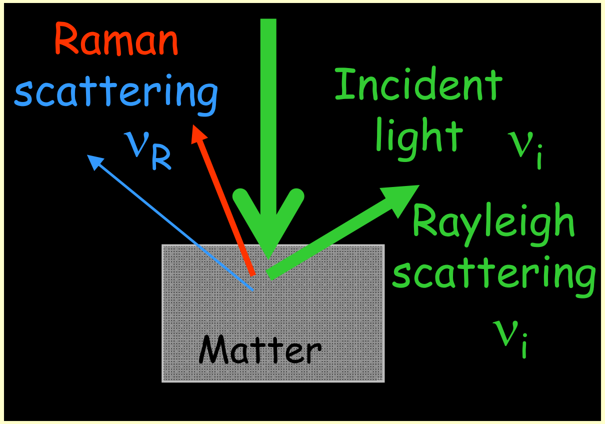

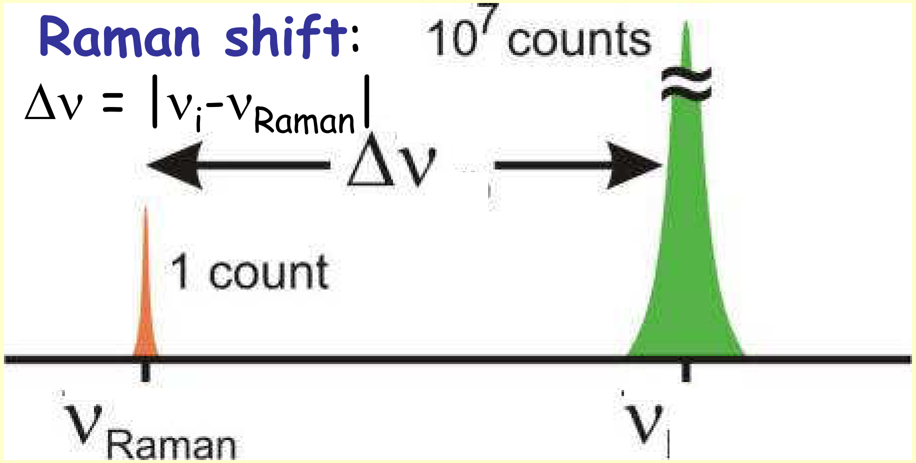

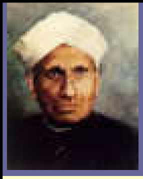

ELASTIC & INELASTIC SCATTERING

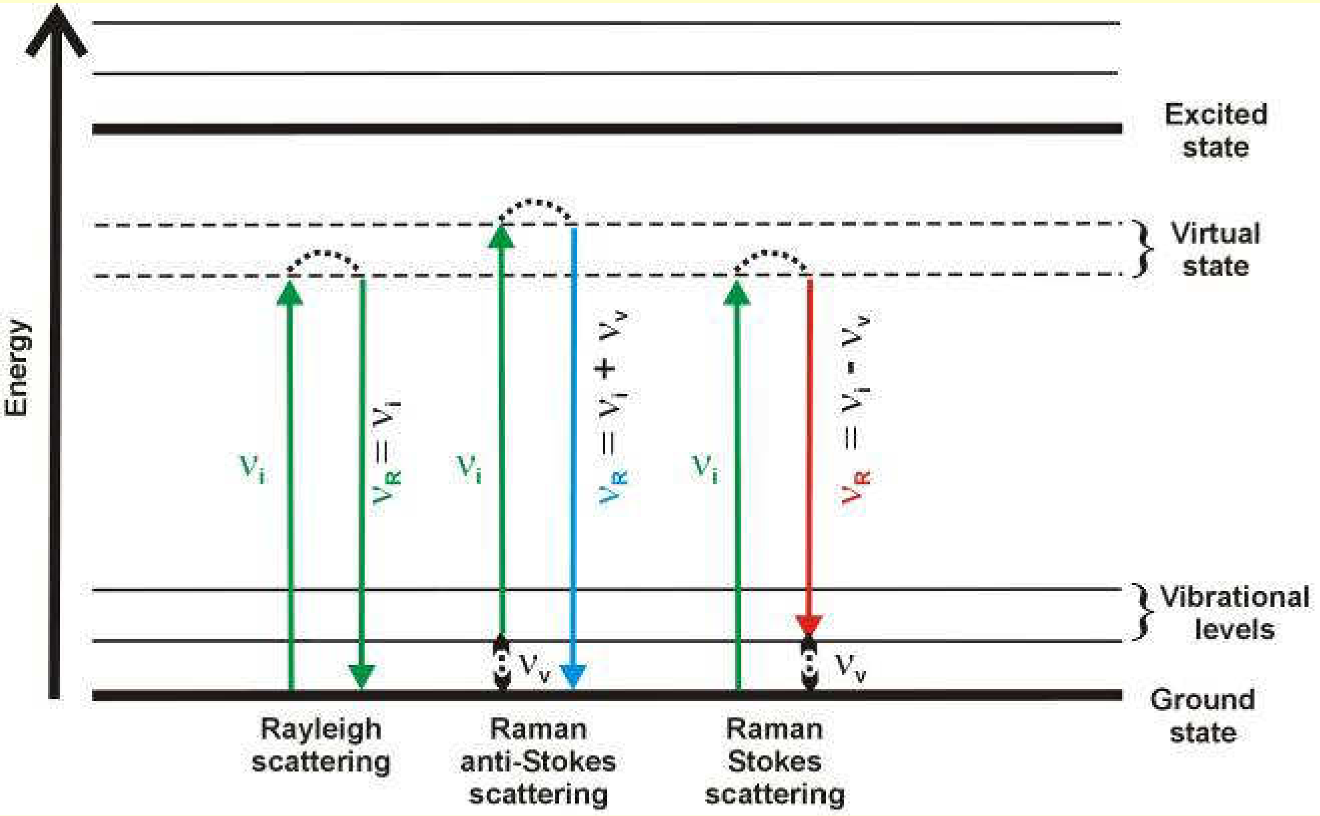

Anti-Stokes scattering: inelastically scattered radiation has higher frequency than exciting line → the molecule loses energy

Stokes scattering: inelastically scattered radiation has lower frequency than exciting line → the molecule gains energy

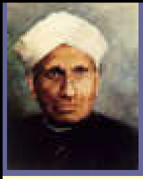

CLASSICAL INTERPRETATION

In classical physics, an applied electric field (E) perturbs the electronic state of a molecule and produces a dipole moment (μ_d)

$\mu_d = \alpha E$

Polarizability (α): tendency of a molecule to distort its charge distribution in presence of an electric field

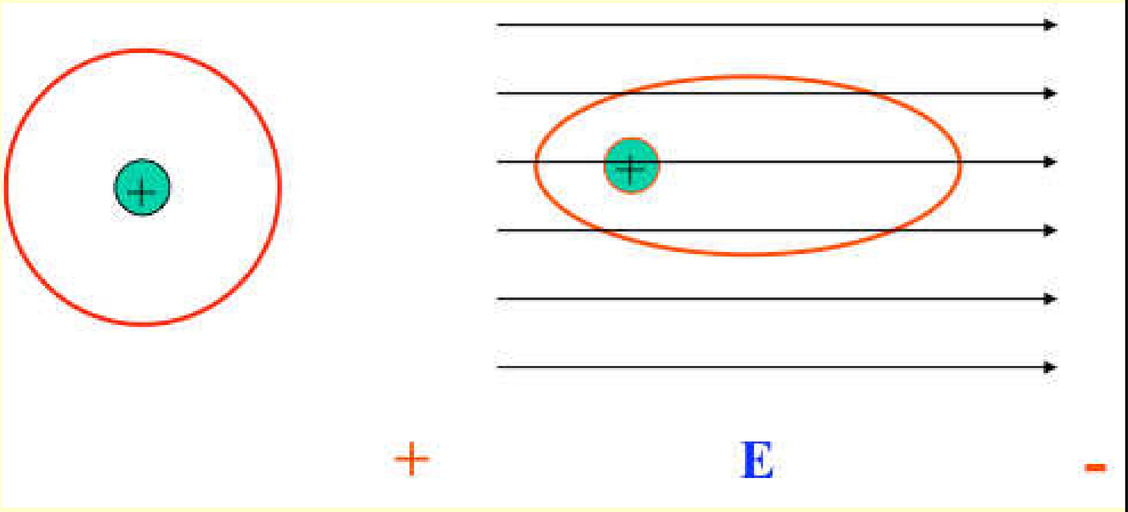

The Raman effect occurs when a "Raman-active" molecule experiences a **variation of its polarizability** because of internal vibrational, rotational or electronic motions of the molecule

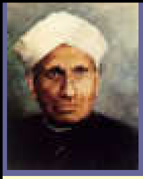

QUANTUM INTERPRETATION

Consider light-matter interaction in terms of particles

Photon: elementary particle (or "quantum") used to describe the electromagnetic field

Phonon: a quasi-particle used to describe the vibrational modes in the matter

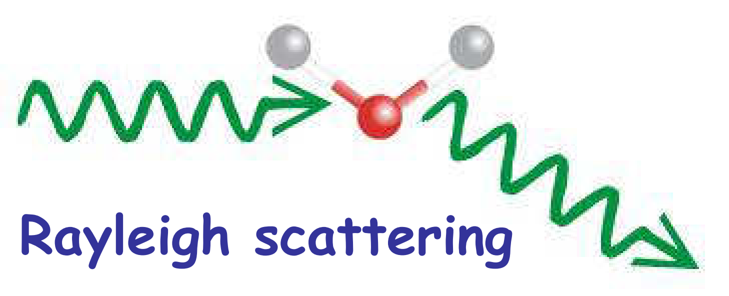

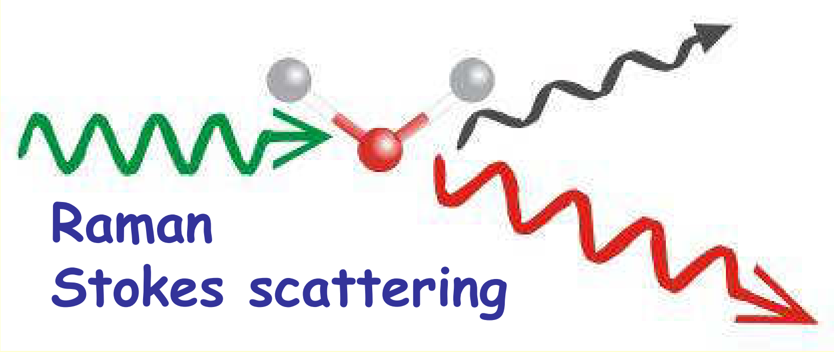

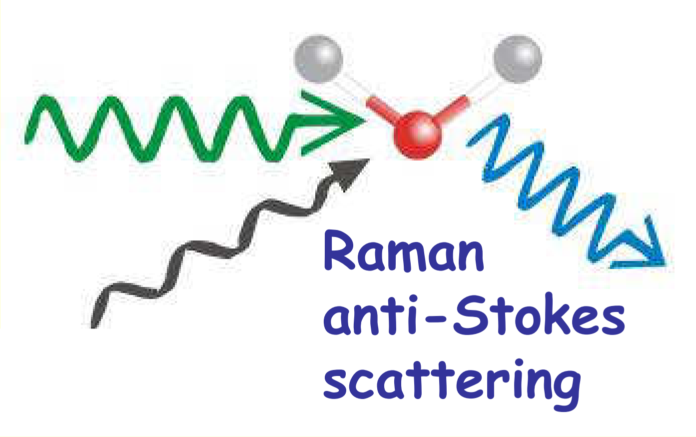

Stokes scattering is a more probable event

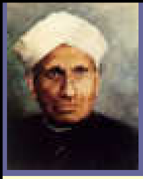

THE RAMAN SPECTRUM

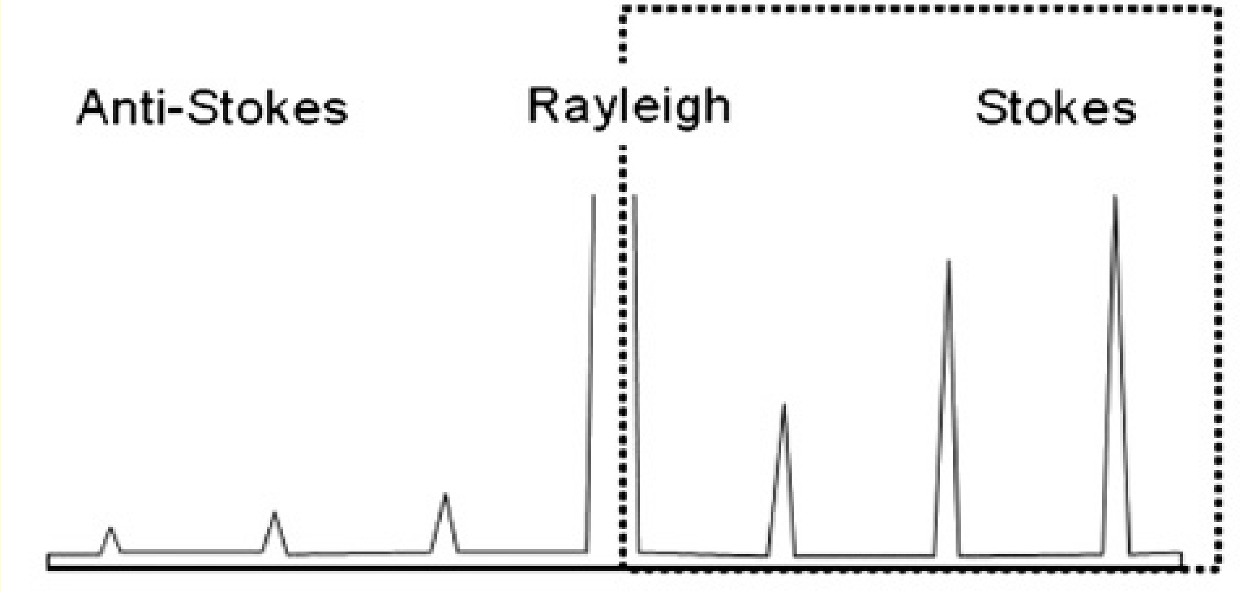

Frezzotti et al. (2012 - J. Geochem. Explor., 112, 1-20

Relative wavenumbers (Raman shift): cm^{-1} →

Absolute wavenumbers: cm^{-1} →

Wavelenght (λ): nm →

Frequency (ν): Hz →

Energy (E): eV →

The Rayleigh scattered frequency lies at 0 cm^{-1} and Raman frequencies are expressed as relative wavenumbers (**Raman shift**)

The Stokes scattering is more frequent → more intense bands

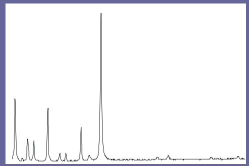

THE RAMAN SPECTRUM

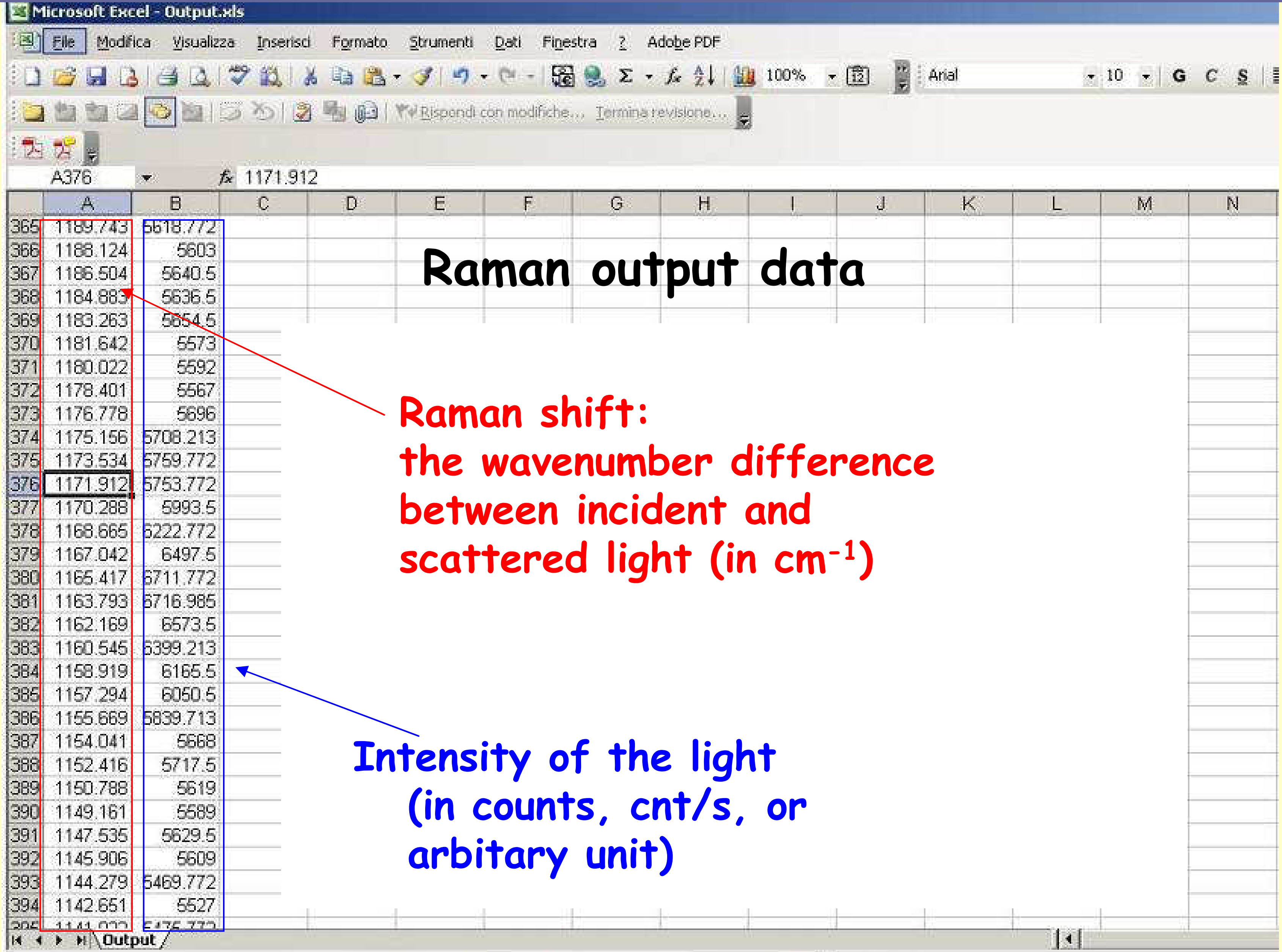

	A	B
365	1189.743	5618.772
366	1188.124	5603
367	1186.504	5640.5
368	1184.883	5636.5
369	1183.263	5654.5
370	1181.642	5573
371	1180.022	5592
372	1178.401	5567
373	1176.778	5696
374	1175.156	5708.213
375	1173.534	5759.772
376	1171.912	5753.772
377	1170.288	5993.5
378	1168.665	6222.772
379	1167.042	6497.5
380	1165.417	6711.772
381	1163.793	6716.985
382	1162.169	6573.5
383	1160.545	6399.213
384	1158.919	6165.5
385	1157.294	6050.5
386	1155.669	5839.713
387	1154.041	5668
388	1152.416	5717.5
389	1150.788	5619
390	1149.161	5589
391	1147.535	5629.5
392	1145.906	5609
393	1144.279	5469.772
394	1142.651	5527

Raman output data

Raman shift:
the wavenumber difference between incident and scattered light (in cm^{-1})

Intensity of the light (in counts, cnt/s, or arbitary unit)

THE RAMAN SPECTRUM

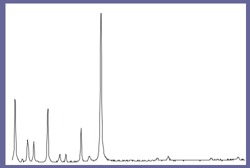

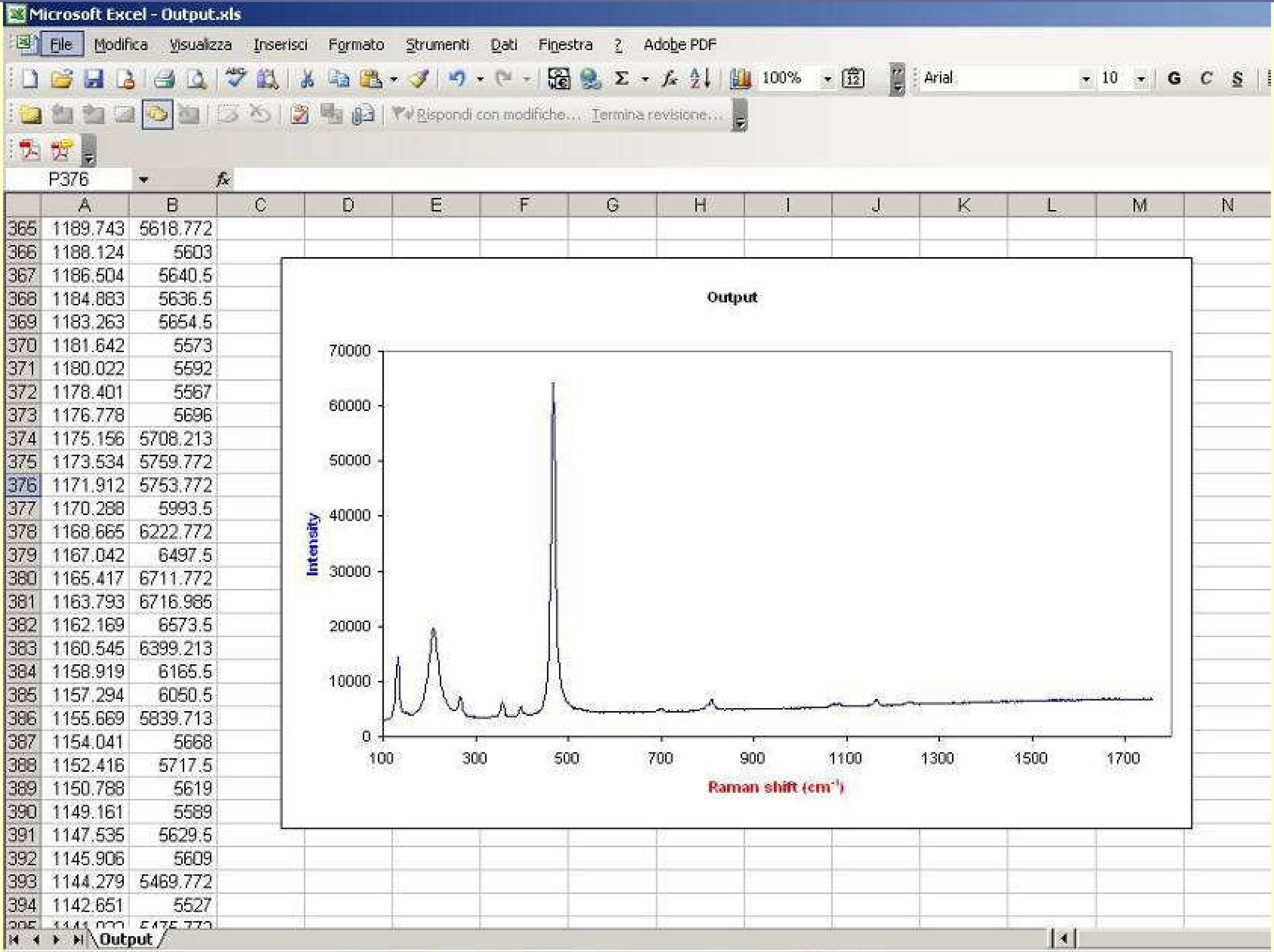

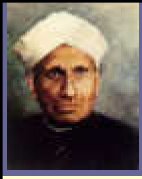

RAMAN-ACTIVE MOLECULAR VIBRATIONS

Every peak, or band, corresponds to one, or a superposition of more, **Raman-active molecular vibrations**.

Main molecular vibrations include:

- **stretching** (stretching of the bond) modes
- **bending** (deformation of the bond angle) modes

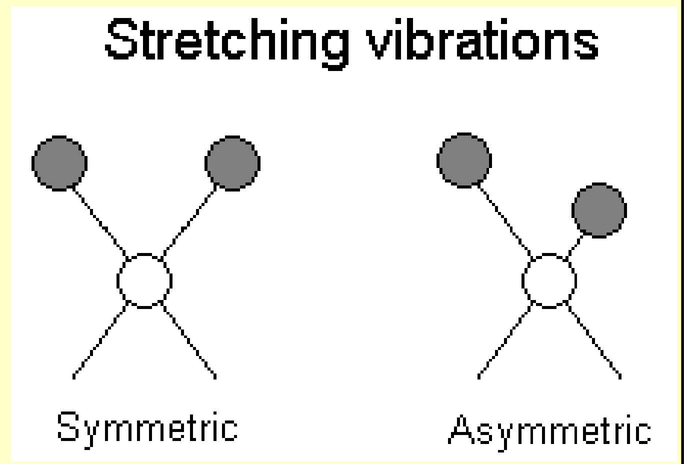

Symmetric vibrations are usually strongly Raman-active whereas asymmetric vibrations are usually nearly Raman inactive.

Stretching frequencies are generally higher than bending frequencies.

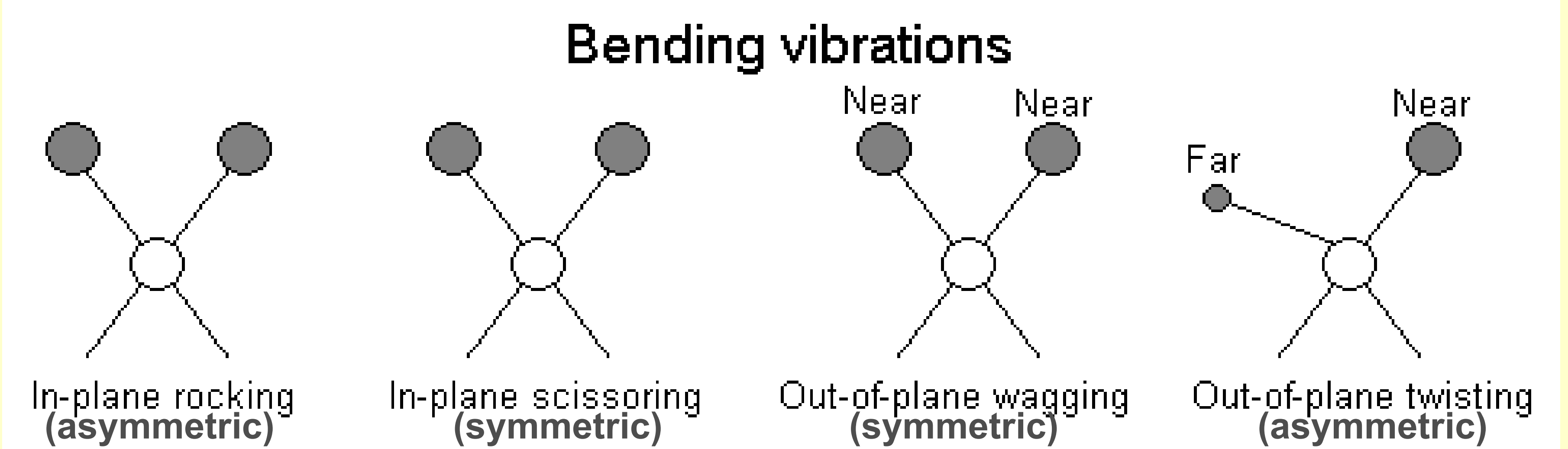

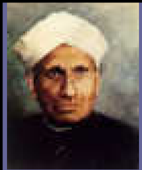

RAMAN-ACTIVE MOLECULAR VIBRATIONS

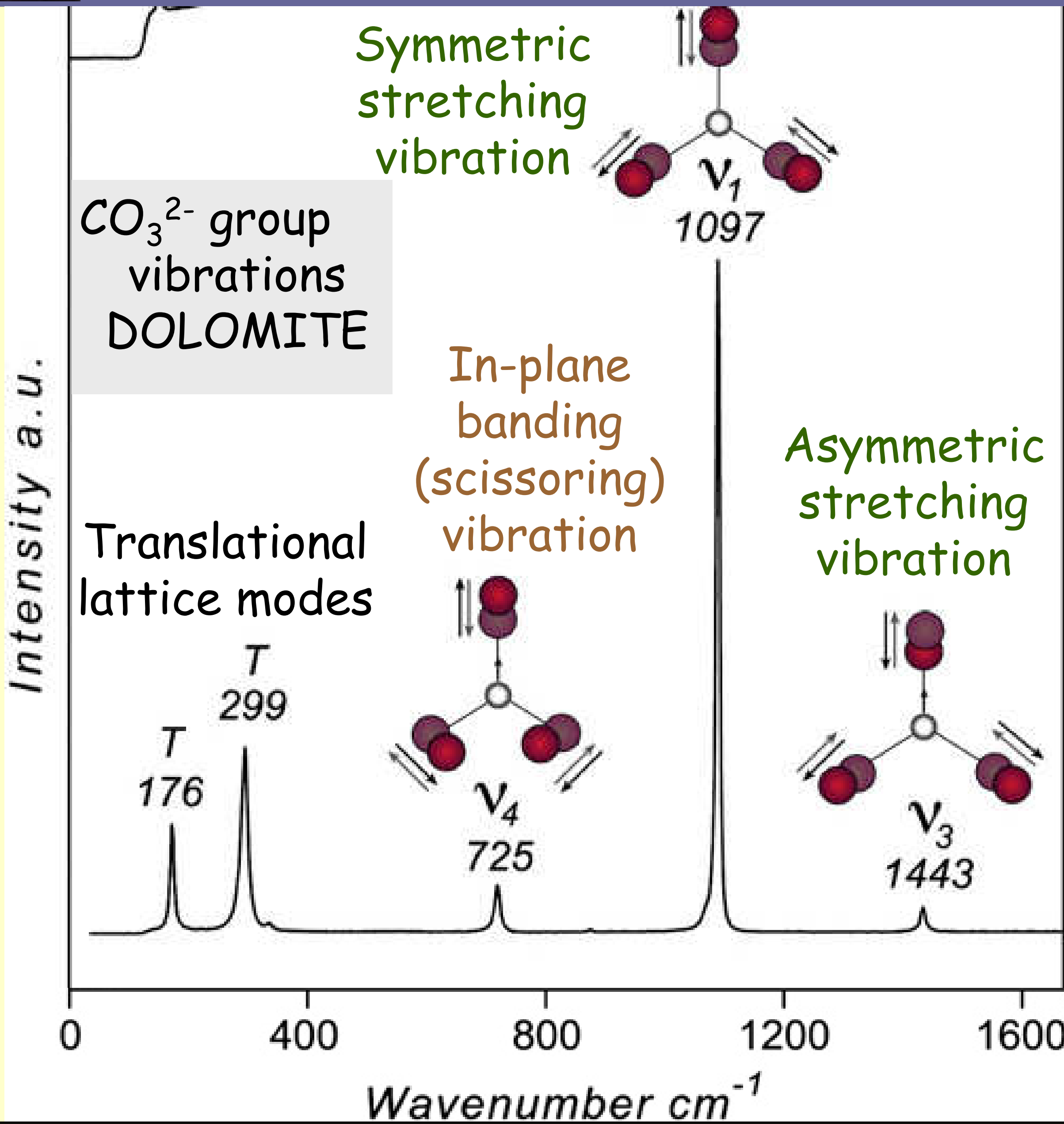

One of the most challenging tasks in Raman spectroscopy is the reliable assignment of observed bands to certain vibrations in the sample

Frezzotti et al. (2012) – J. Geochem. Explor., 112, 1-20

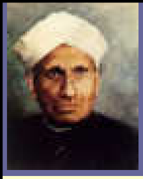

RAMAN vs IR

Complementary character:
IR-active transitions are not Raman-active, and viceversa.

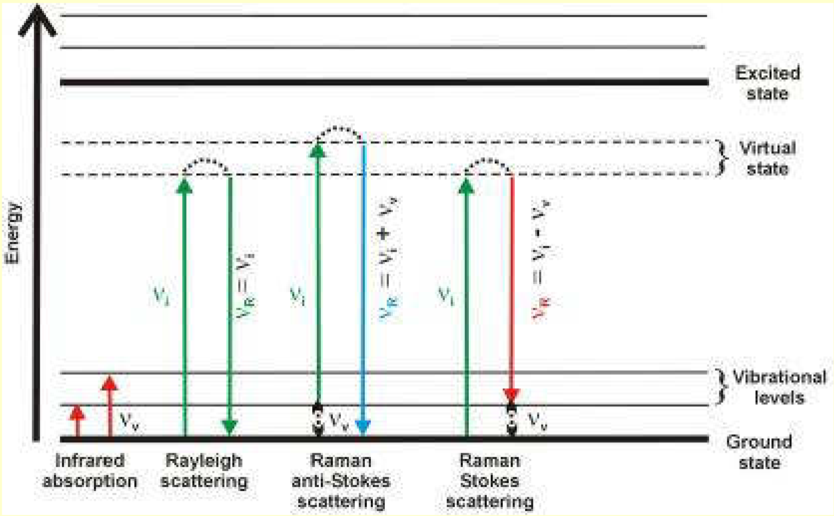

Raman : change in polarizability

Higher sensitivity to polar functional groups

Low sensitivity to water

IR : change in dipole

Higher sensitivity to aromatic & carbon backbone & water

"Blind" to many common polar solvents in acqueous samples

A typical μ-Raman spectrometer

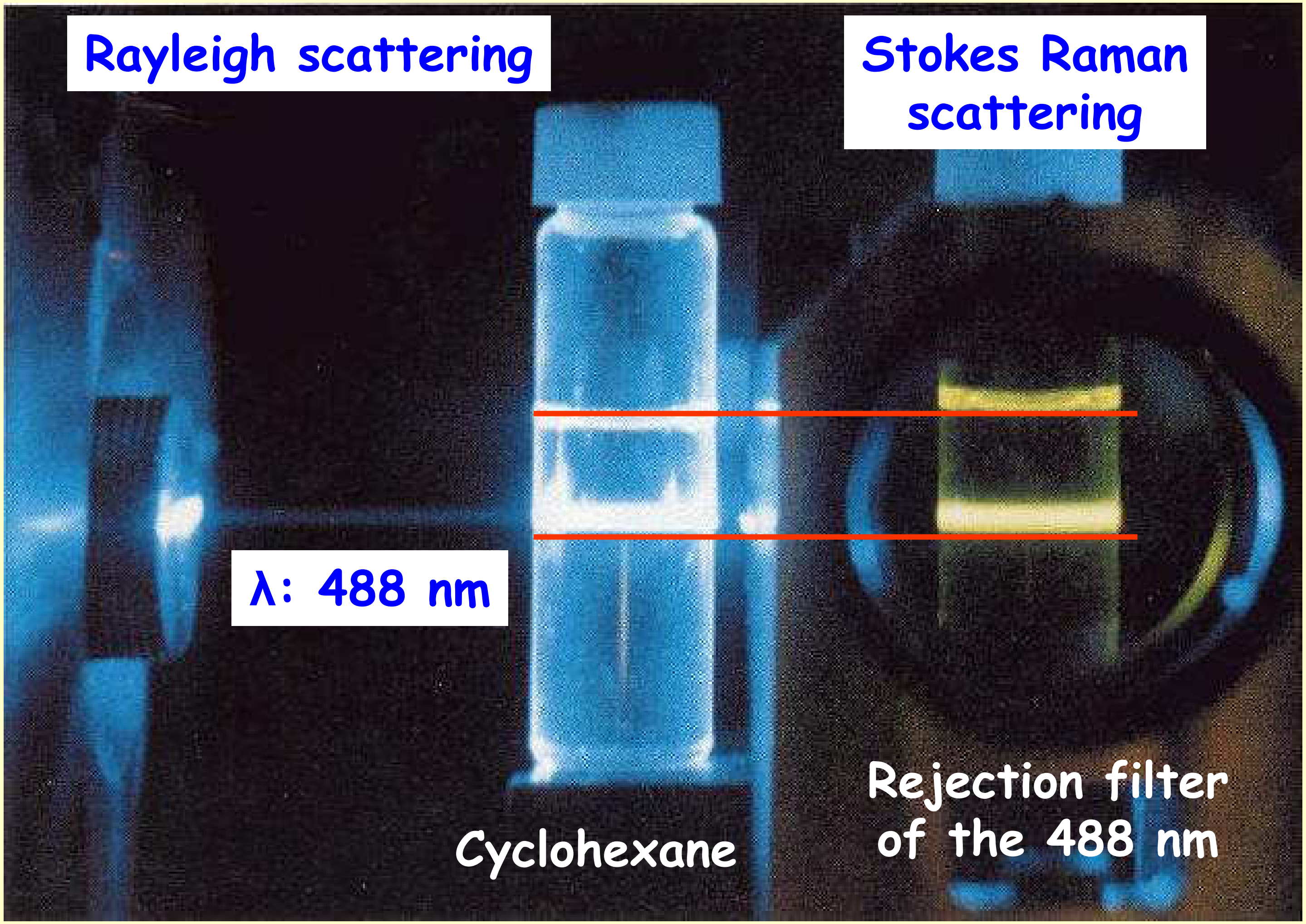

RAMAN APPARATUS

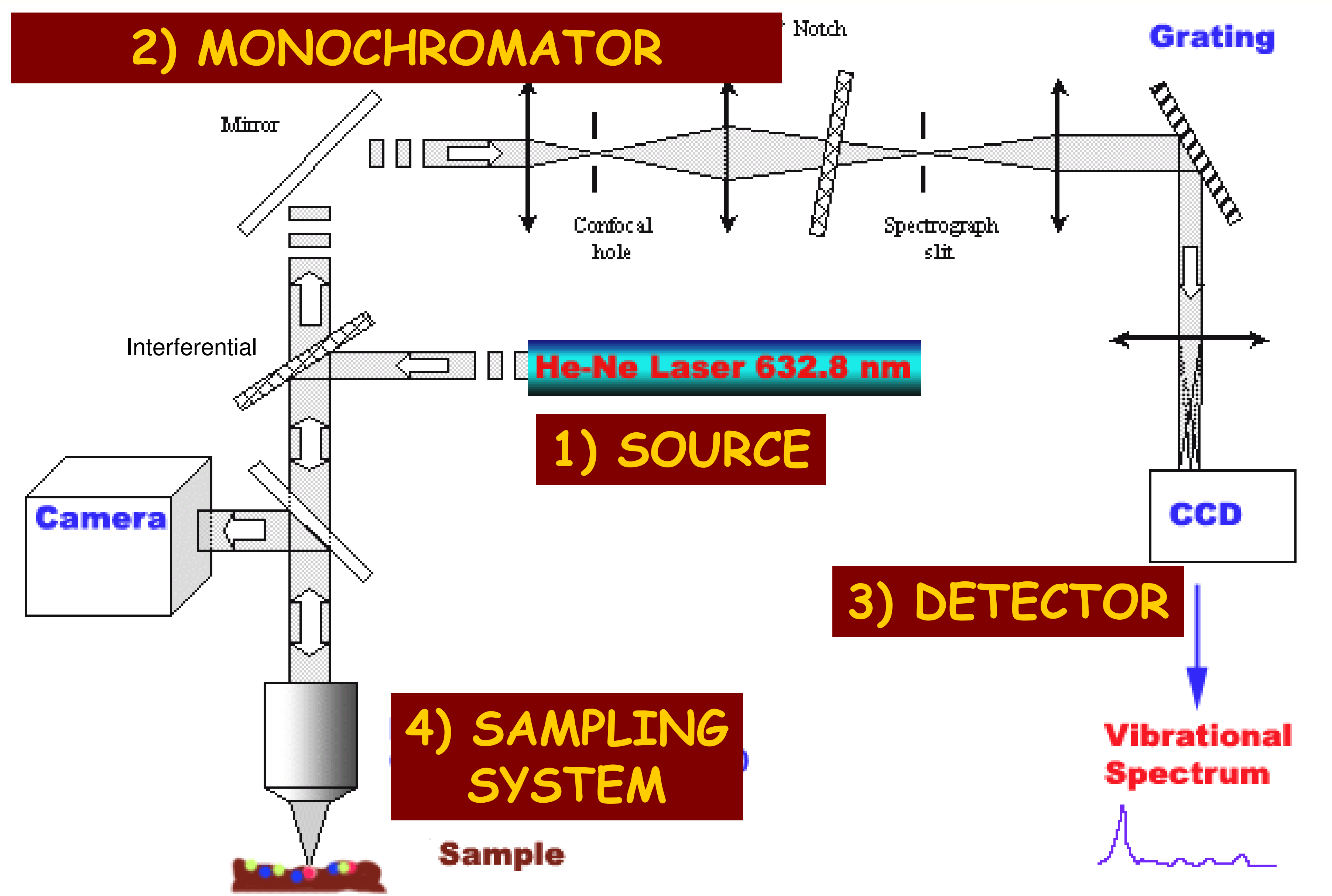

1) EXCITATION SOURCES: LASER

Why? High power. High monochromaticy. High stability.

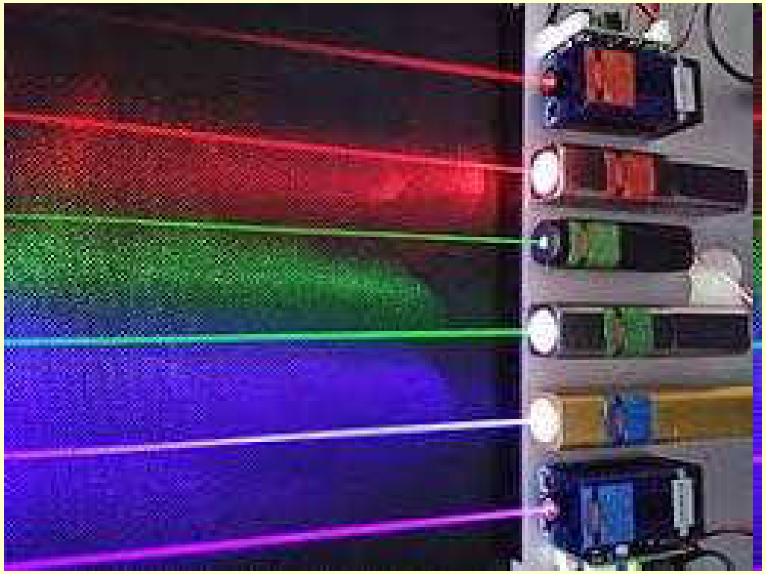

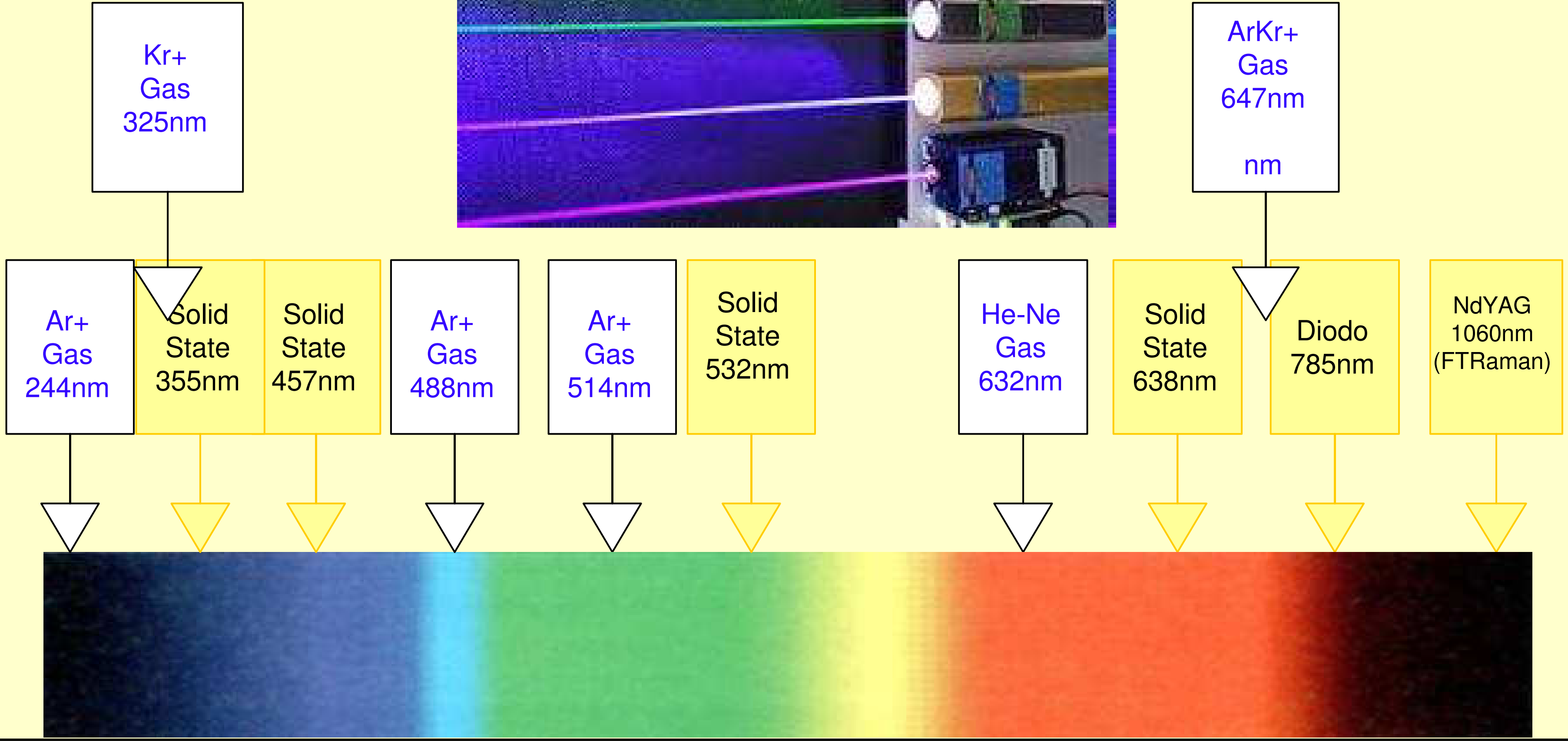

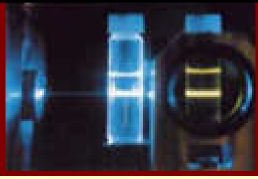

2) MONOCHROMATOR

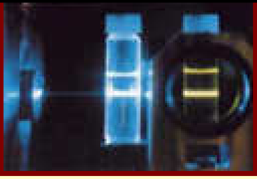

MONOCHROMATOR: allow to separate different wavelengths & to focalize them on the image plane of the detector

The **filter** **(Notch or Edge)** excludes the Rayleight component

The **slit** avoids stray light and control the bandpass

The **grating** disperse the incident light separating it into its constituent components (like a prism, but works in reflection)

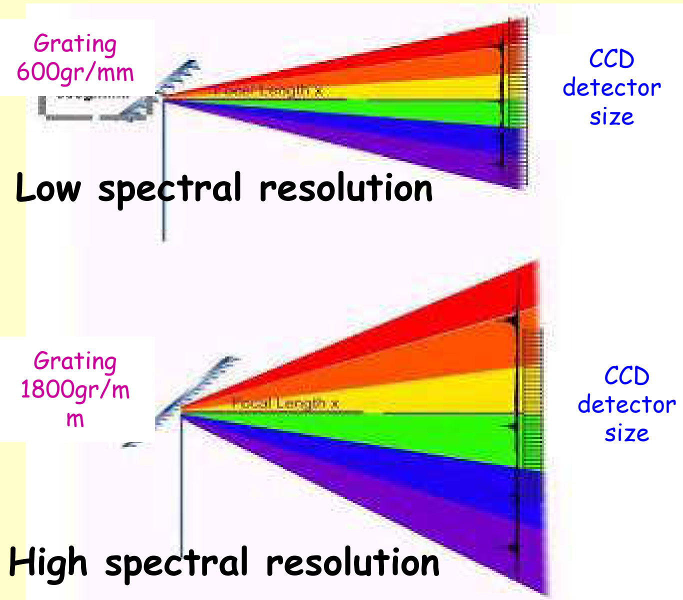

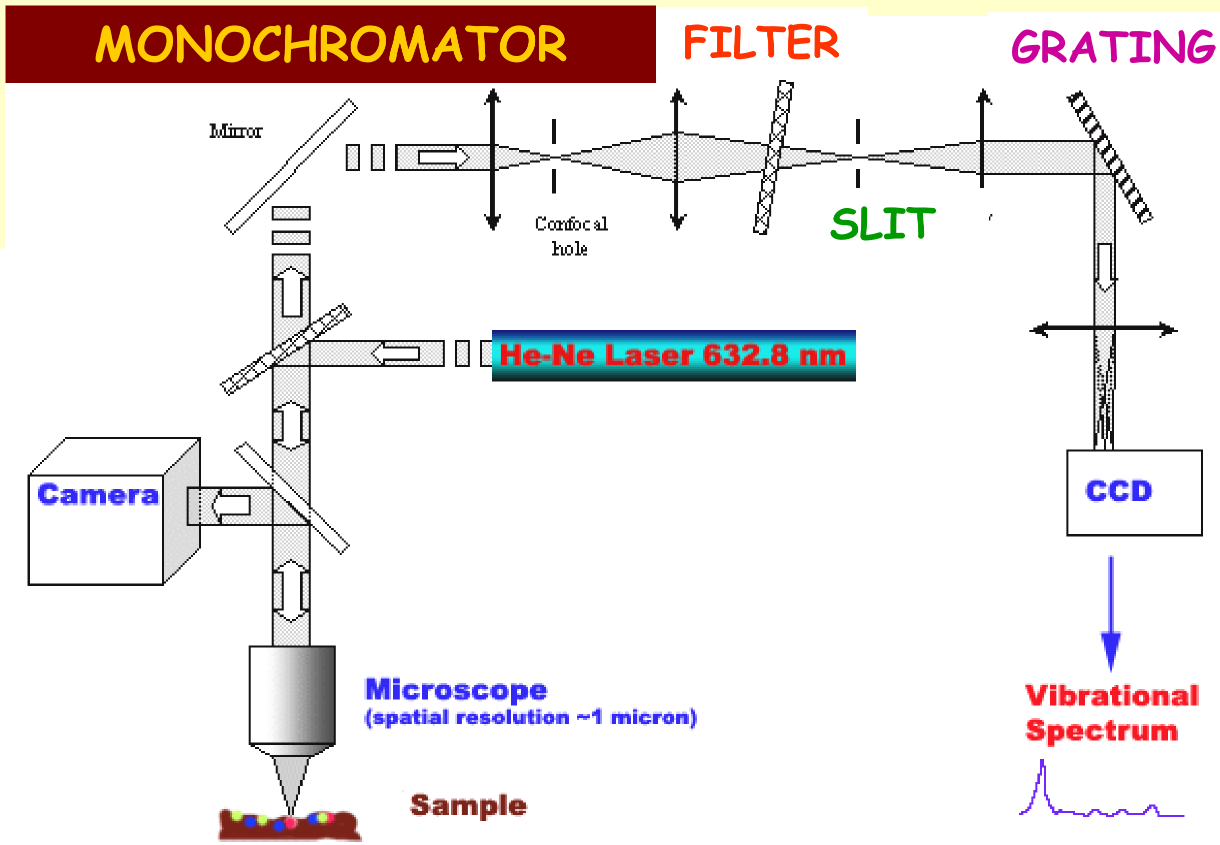

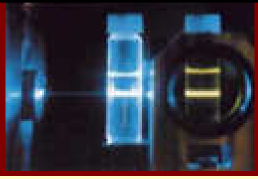

3) DETECTOR: PMT vs CCD

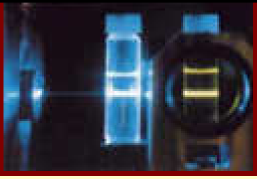

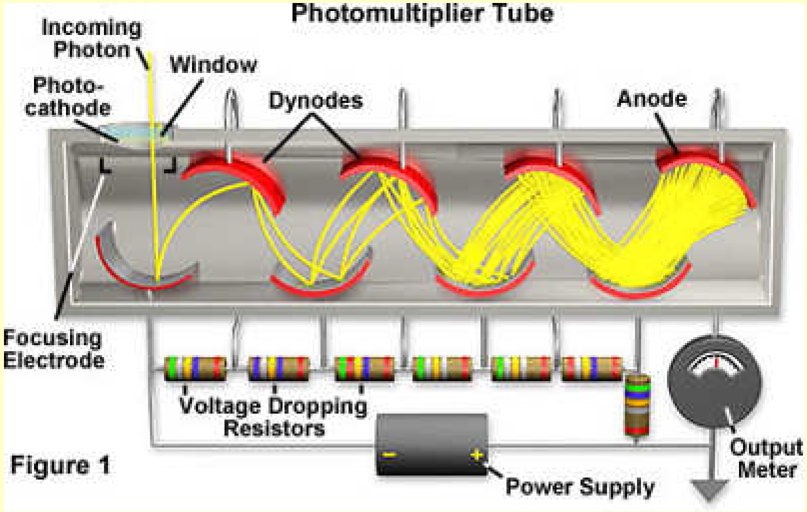

Single channel detector: photomultiplier tube (PMT)

- ☺ cheaper
- ☹ worse signal-to-noise ratio
- ☹ longer acquisition time

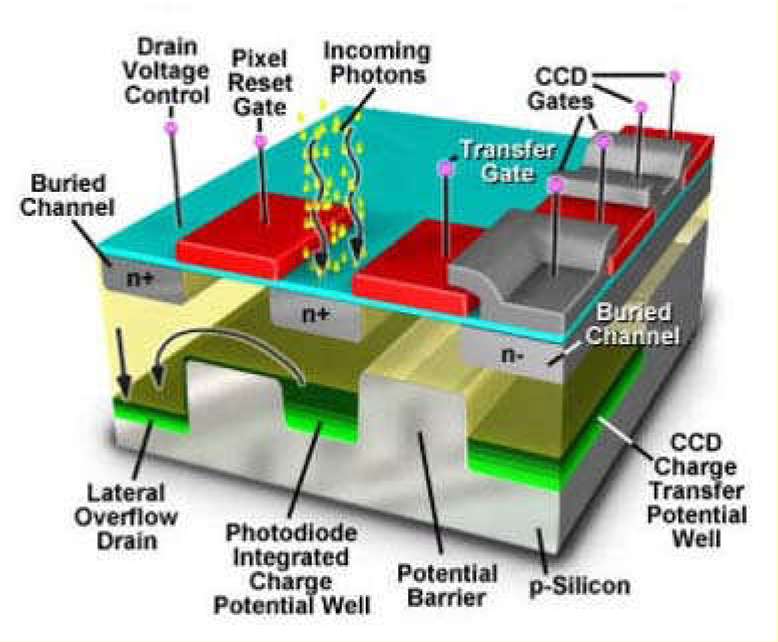

Multichannel detectors: Charge Coupled Device (CCD)

- ☹ more expensive
- ☺ better signal-to-noise ratio
- ☺ shorter acquisition time

4) SAMPLING SYSTEMS

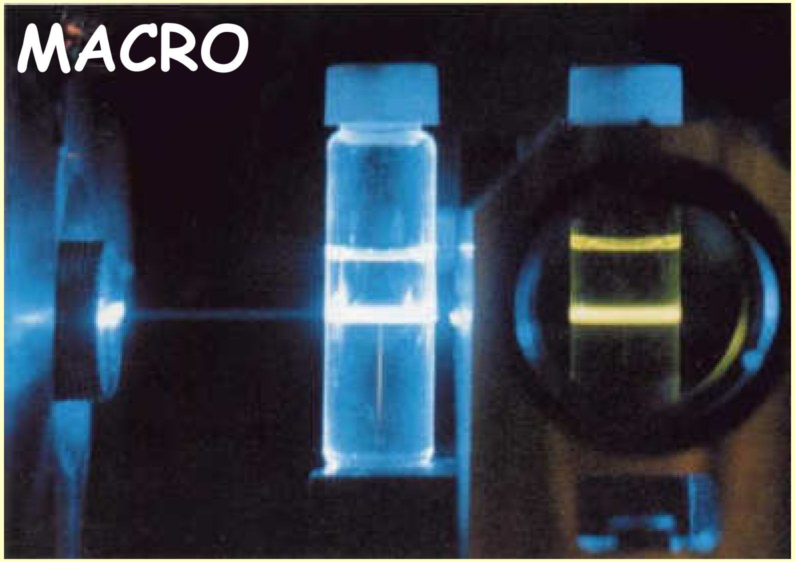

Nasdala et al.,(2004). EMU Notes, 6, 281-343

4) SAMPLING SYSTEMS

Confocality: selectivity along axial direction (axial resolution)

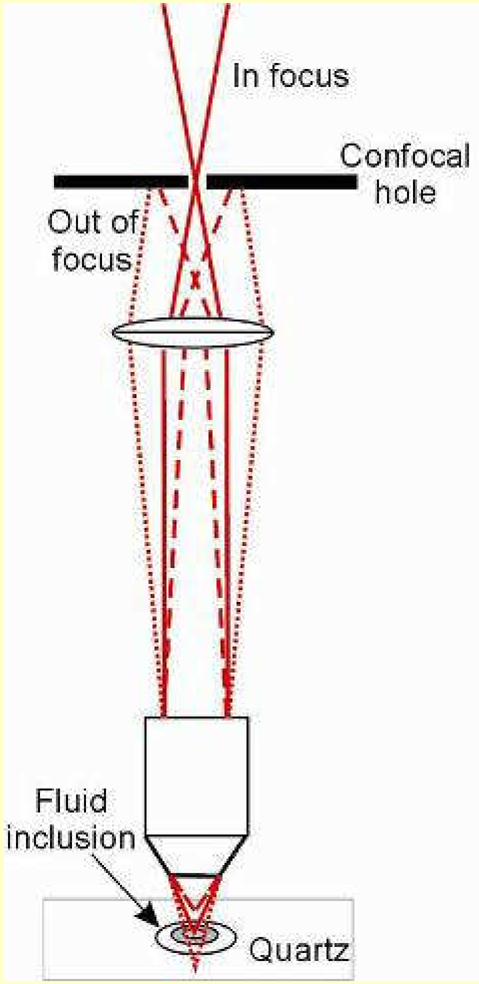

Depends on:
- NA of objective
- laser wavelength
- confocal hole aperture

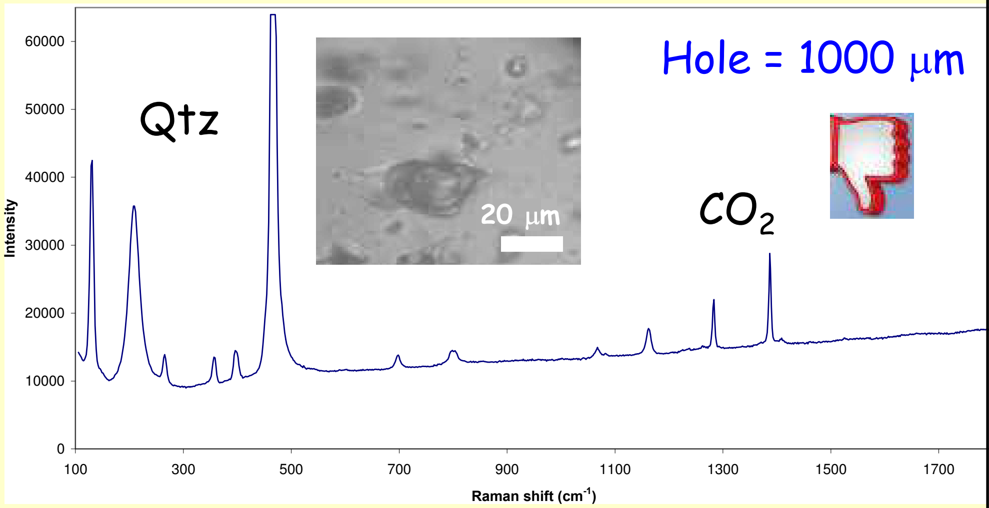

Ferrando, Rossetti

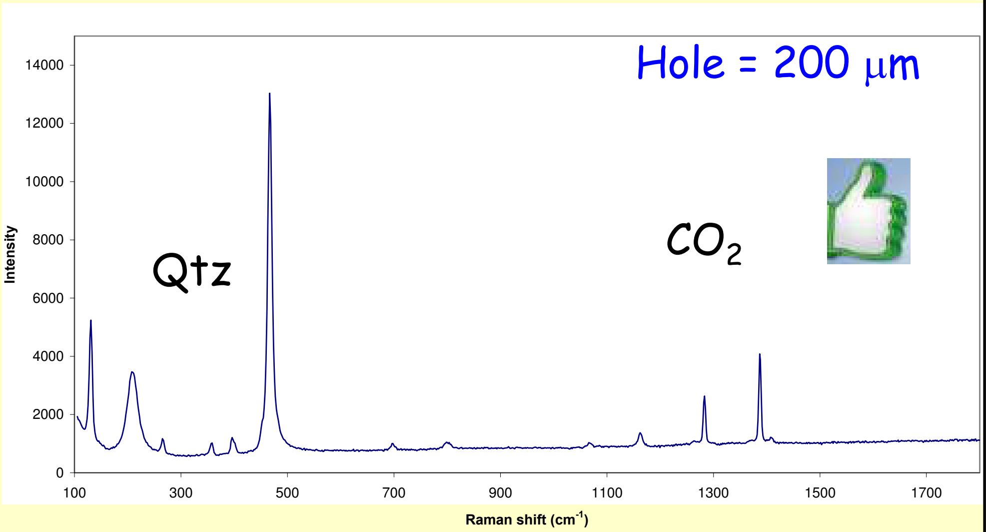

THE RAMAN MICRO-SPECTROMETER OF THE INTERDIPARTIMENTAL CENTER "SCANSETTI"

Horiba Jobin Yvon Raman micro-spectrometer LABRAM HR800

Excitation: He-Ne laser 633 nm (20 mW)
Solid state Nd laser 532 nm (up to 250 mW)

Filters: interferential and edge

Grating:
600 grooves/mm
1800 grooves/mm

Confocal microscope Olympus BX41

Objectives: 4, 10, 20, 50, 100 x (spatial resolution <1 μm)

Transmicted and refleted polarized light (with videocameras)

Automated X-Y mapping stage

Spectral resolution: 1-3 cm^{-1} (depending on the configuration)
Accuracy and precision: ≤1 cm^{-1} (depending on the configuration)

Setting for macro-analyses:
- objective 4x
- 90° mirror/prism

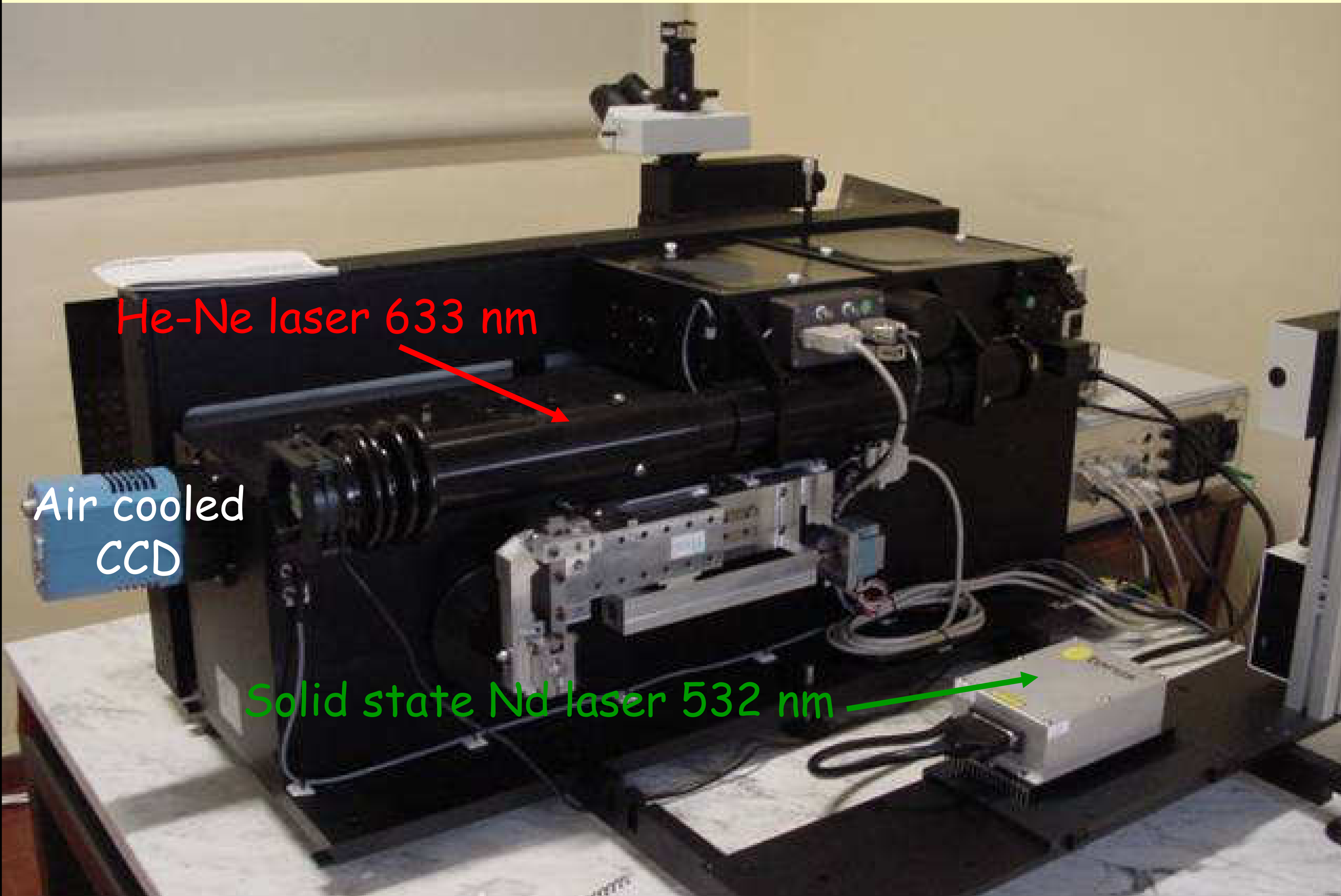
He-Ne laser 633 nm
Air cooled
CCD
Solid state Nd laser 532 nm

Toward grating and CCD

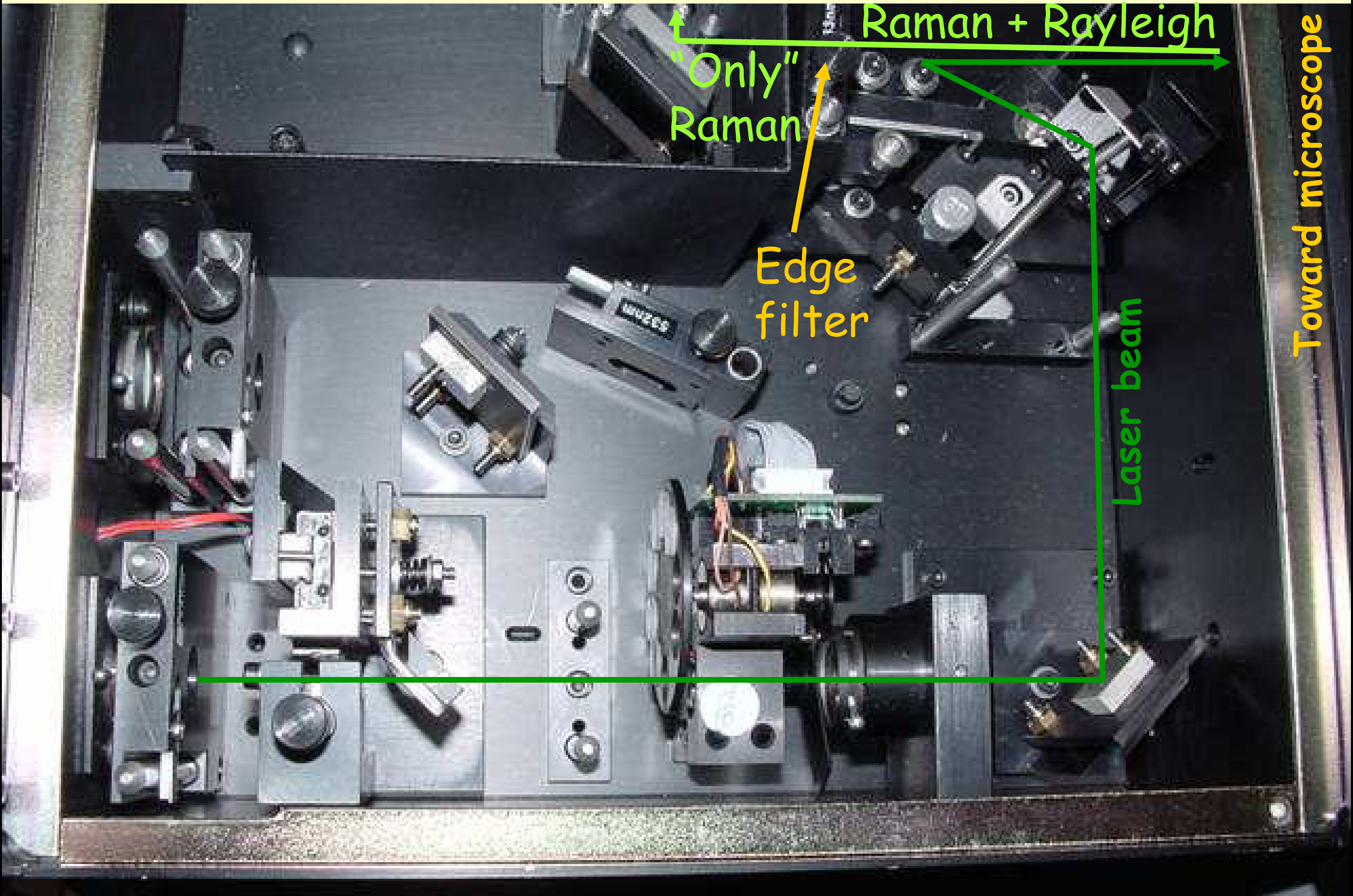

Applications

Beneficial possibilities of Raman spectroscopy…

non-destructive
not special sample preparation
analysis of solid, liquid and gaseous phases
structural and chemical information
fast measure
low analytical costs
water and moisture does not interfere with analysis
analyses at and under the surface of transparent media

…& of Raman microspectroscopy (CONFOCAL configuration)

in situ analyses
analysis of small volumes (1x1x5 μm^3)

SAMPLE *TAL QUALE* VS THIN SECTION

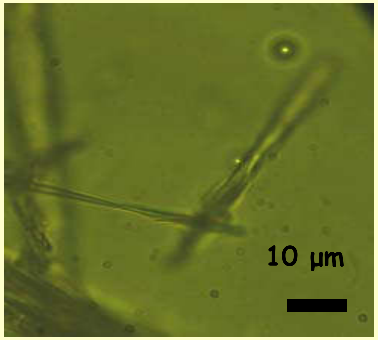

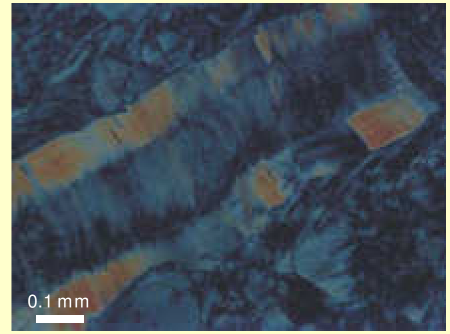

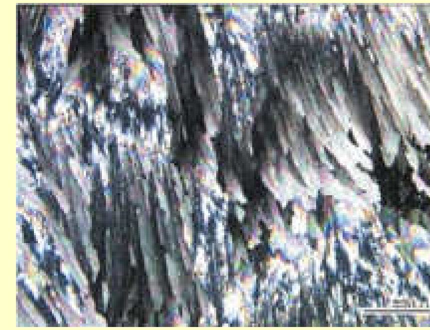

	Sample *tal quale*	Thin section
Sample preparation (distructive)	NO	YES
Acquisition time (for a spectrum of similar quality)	>	<
Focus problem	>	<
Other problems	Possible electrostatic charge at high magnification and interference with protective matter	Possible interference with resins

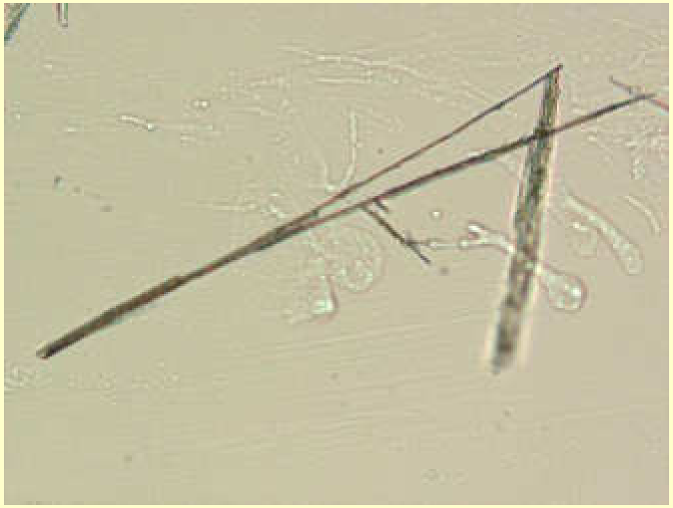

Mineral characterization

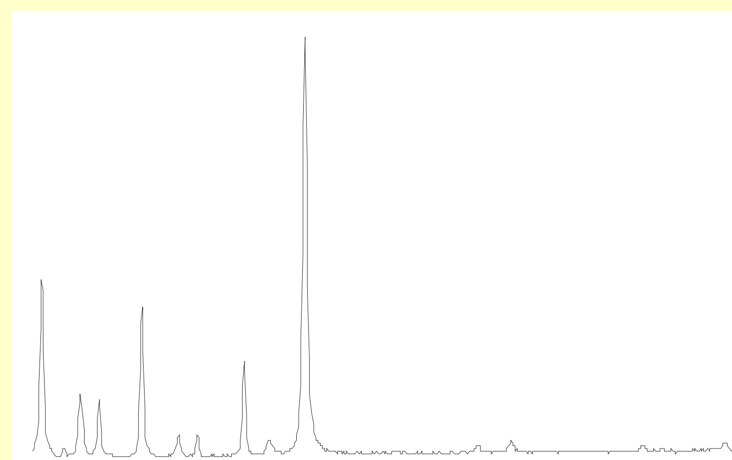

video

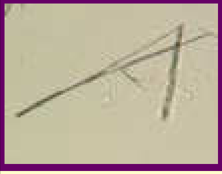

MINERAL CARACTERIZATION
Raman spectra interpretation

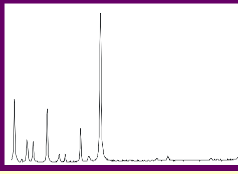

Main vibrational regions of minerals

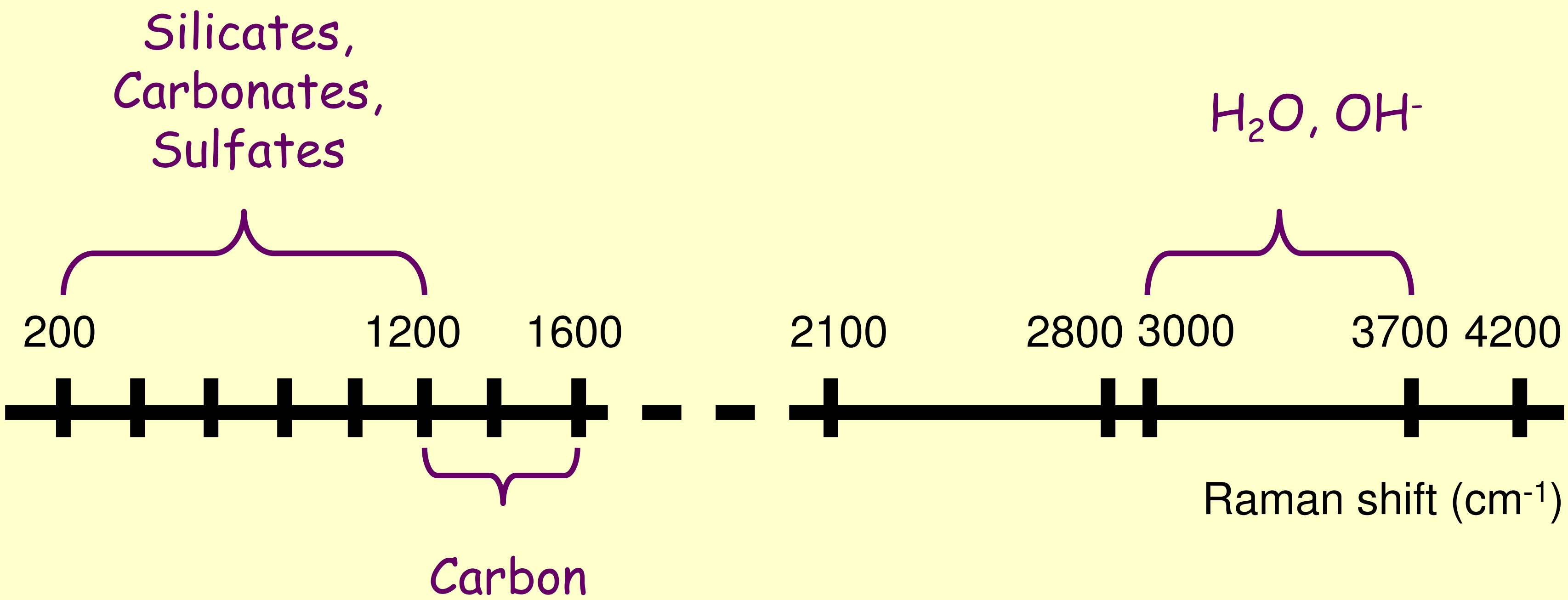

N.B. Hydrous and OH-bearing minerals show **DIAGNOSTIC** broad bands at 3000-3700 cm^{-1}

MINERAL CARACTERIZATION
Raman spectra interpretation

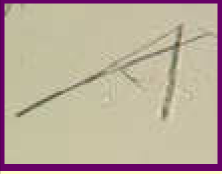

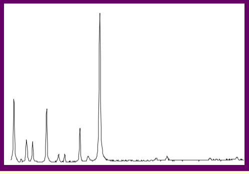

Main vibrational regions of most common minerals

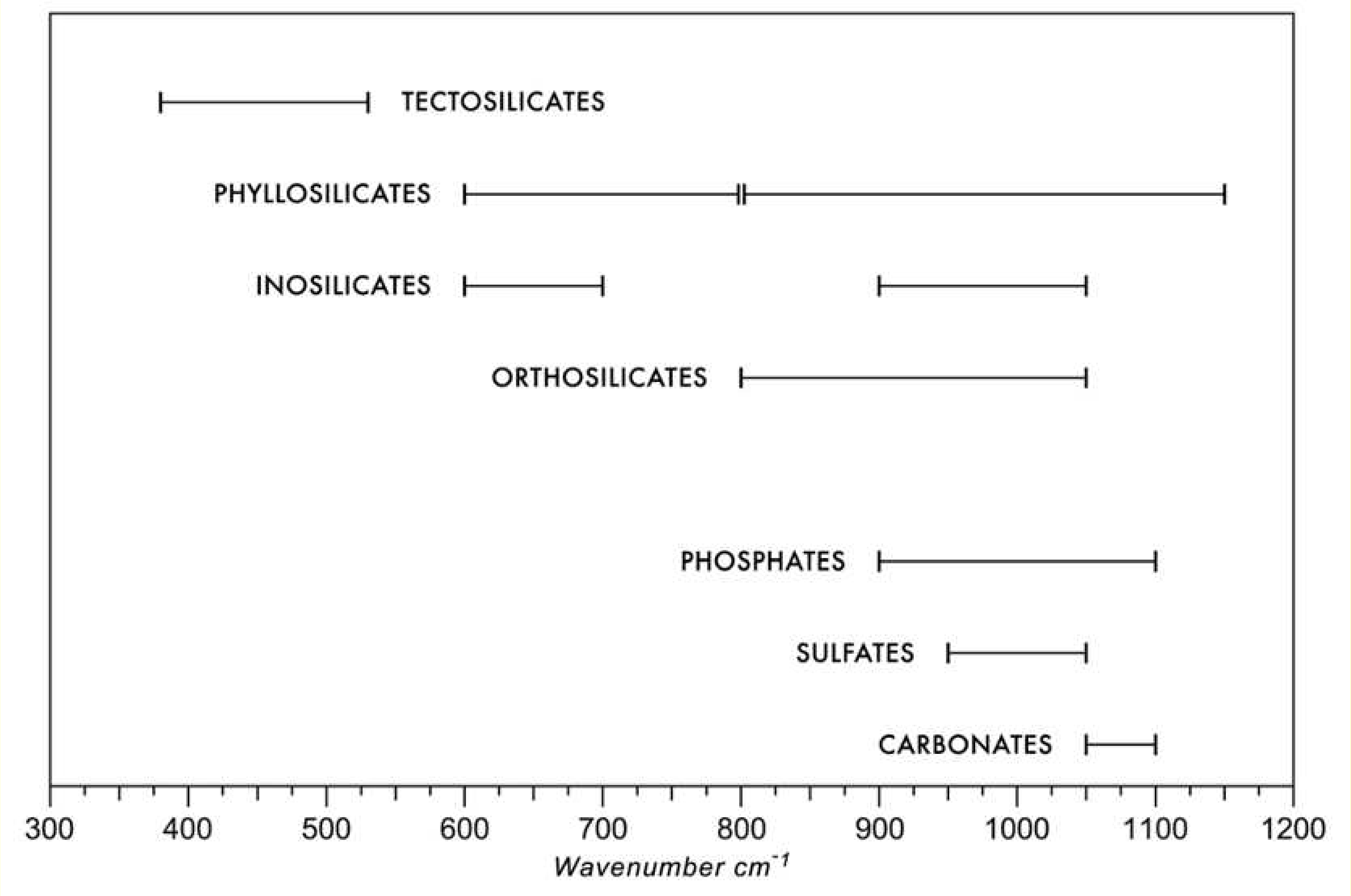

Modified from Frezzotti et al. (2012) – J. Geochem. Explor., 112, 1-20

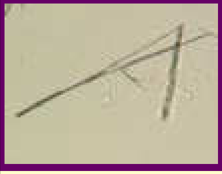

MINERAL CARACTERIZATION
Raman spectra interpretation

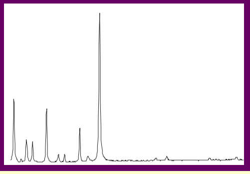

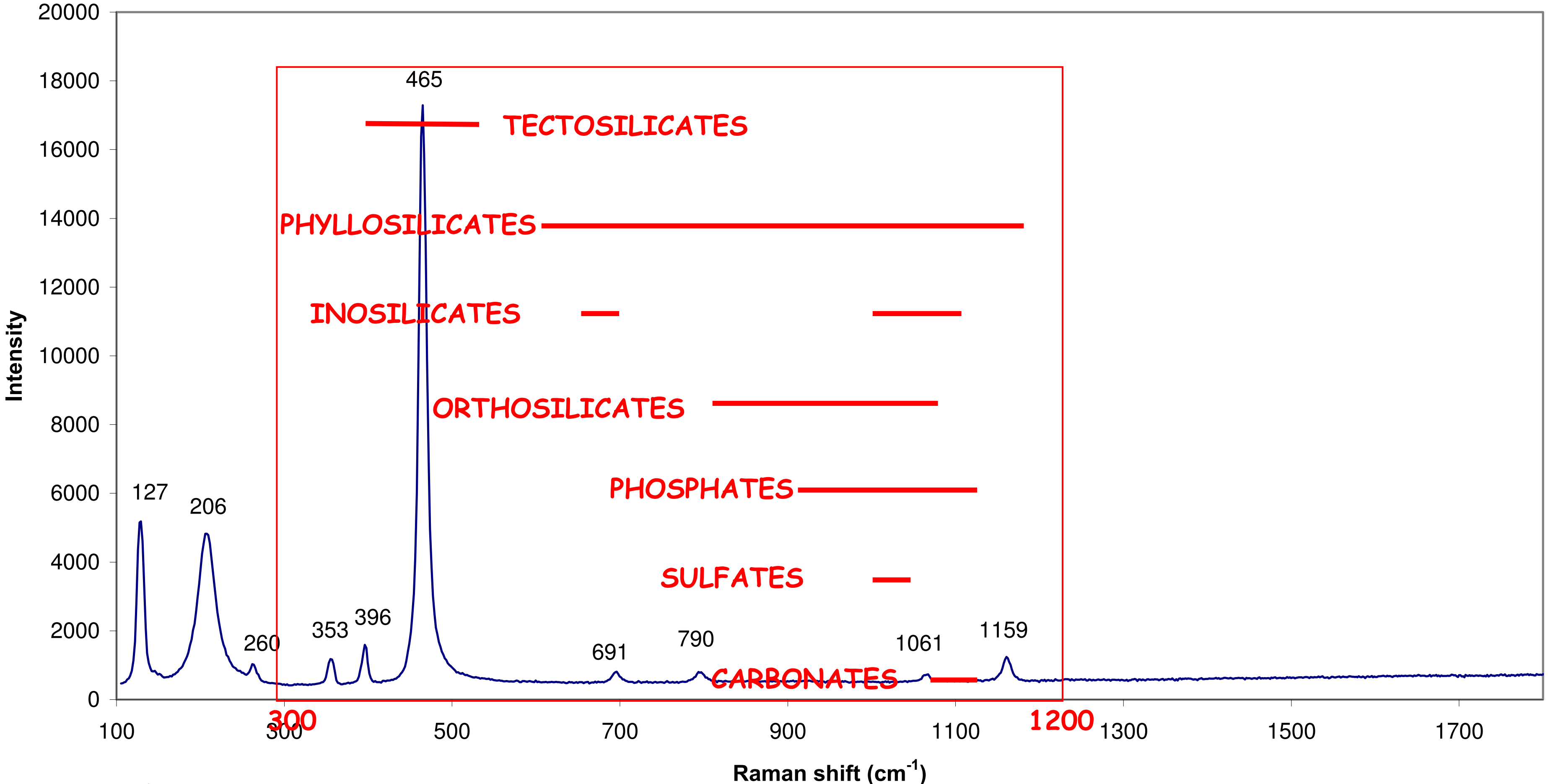

Ferrando

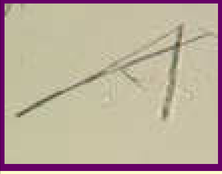

MINERAL CARACTERIZATION
Raman spectra interpretation

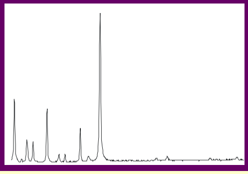

To identify a mineral,
all peaks must be numbered
and be assigned to a phase
by comparison with STANDARDS…

…present in literature

Tectosilicates	Main vibrations											Ref.
Orthoclase $KAlSi_3O_8$	157 177 197	284		458 477	514 583		751	814	967	1035 1062	1137	[1]
Microcline $KAlSi_3O_8$	159 178 199	263 267 286		455 475	514	651	749	813		1007	1128 1142	[1]
Sanidine $KAlSi_3O_8$	163	284		462 475	514		767	813			1123	[1]
Albite $NaAlSi_3O_8$	183	210 292		457 480	508		764	816	977	1032 1098		[2]; 5
Quartz SiO_2	128	206 265	356	402 464 485	520	608 698		807		1066	1161	6
Coesite SiO_2	116 151 176	204 269	326 355	427 466	521		785	815 837		1036 1065	1144 1164	6
Cristobalite SiO_2	114	230 273 286		420			792			1075		[2]

Frezzotti et al. (2012) – J. Geochem. Explor., 112, 1-20

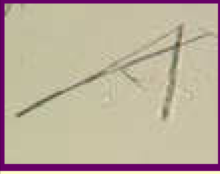

MINERAL CARACTERIZATION
Raman spectra interpretation

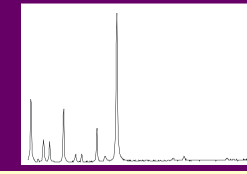

…present within databases

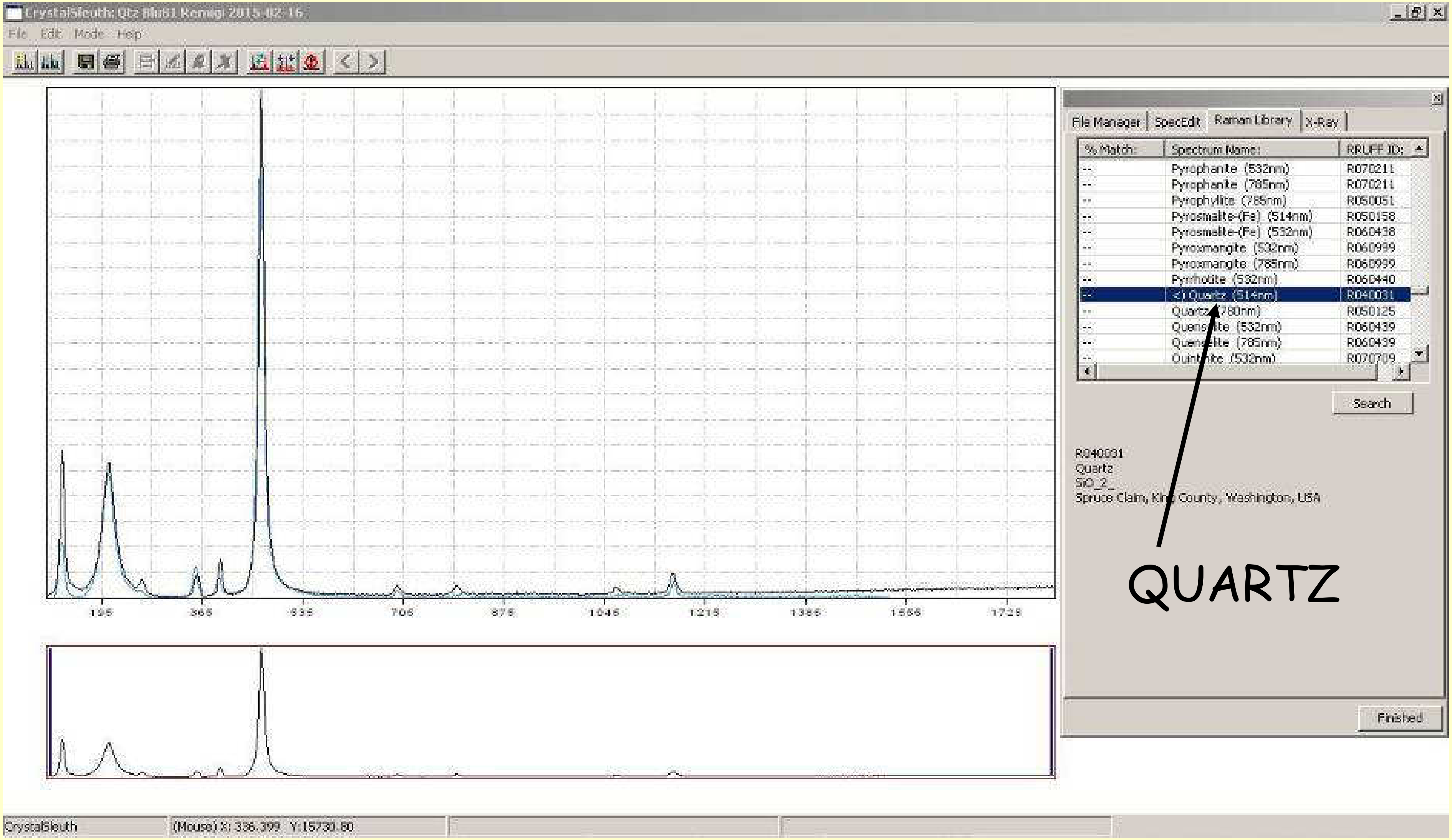

RRUFF project

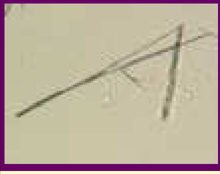

MINERAL CARACTERIZATION
Raman spectra interpretation

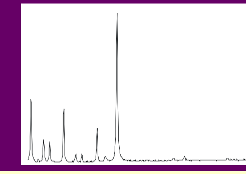

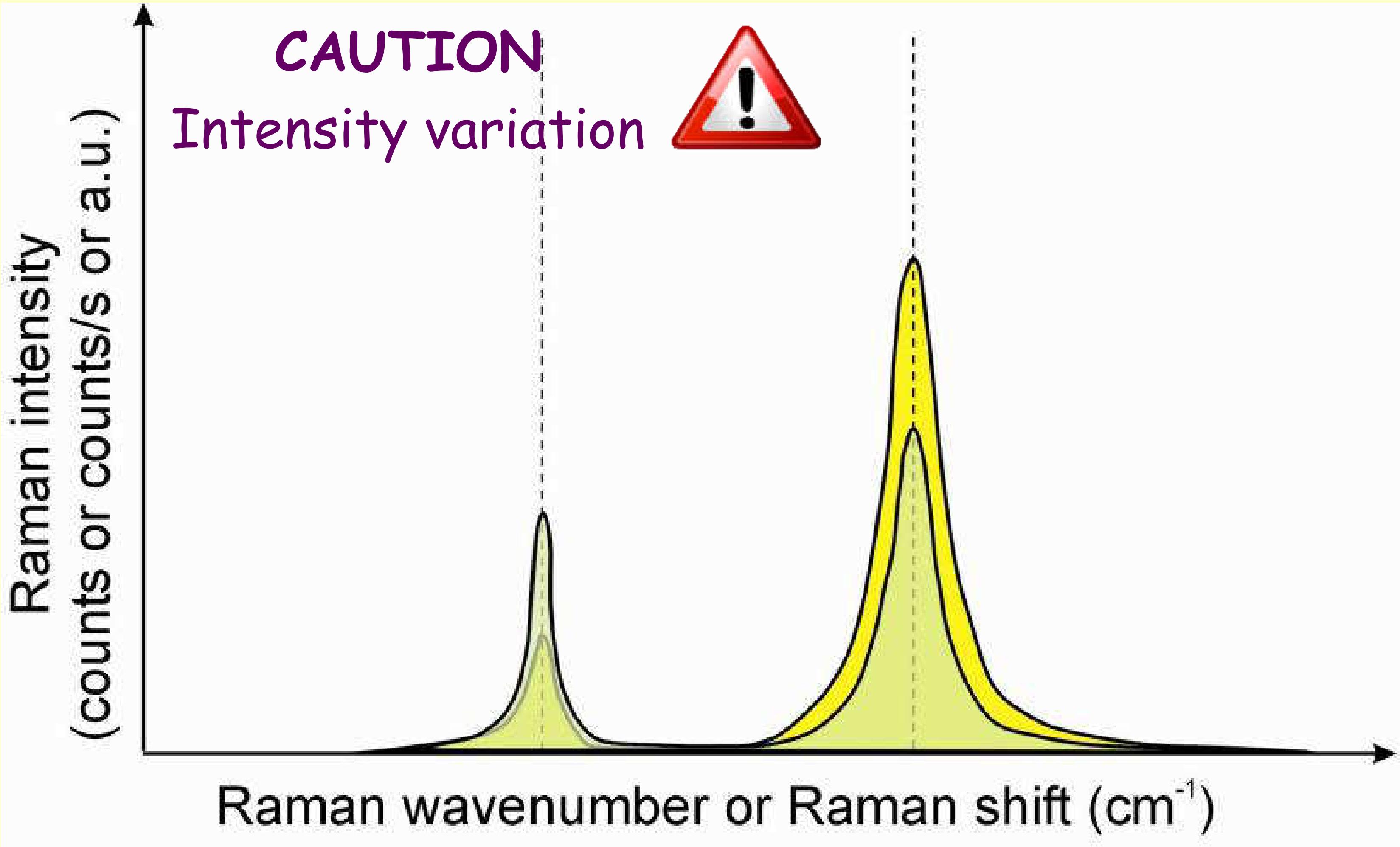

If the incident light is polarized, the polarizability of a molecular vibration may change with mineral orientation

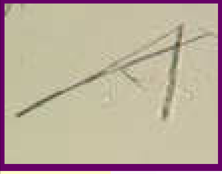

MINERAL CARACTERIZATION
Raman spectra interpretation

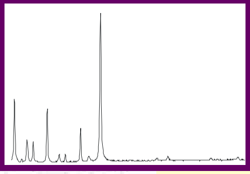

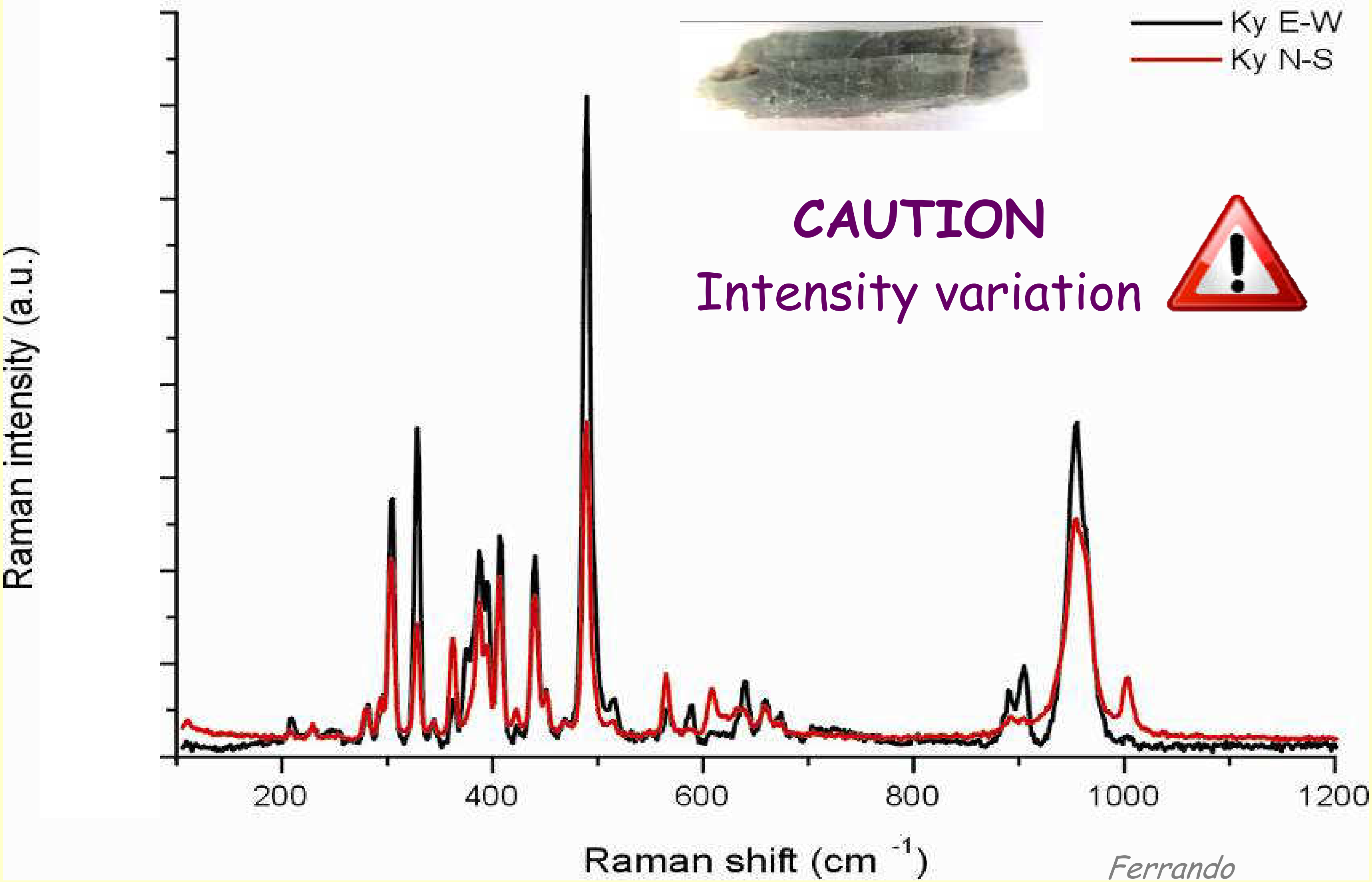

CAUTION

Intensity variation

The absence of a Raman bands in a spectrum does not necessarily mean the vibration does not exist

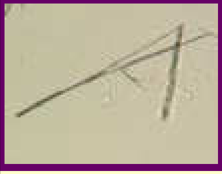

MINERAL CARACTERIZATION
Asbestos & other harmful fibrous minerals

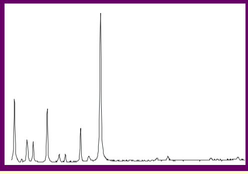

Balangero asbestos mine (TO): 1918-1990

The exposure to fine fibrous asbestos powder is linked to diseases such as pleural mesothelioma and asbestosis.

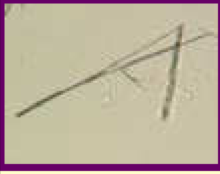

MINERAL CARACTERIZATION
Asbestos & other harmful fibrous minerals

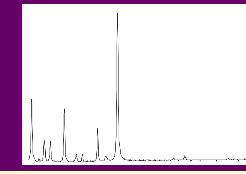

Mineral	Chemical formula	Asbestos D.L. 81/08	Verified pathogenicy	Mineral group
Chrysotile	$Mg_3[Si_2O_5](OH)_4$	*	yes	Serpentine
Antigorite	$Mg_{3m-3}Si_{2m}O_{5m}(OH)_{4m-6}$, m = n° of tetrahedra along an entire wavelength		under evaluation	Serpentine

CHRYSOTILE

ANTIGORITE

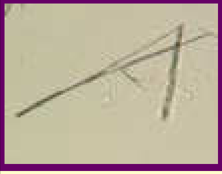

MINERAL CARACTERIZATION
Asbestos & other harmful fibrous minerals

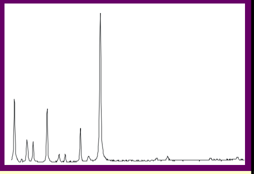

MAIN BANDS & RELATED MOLECULAR VIBRATIONS

< 650 cm^{-1}

Distinct molecular vibrations:
- Mg-OH;
- *bending* mode of SiO_4 tetrahedra;
- O-H-O bonds

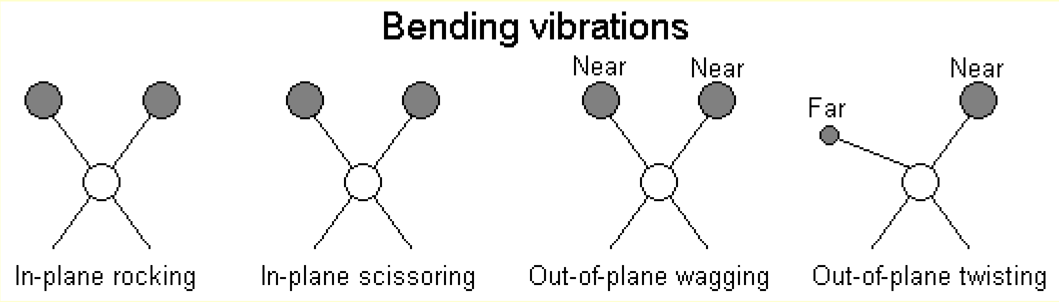

650-1000 cm^{-1}

Stretching modes (symmetric and asymmetric) of Si-O_b-Si bonds (O_b=oxygen in the tetrahedral plane)

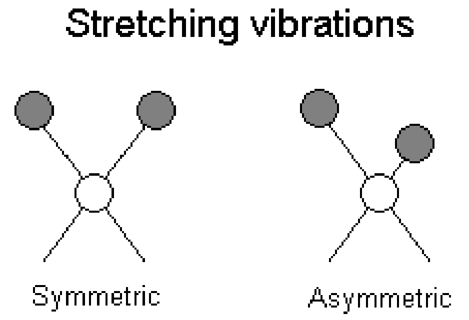

1000-1150 cm^{-1}

Stretching modes of Si-O_{nb} bonds (O_{nb}=oxygen out of the tetrahedral plane)

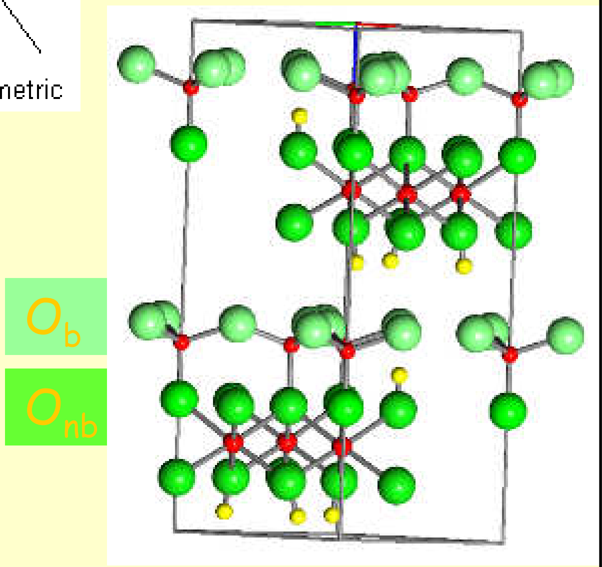

3000-4000 cm^{-1}

Vibrational modes of OH groups

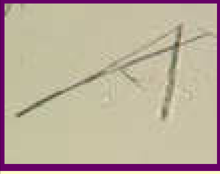

MINERAL CARACTERIZATION
Asbestos & other harmful fibrous minerals

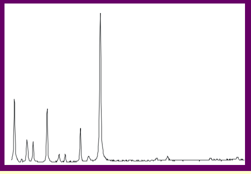

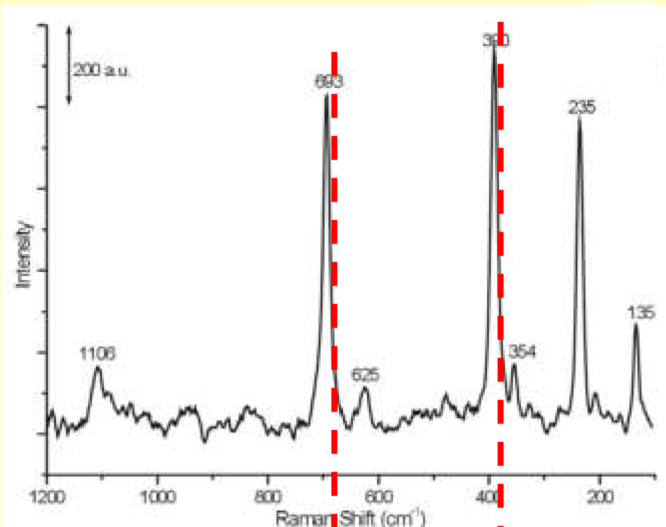

CHRYSOTILE

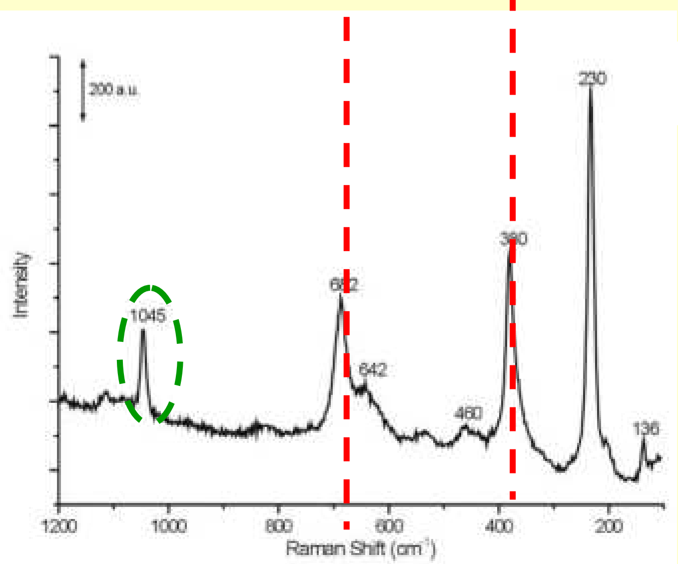

ANTIGORITE

	CRHYSOTILE	ANTIGORITE
	IDENTIFICATION	
SiO_4 tetrahedra bending modes	389-391	378-382
symmetric $Si-O_b-Si$ stretching vibrations	690-692	680-684
antisymmetric $Si-O_b-Si$ stretching vibrations	-	1043-1045
OH vibrations	3684-3685	3669-3670

*Rinaudo et al. (2003) - Canadian Mineralogist, **41**, 883-890*

*Groppo et al. (2006) - European Journal of Mineralogy, **18**, 319-329*

Groppo & Compagnoni (2007) - Periodico di Mineralogia, 76, 127-153

Bloise et al. (2014) – Environ. Earth Sci., 71, 3773-3786

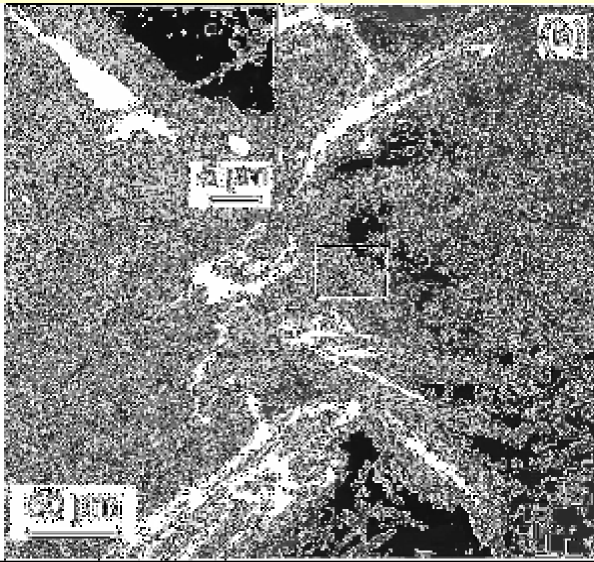

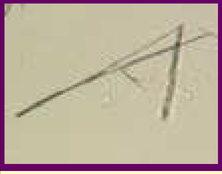

MINERAL CARACTERIZATION
Asbestos & other harmful fibrous minerals

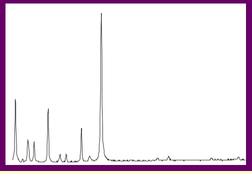

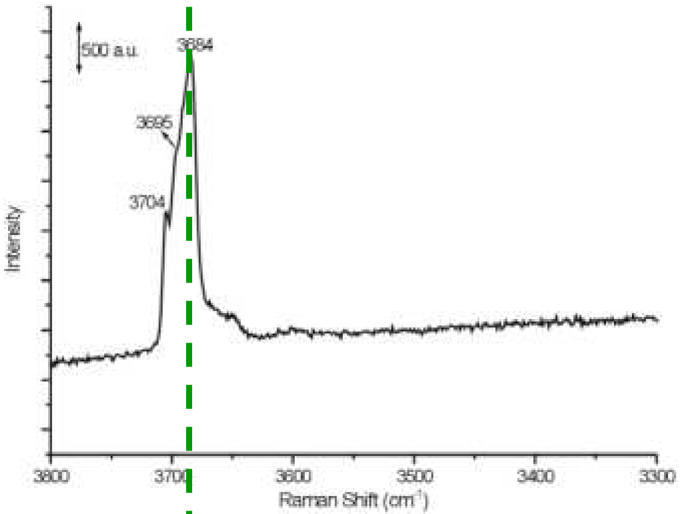

CHRYSOTILE

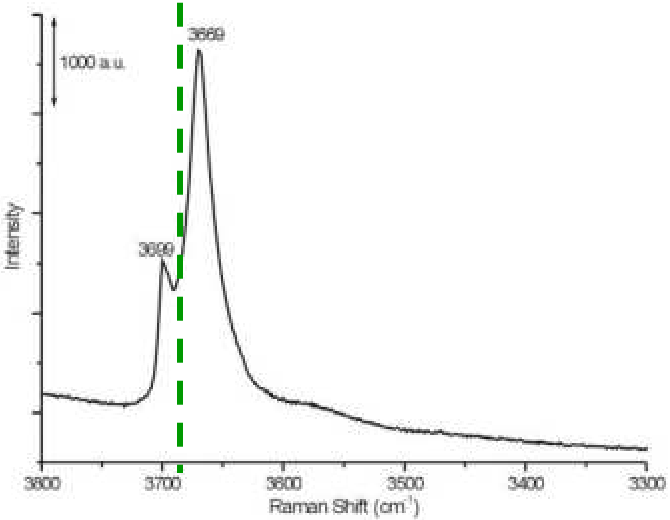

ANTIGORITE

	CRIHYSOTILE	***ANTIGORITE***
	IDENTIFICATION	
SiO_4 tetrahedra bending modes	389-391	378-382
symmetric Si-O_b-Si stretching vibrations	690-692	680-684
antisymmetric Si-O_b-Si stretching vibrations	-	1043-1045
OH vibrations	$\boxed{3684}$-3695	$\boxed{3668}$-3699

*Rinaudo et al. (2003) - Canadian Mineralogist, **41**, 883-890*
*Groppo et al. (2006) - European Journal of Mineralogy, **18**, 319-329*
Groppo & Compagnoni (2007) - Periodico di Mineralogia, 76, 127-153

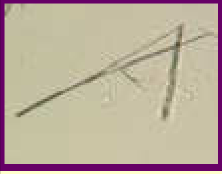

MINERAL CARACTERIZATION
Asbestos & other harmful fibrous minerals

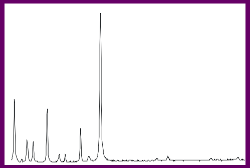

Raman imaging

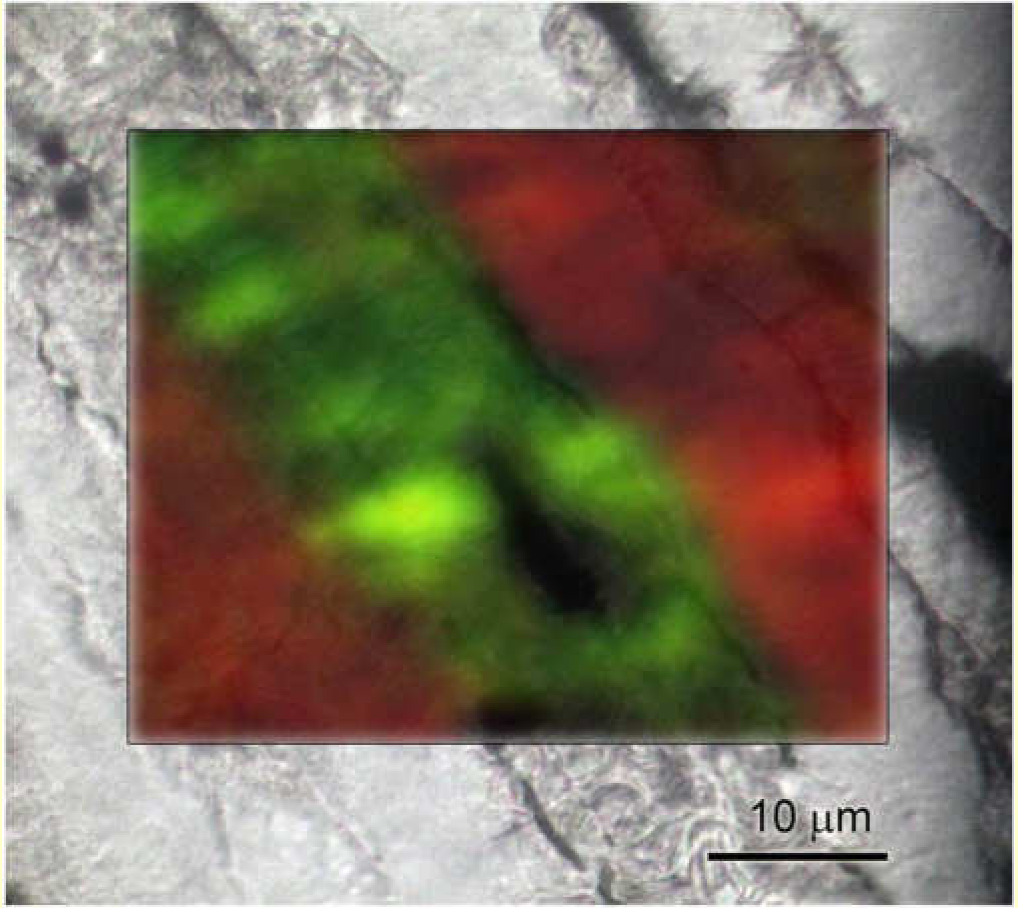

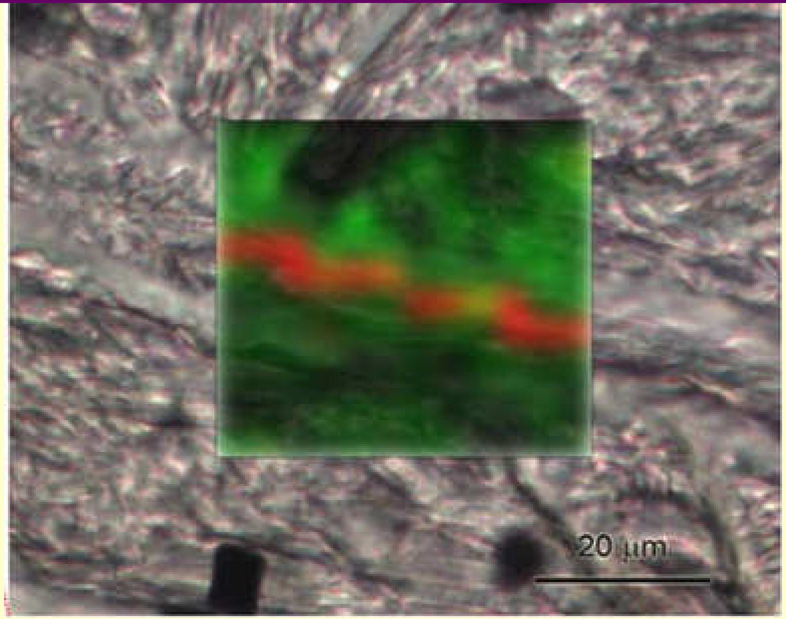

Green: OH-bond in chrysotile

Red: OH-bond in antigorite

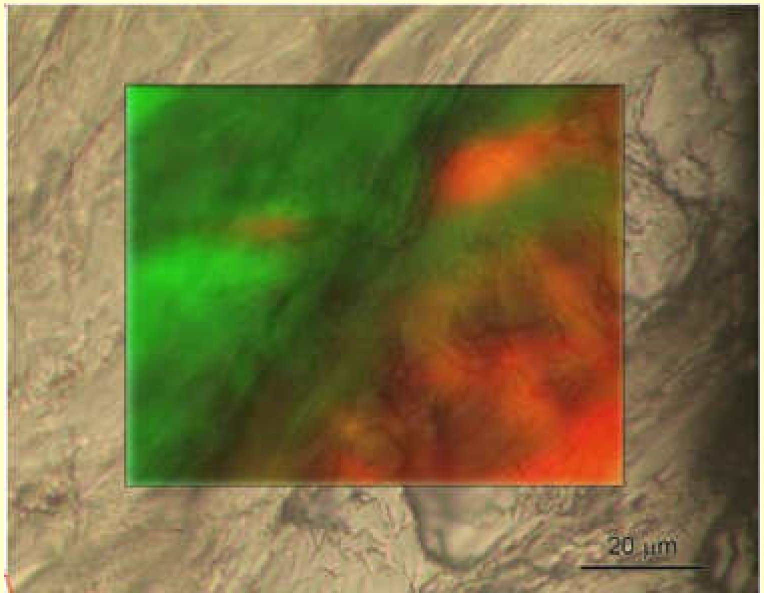

*Petriglieri et al. (2015) - Journal of Raman Spectroscopy, **46**, 953-958*

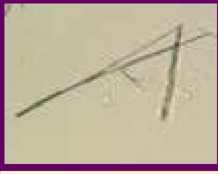

MINERAL CARACTERIZATION
Asbestos & other harmful fibrous minerals

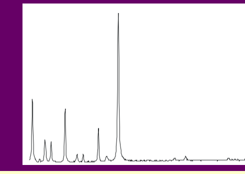

Mineral	Chemical formula	Asbestos D.L. 81/08	Verified pathogenicy	Mineral group
Anthophyllite	$(Mg)_7[Si_8O_{22}](OH,F)_2$	*	yes	Orthoamphibole
Gedrite	$(Mg)_5Al_2[Si_6Al_2O_{22}](OH,F)_2$			Orthoamphibole
Amosite (Grunerite)	$(Mg,Fe^{2+})_7[Si_8O_{22}](OH,F)_2$	*	yes	Clinoamphibole
Actinolite	$Ca_2(Mg,Fe^{2+})_5[Si_8O_{22}](OH,F)_2$	*	yes	Clinoamphibole
Tremolite	$Ca_2(Mg)_5[Si_8O_{22}](OH)_2$	*	yes	Clinoamphibole
Mg-hornblende	$Ca_2(Mg)_4Al[Si_7AlO_{22}](OH)_2$			Clinoamphibole
Crocidolite (Riebeckite)	$Na_2Fe^{2+}{}_3Fe^{3+}{}_2[Si_8O_{22}](OH,F)_2$	*	yes	Clinoamphibole
Fluoro-edenite	$NaCa_2Mg_5[(Si_7Al)O_{22}]F_2$		yes	Clinoamphibole
Whincite	$NaCa(Mg_4Al)[Si_8O_{22}](OH,F)_2$		yes	Clinoamphibole
Richterite	$(Na)NaCaMg_5[Si_8O_{22}](OH,F)_2$		yes	Clinoamphibole

TREMOLITE

ACTINOLITE

CROCIDOLITE/RIEBECKITE

AMOSITE/GRUNERITE

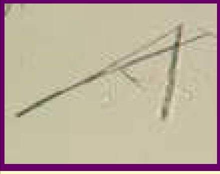

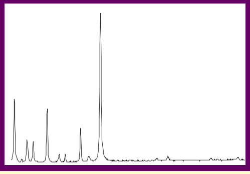

MAIN BANDS & RELATED MOLECULAR VIBRATIONS

< 600 cm^{-1}

Distinct molecular vibrations:

- translational modes of metal-oxygen bonds
- rotational modes of SiO_4 tetrahedra
- O-H-O bonds

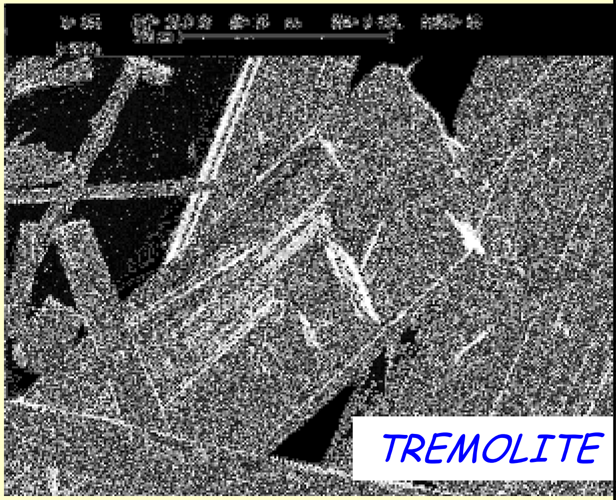

TREMOLITE

600-1150 cm^{-1}

Stretching modes (symmetric and asymmetric) of Si-O_b-Si bonds

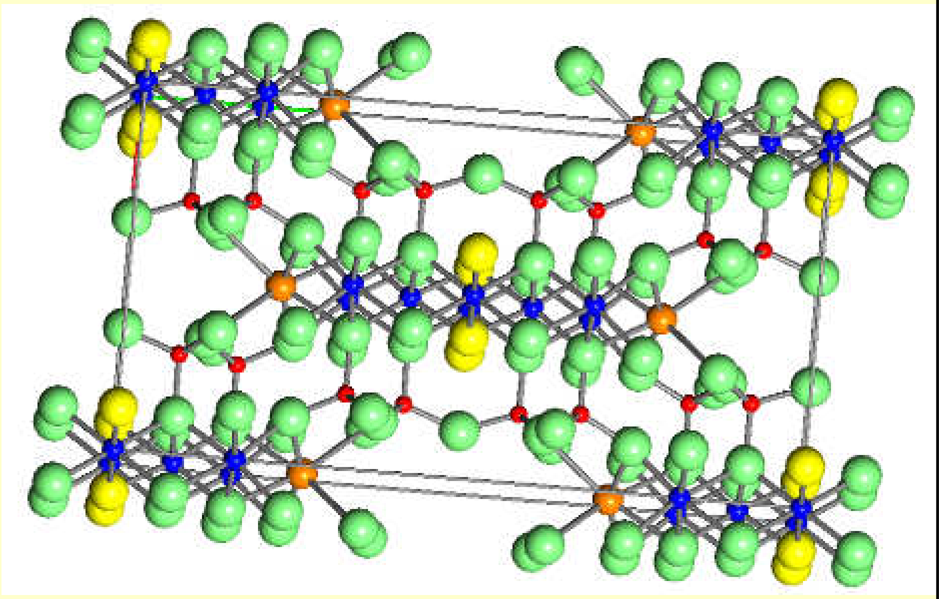

3000-4000 cm^{-1}

Vibrational modes of OH groups

MINERAL CARACTERIZATION
Asbestos & other harmful fibrous minerals

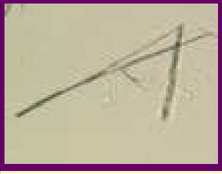

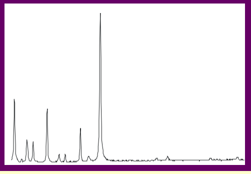

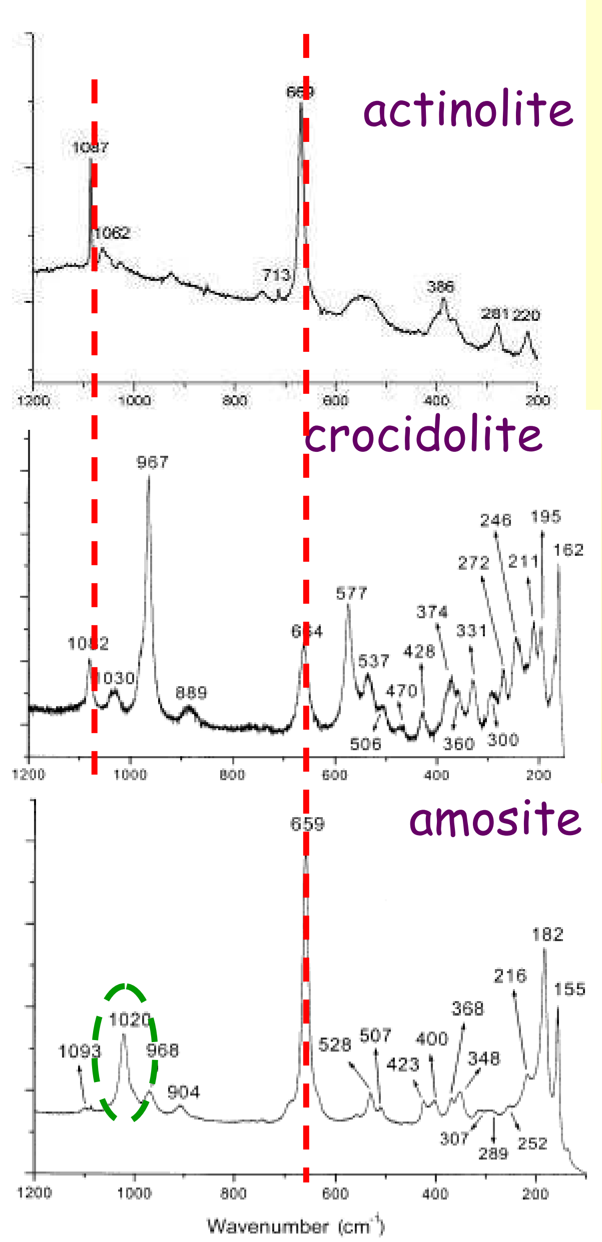

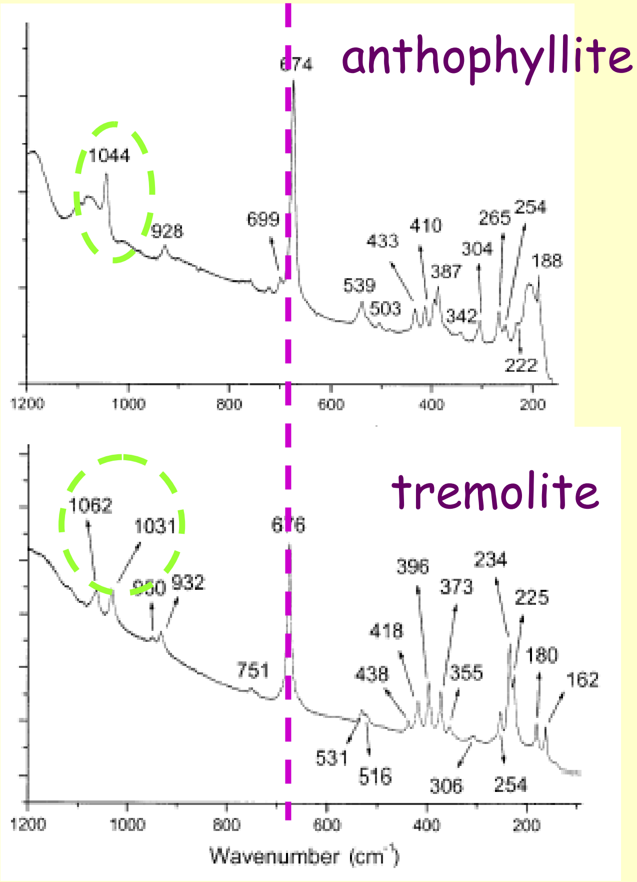

IDENTIFICATION

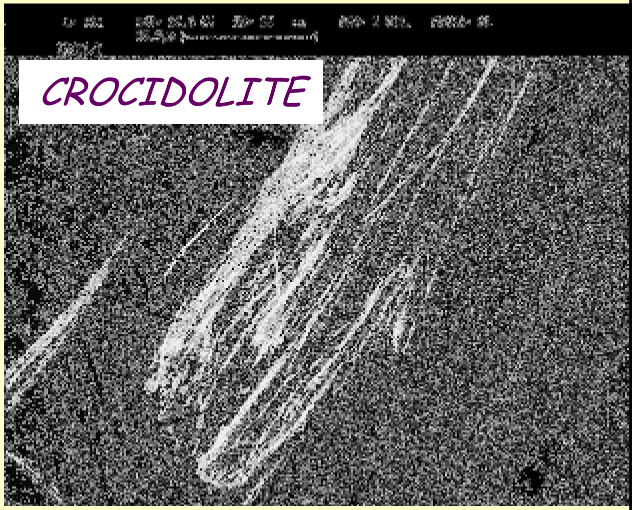

*Rinaudo et al. (2004) – Mineralogical Magazine, **68**, 455-465*

	Act	Croc	Amos	Anth	Tr
symmetric Si-O_b-Si stretching vibrations	669	664	658	674	676
antisymmetric Si-O_b-Si stretching vibrations	1087	1082	1020	1044	1062

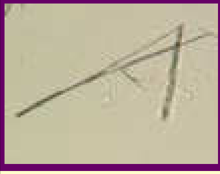

MINERAL CARACTERIZATION
Asbestos & other harmful fibrous minerals

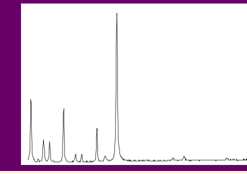

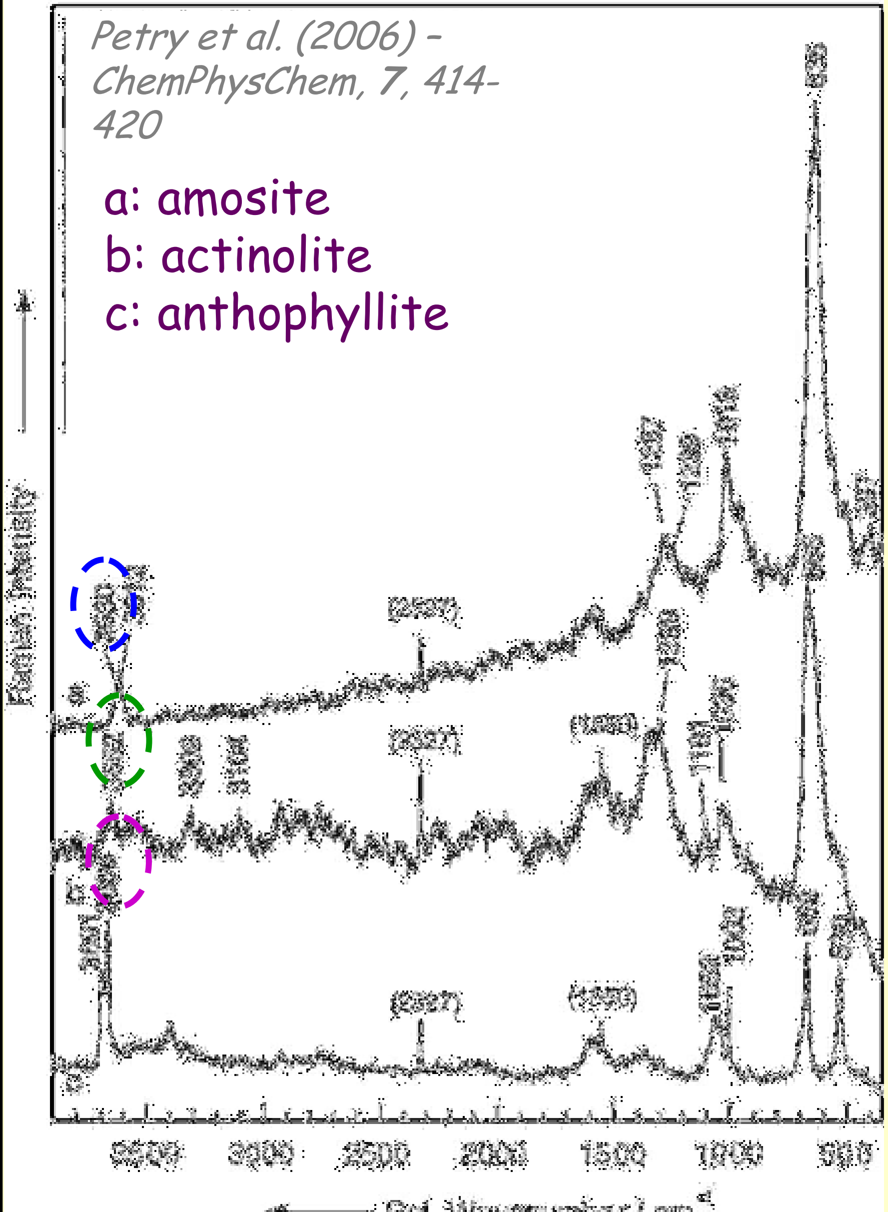

IDENTIFICATION

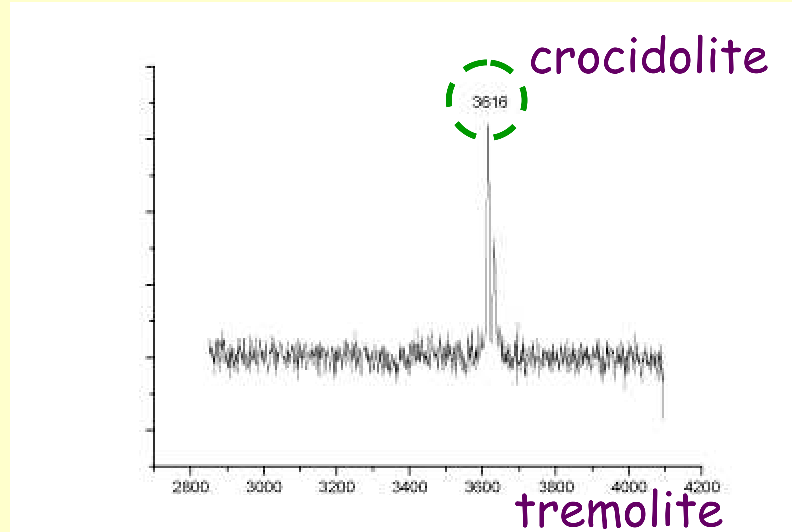

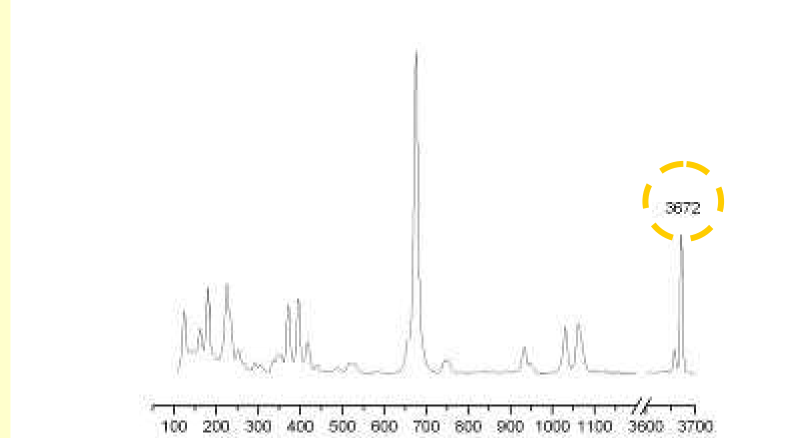

Ferrando, Turci

	Act	Croc	Amos	Anth	Tr
OH vibrations	3652	3616	3630	3666	3672

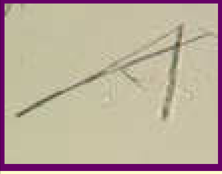

MINERAL CARACTERIZATION
Sedimentology

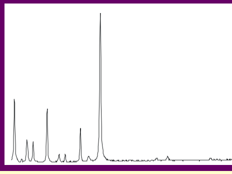

Gypsum with filamentous fossils. The Raman identification of the minerals phases included indicates that they probably are sulfide-oxidizing bacteria

Dela Pierre et al. (2015) - Geology, 42, 855-858

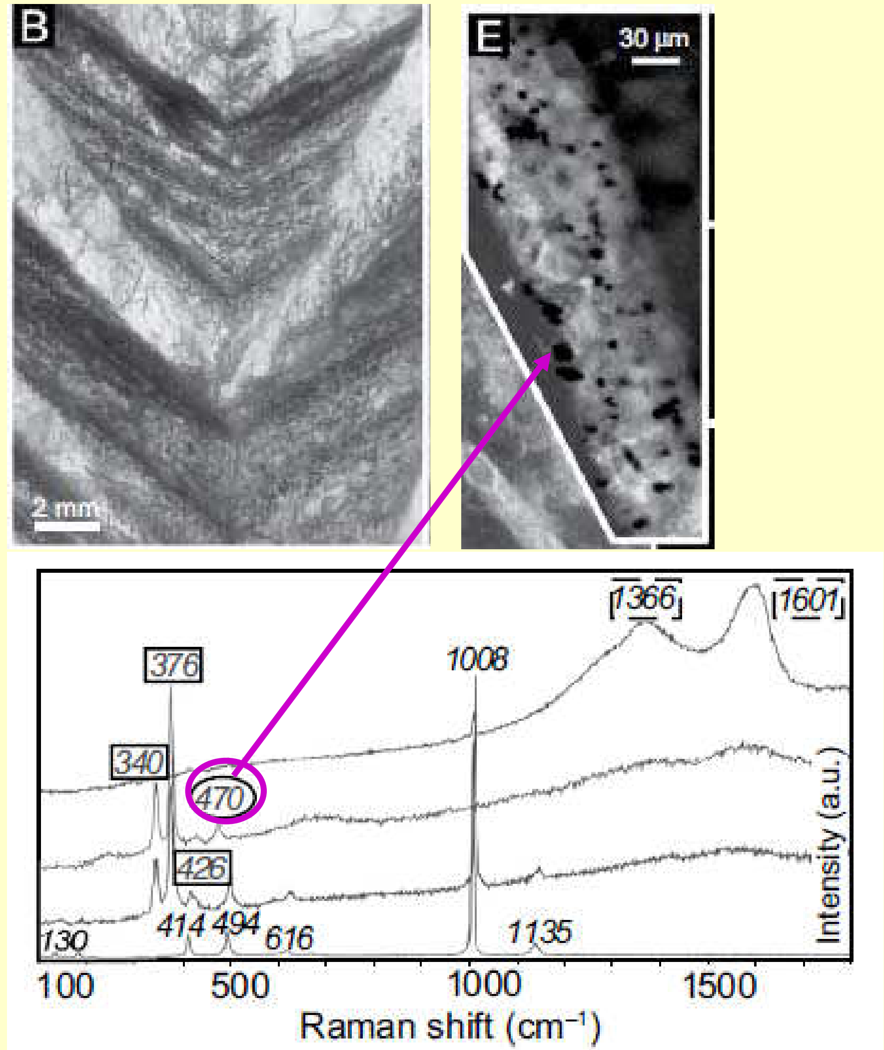

Figure 3. From the bottom to the top, Raman spectra of gypsum with filaments, pyrite (rectangles), pyrite with polysulfide (circle), and carbonaceous material (dotted rectangles).

Modern sulfur bacteria: presence of zero-valent sulfur globules stored within membrane-bounded vesicles

The presence of polysulfide (S_n^{-2}) may represents remnant of elemental sulfur stored by the bacteria. The other S reacted with Fe and forms pyrite

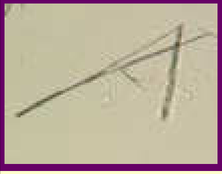

MINERAL CARACTERIZATION
Polymorph & allotrope

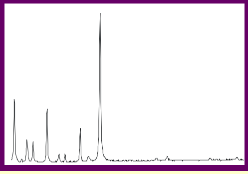

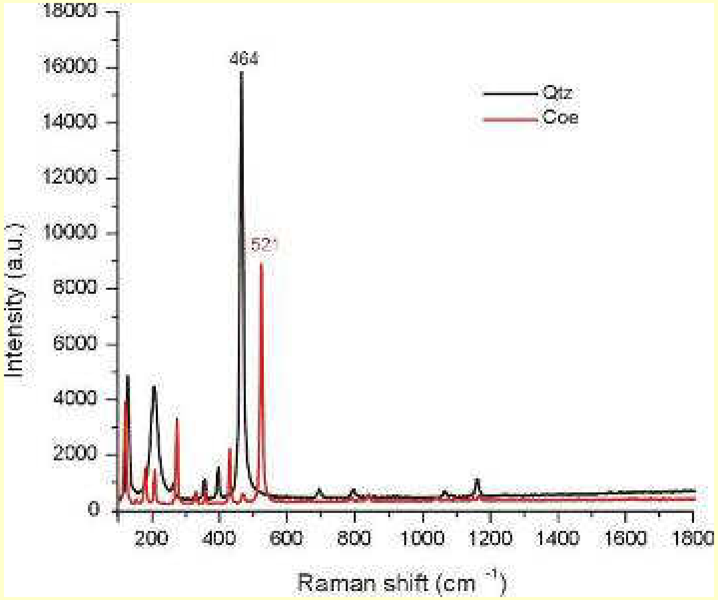

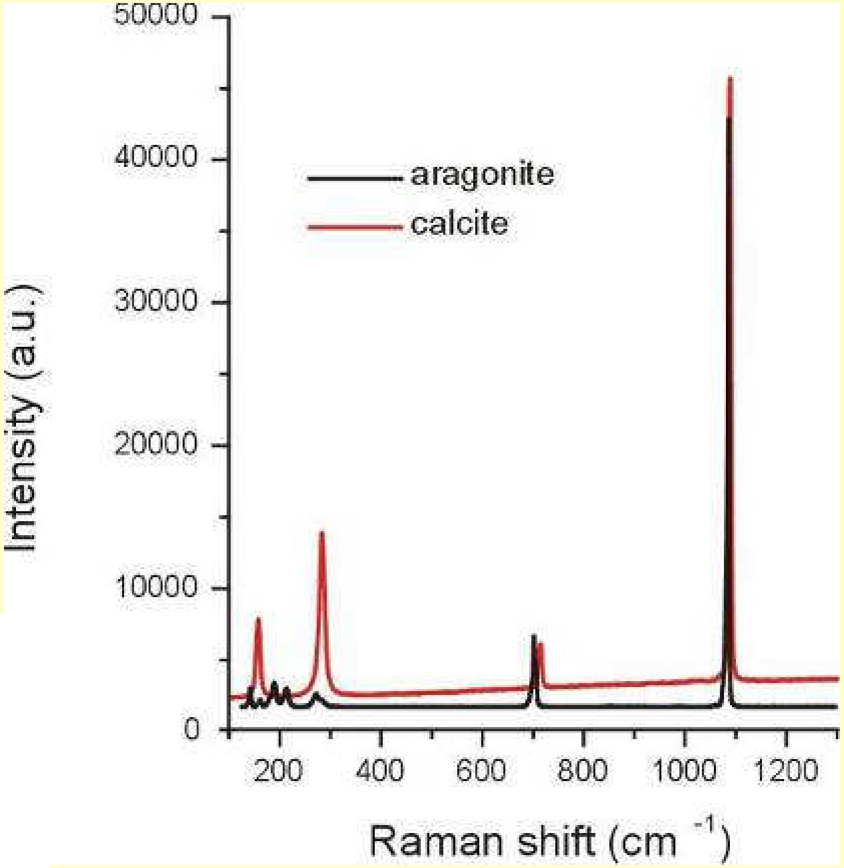

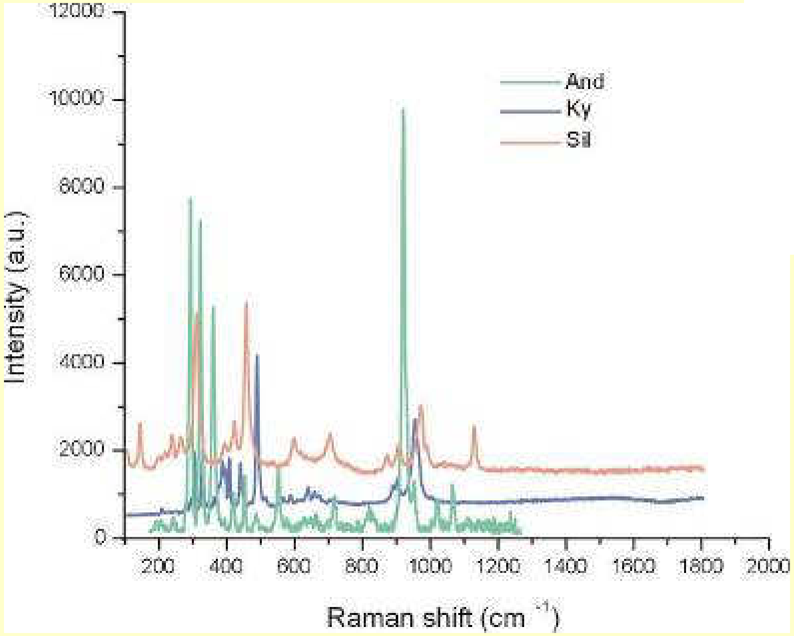

Ferrando

MINERAL CARACTERIZATION
Polymorph & allotrope

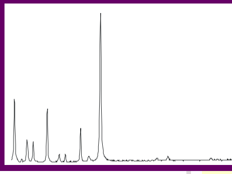

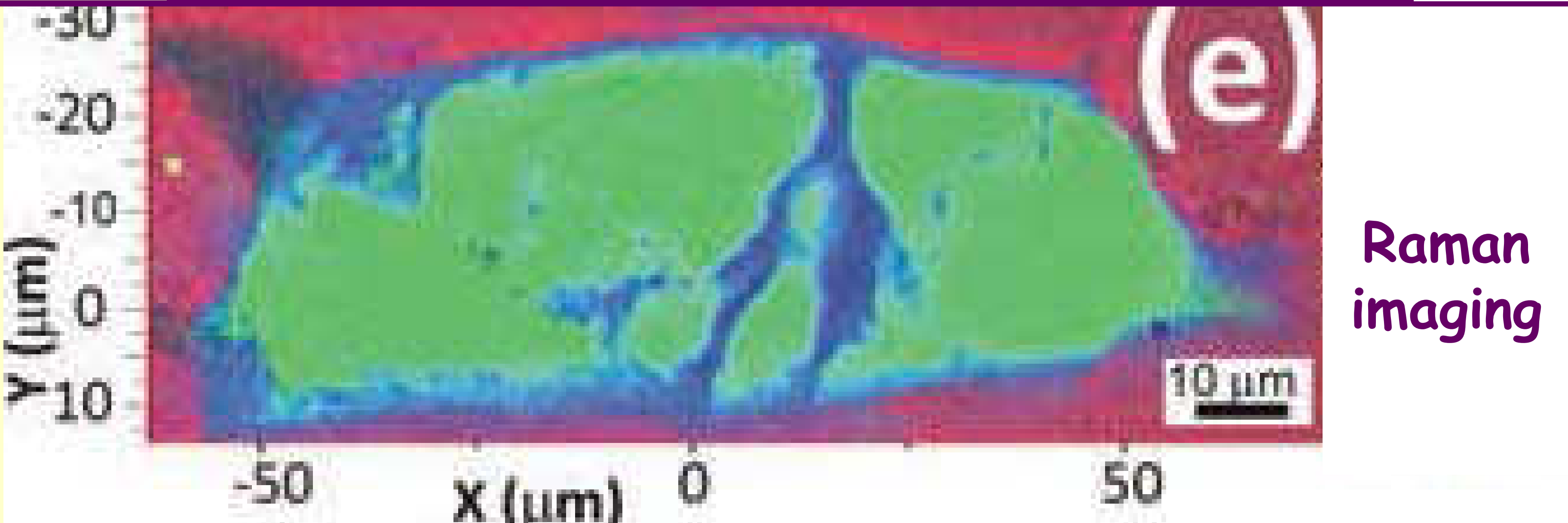

Raman imaging

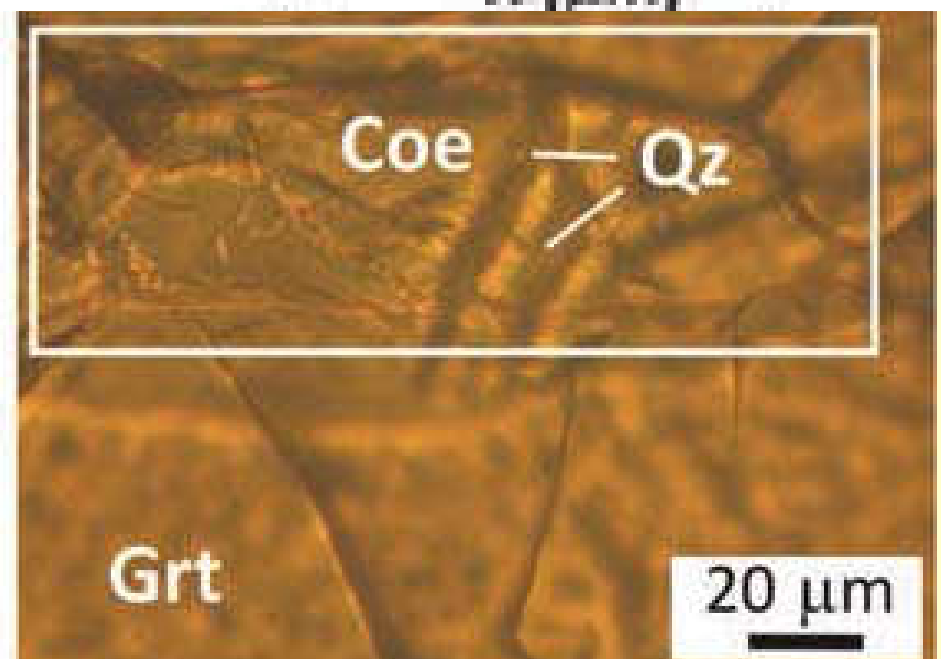

Green: coesite
Blue: quartz
Red: garnet

Groppo et al. (2016) - Eur. J. Mineral., 28, 1215-1232

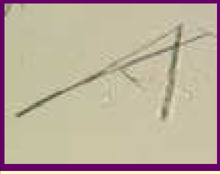

MINERAL CARACTERIZATION
Polymorph & allotrope

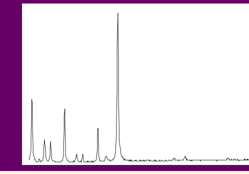

MAIN CARBON PHASES

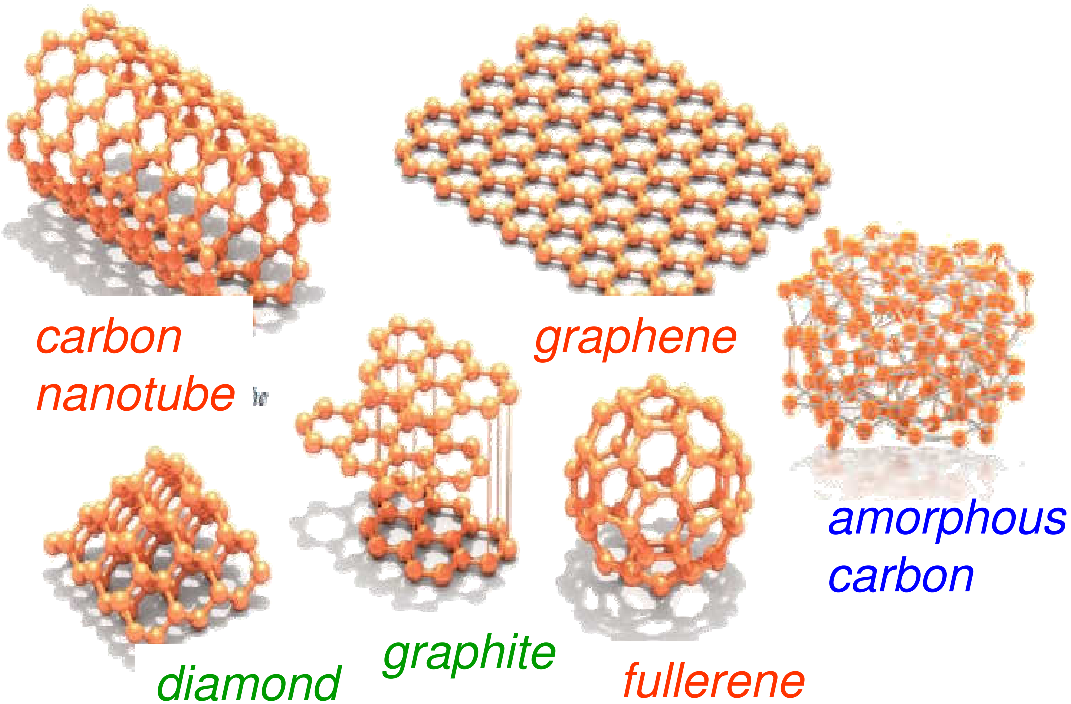

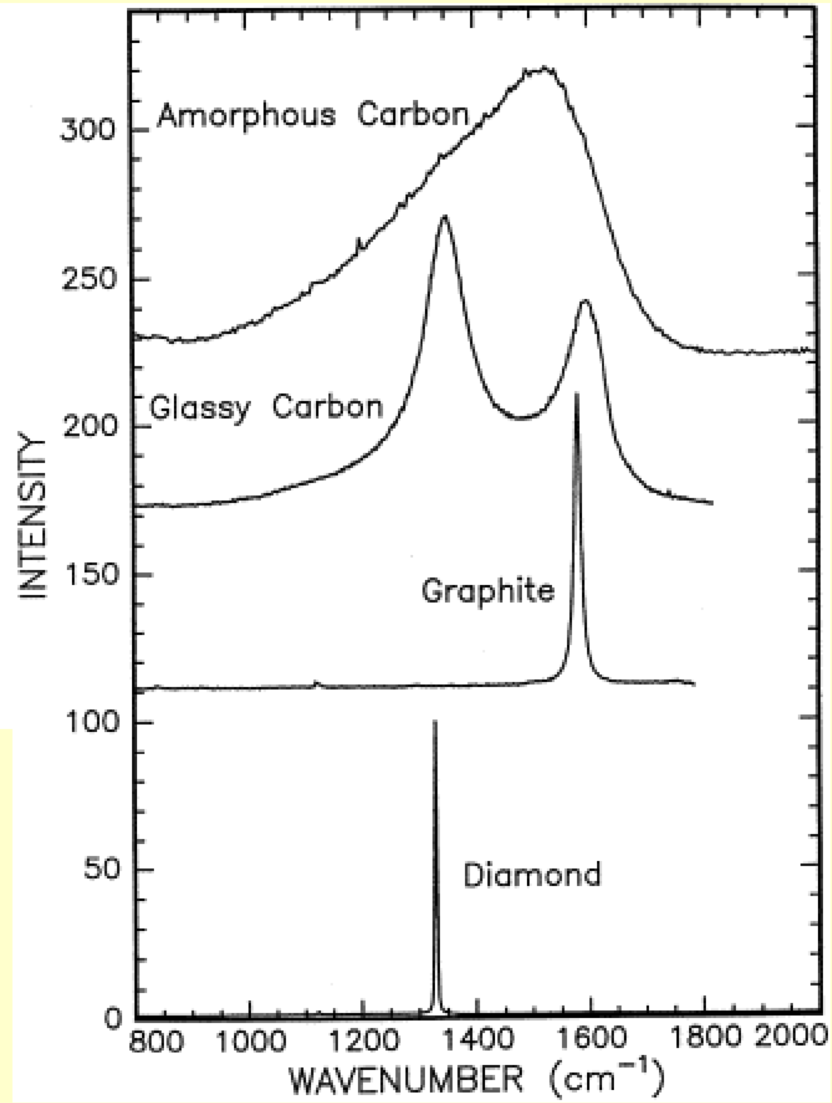

Green: crystalline C phases
Blue: disordered C phases
Red: molecular C phases

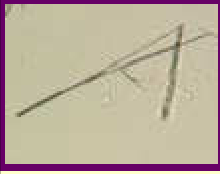

MINERAL CARACTERIZATION
Polymorph & allotrope

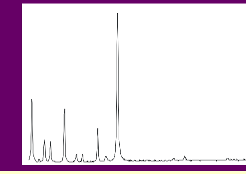

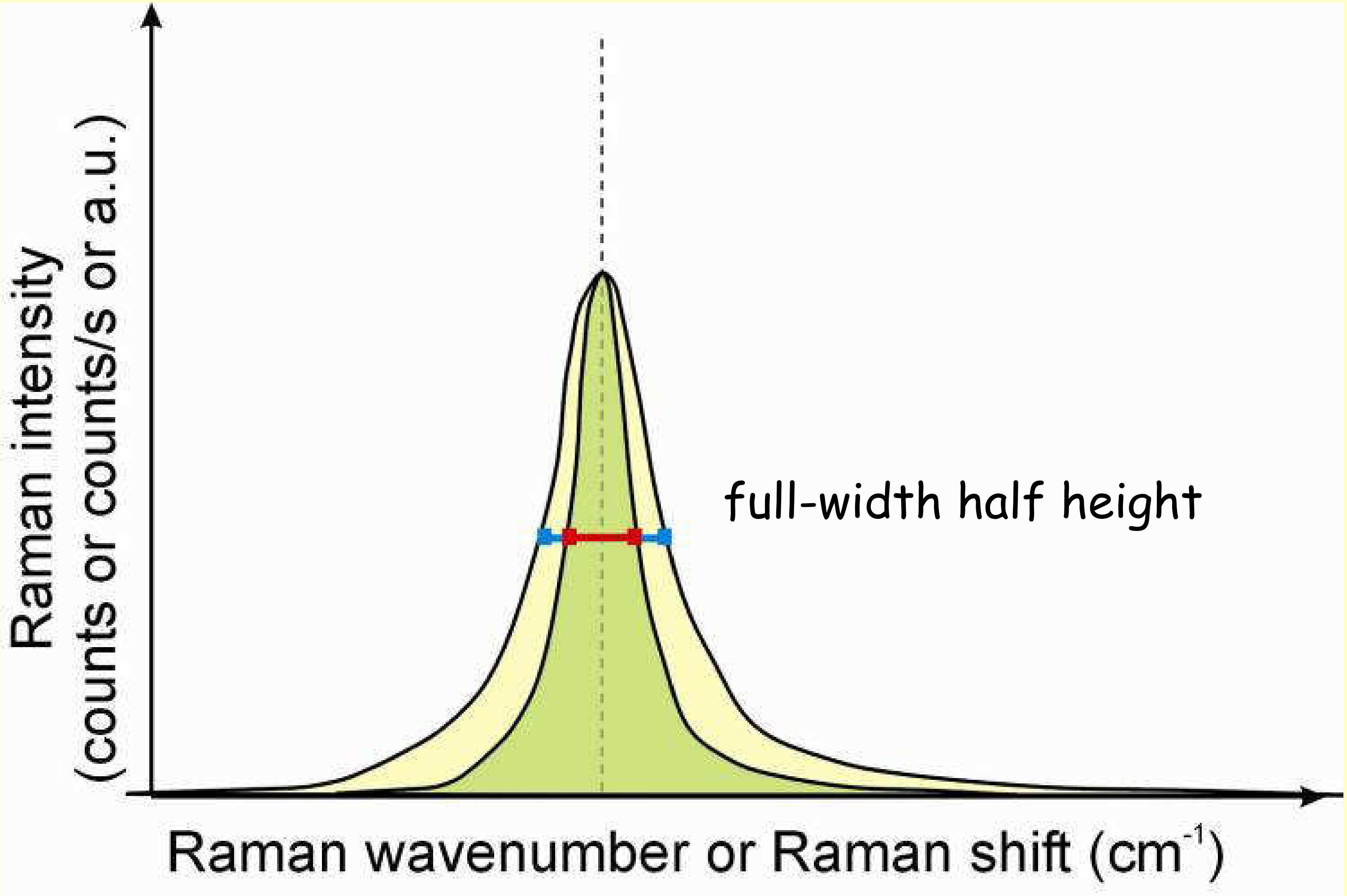

The **bandwidth** increases increasing disorder at the bond scale

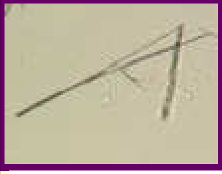

MINERAL CARACTERIZATION
Polymorph & allotrope

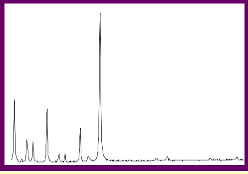

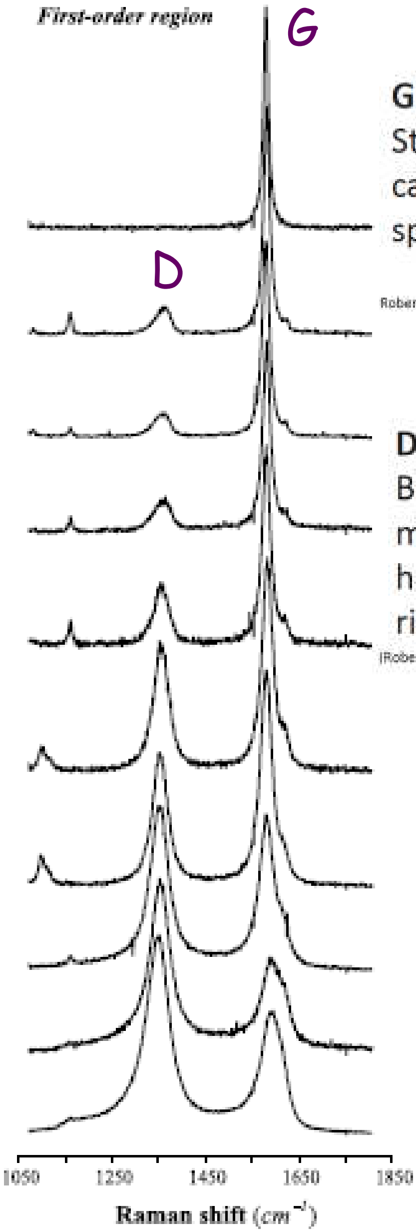

G band
Stretching of carbon-carbon sp^2 bonds

Robertson 2002)(Ado *et. al.* 2010)(Gupta *et. al.* 2008)

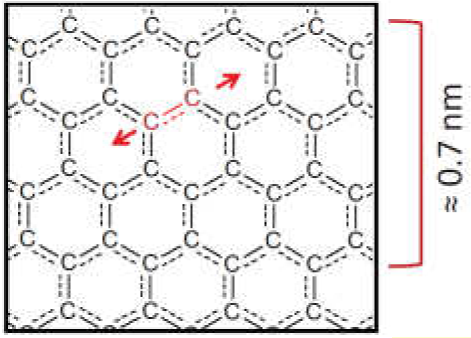

D band
Breathing mode of hexagonal rings

Only seen in Raman spectrum if ring is close (< 10 nm) to sheet edge or other defect

(Robertson 2002)(Ado *et. al.* 2010)(Gupta *et. al.* 2008)

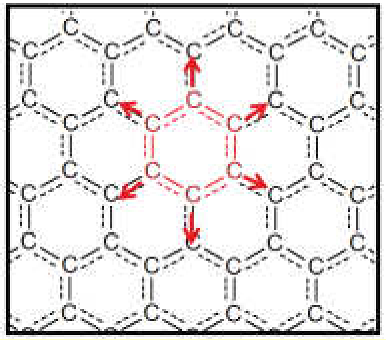

G band 1582 cm^{-1}: related to sp^2 bonds in crystalline carbon

D band 1357 cm^{-1}: is related to a lost of symmetry

Geothermometry of metamorphic graphite

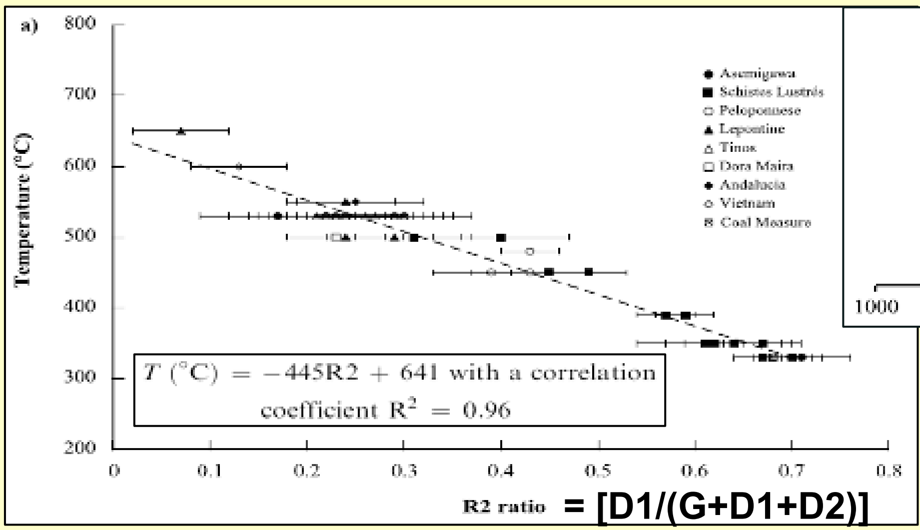

= [D1/(G+D1+D2)]

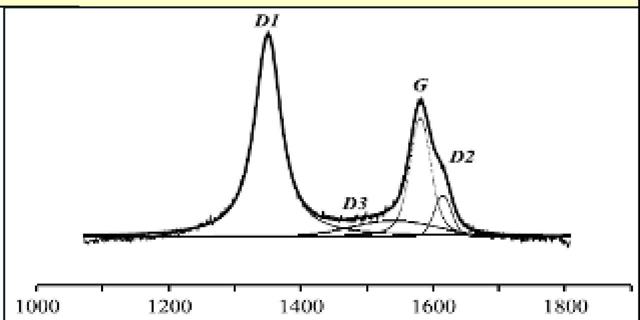

Beyssac et al. (2002) – J. Metam. Geol., 20, 859-871

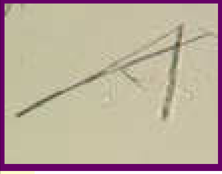

MINERAL CARACTERIZATION
Polymorph & allotrope

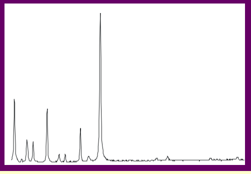

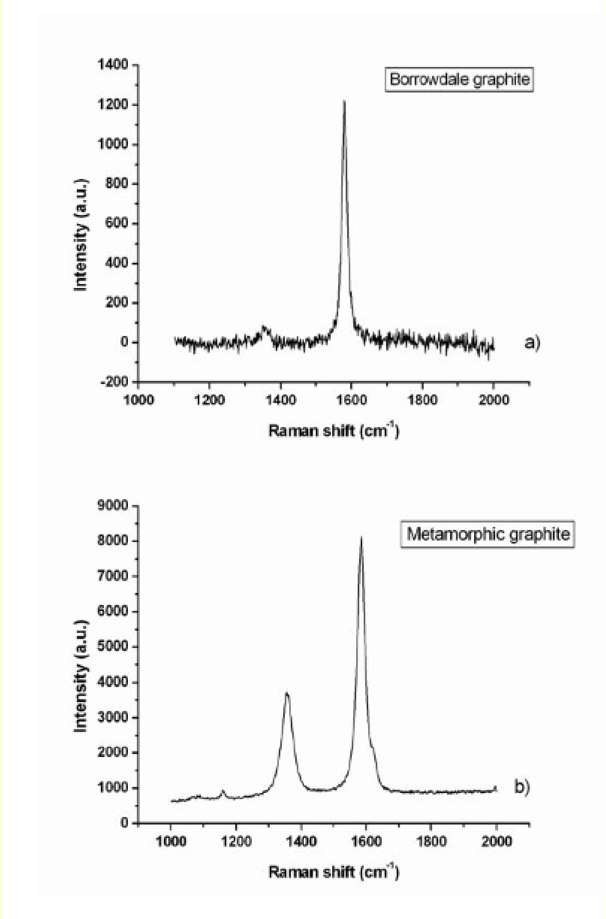

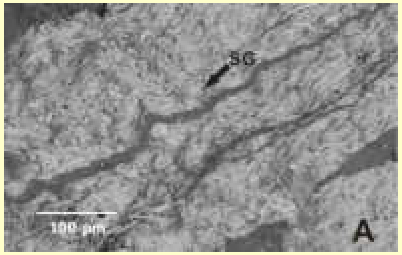

CAUTION

Highly crystalline graphite can precipitate from moderate-T fluids

In the Borrowdale deposit (UK), graphite-epidote intergrowths show that fully ordered graphite precipitated during the propylitic hydrothermal alteration of the volcanic host rocks at temperatures of ~500 °C at FMQ redox conditions.

Luque et al. (2007) - Geology, 37, 275-278

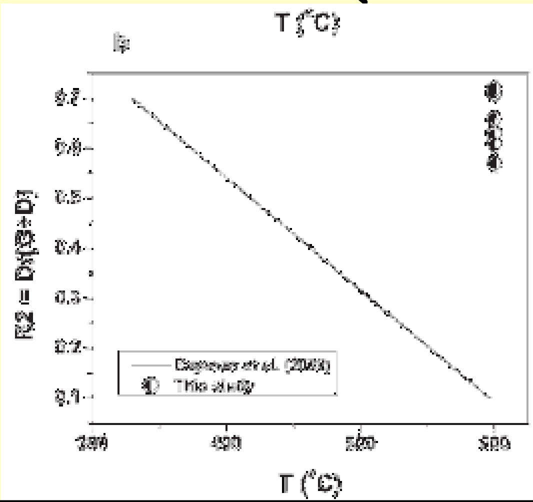

"…the existing Raman geothermometers appear inadequate to address graphite formation under conditions of *metastable equilibria..:"*

Foustoukos (2012) - Am. Mineral., 97, 1373-1380

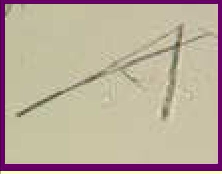

MINERAL CARACTERIZATION
Solid inclusions in minerals

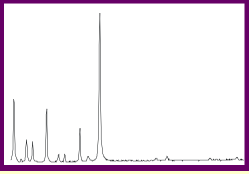

Metamorphic mineral assemblage within zoned zircon

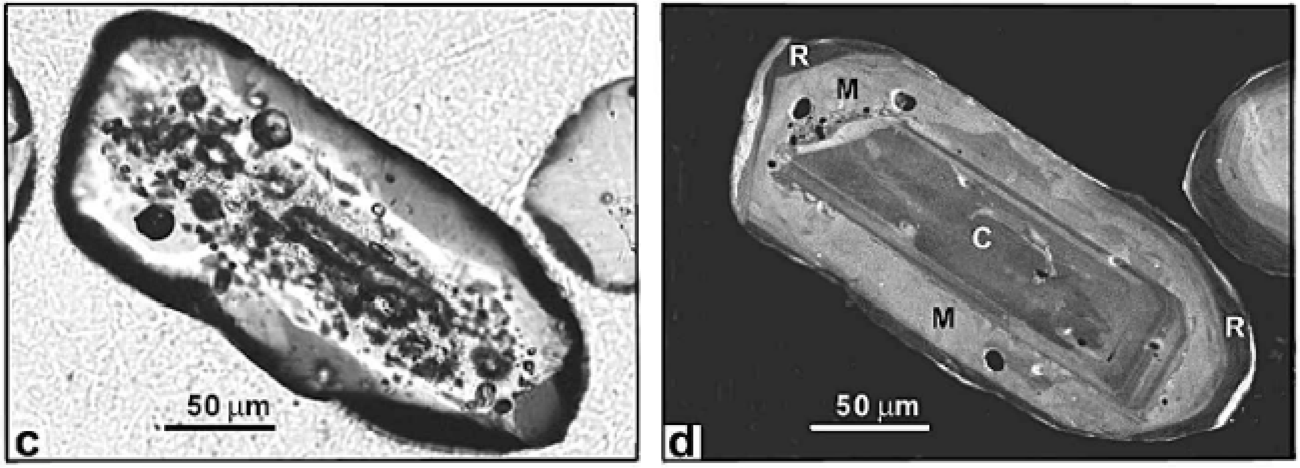

The identification of solid inclusions in zircon allows to characterize the metamorphic evolution of the hosting rock.

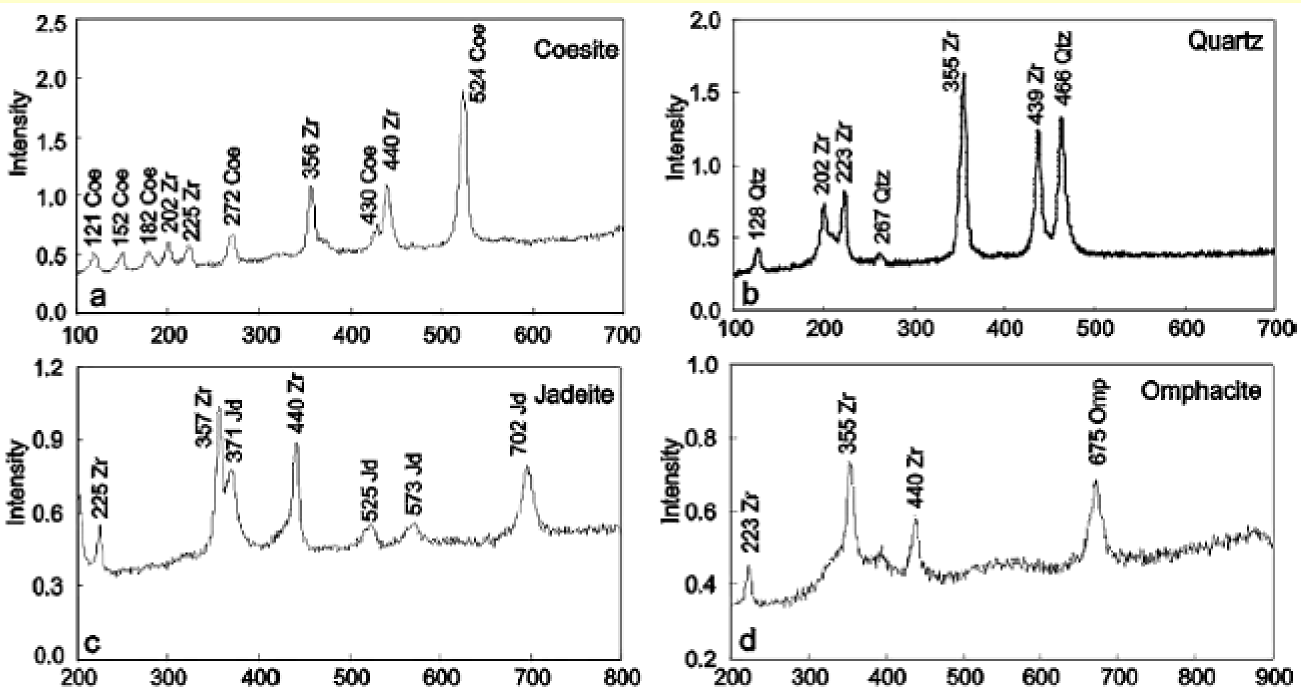

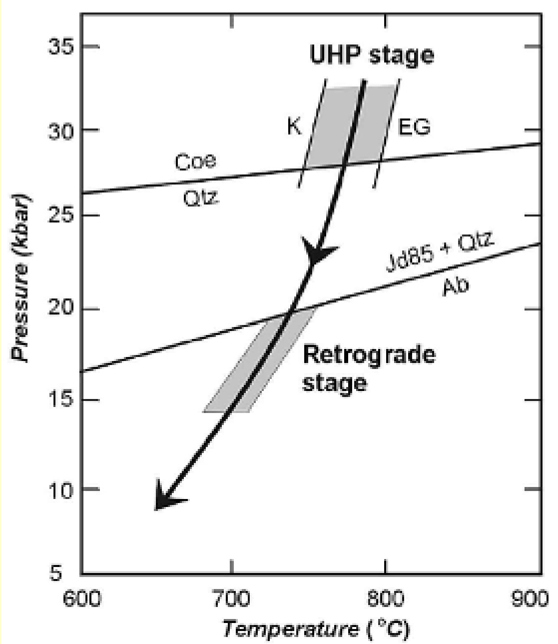

Liu et al. (2002) – Eur. J. Mineral., 14, 499-512

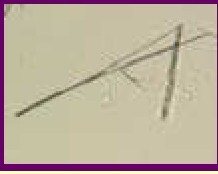

MINERAL CARACTERIZATION
Solid inclusions in minerals

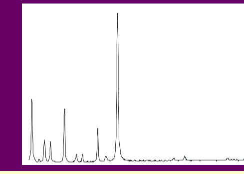

Bandshift

A **compression stress** reduces the distance between two, or more, atoms, leading to an increase of the vibrational frequency (shift towards **higher wave numbers**). A **tensile stress** increases the distance, leading to a decrease of the vibrational frequency (shift toward **lower wave numbers**)

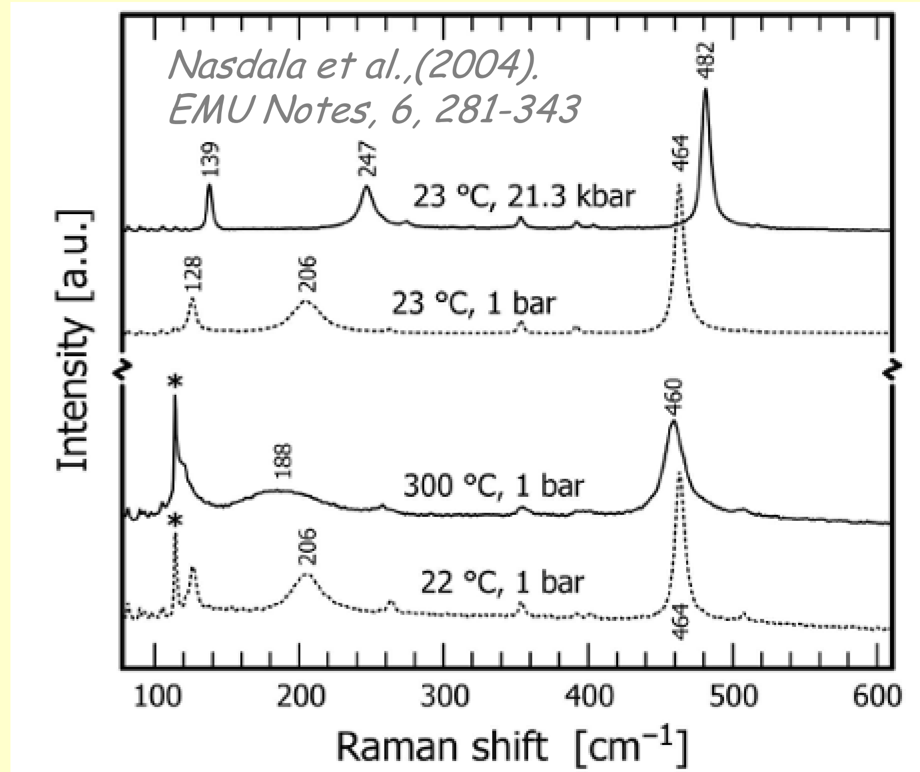

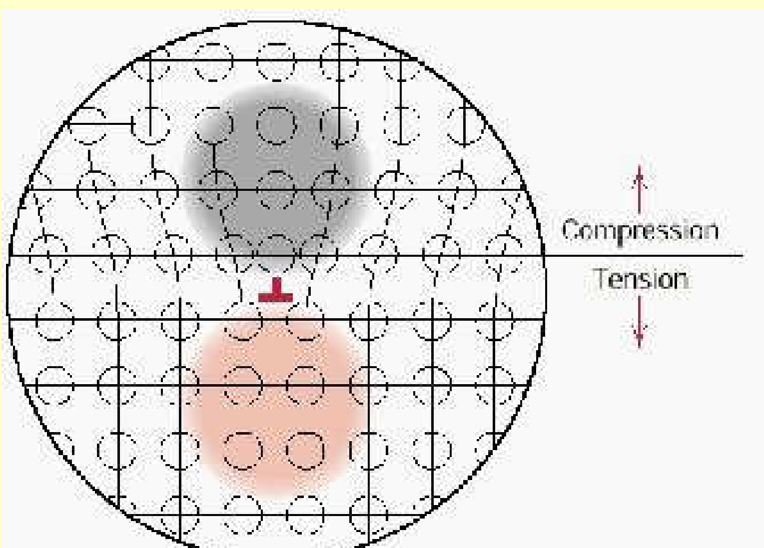

If the deformation of the structure shows elastic behavior the shift will vary linearly with the stress amplitude. Thus the Raman band position can be used to quantify stress.

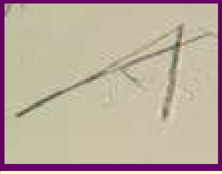

MINERAL CARACTERIZATION
Solid inclusions in minerals

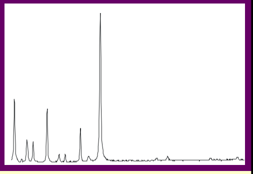

Quartz geobarometer

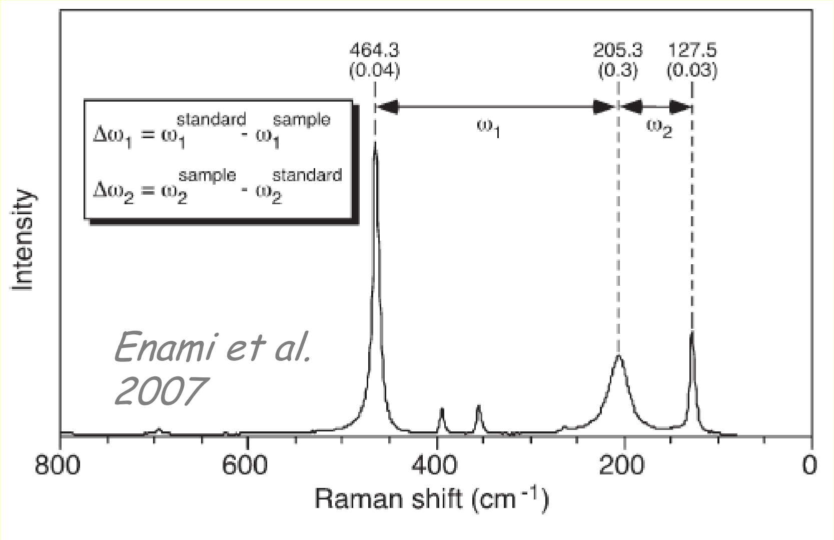

In garnet

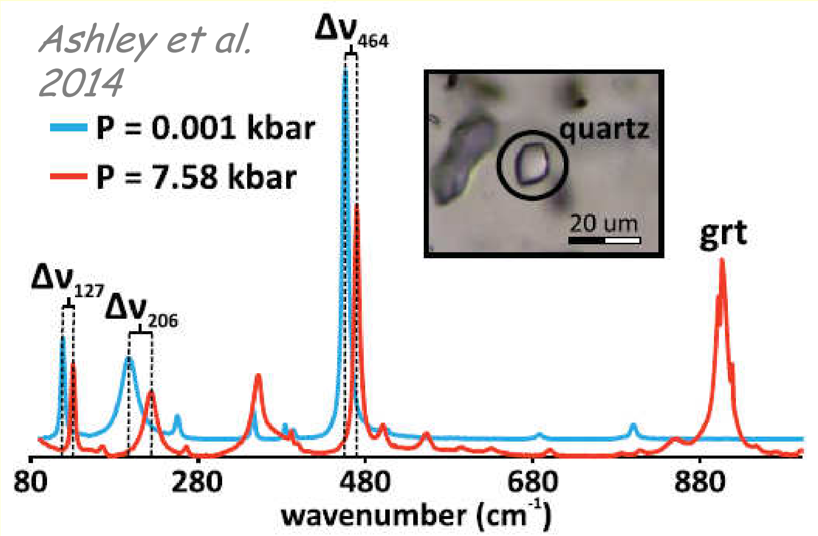

$CaSiO_3$-walstromite

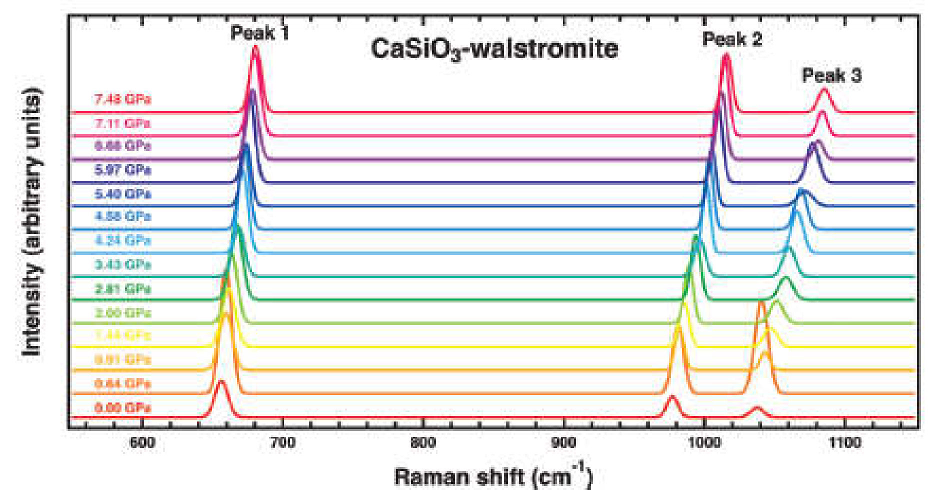

In diamond

Anzolini et al. (2018) – Am. Mineral., ***103****, 69-74*

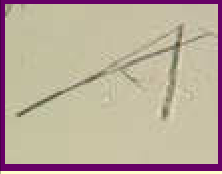

MINERAL CARACTERIZATION
Mineral composition

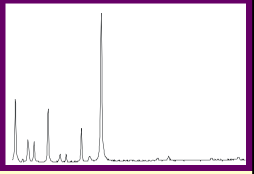

Variation in band position is due to substitutional atoms in the crystalline lattice → **variation in chemical composition**

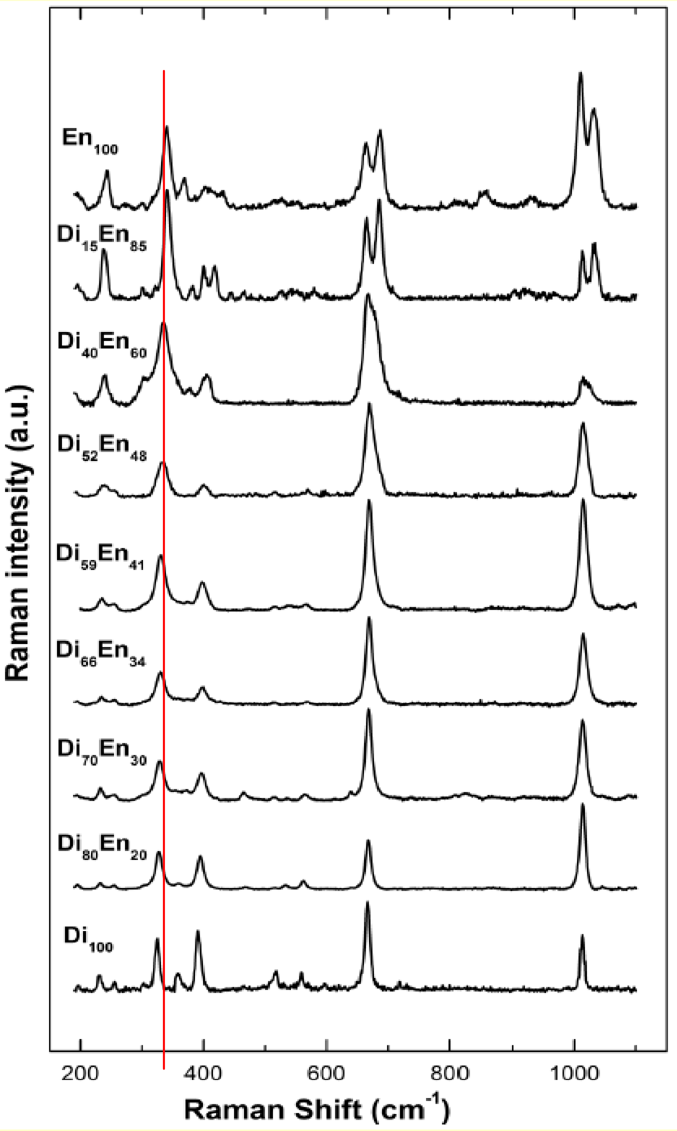

Tribaudino et al. (2012) - Am Mineral., 97, 1339-1347

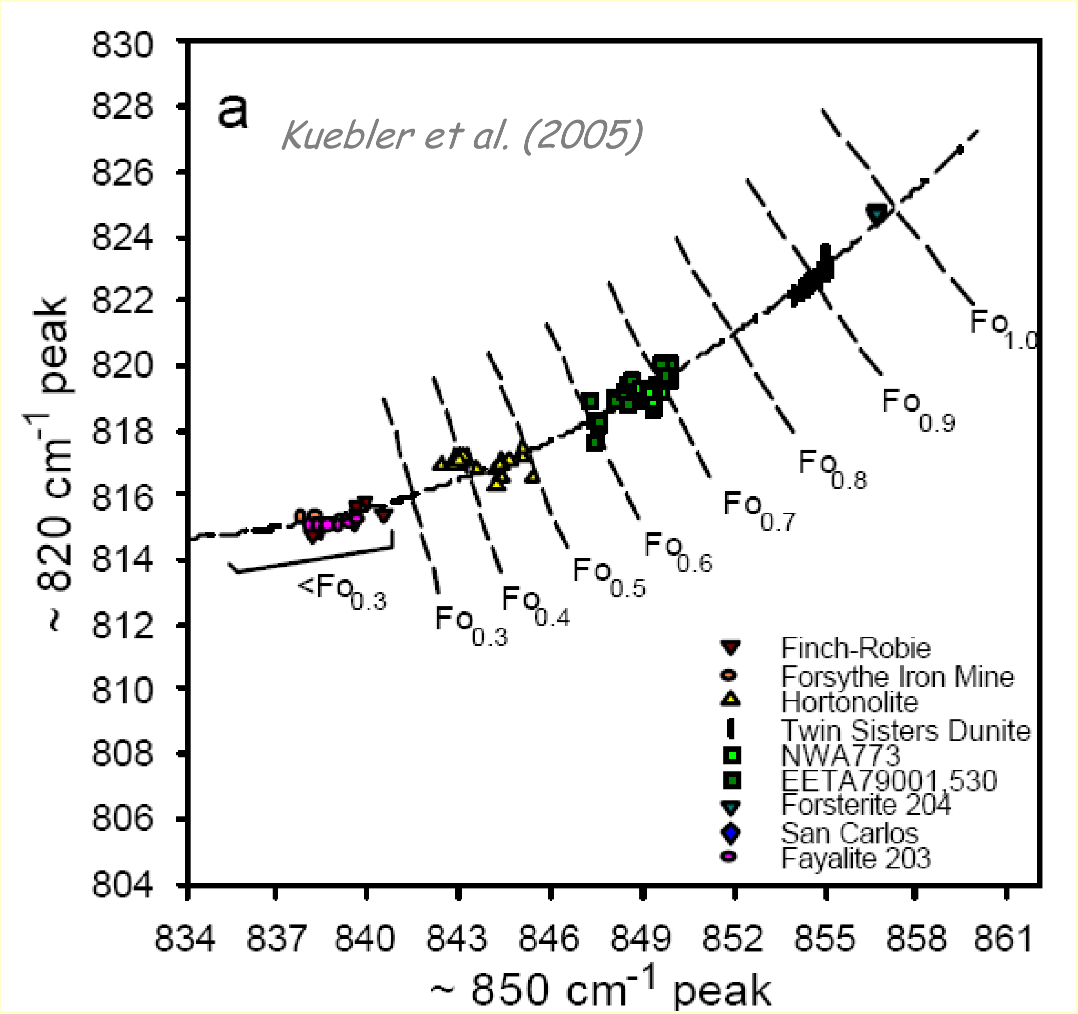

MINERAL CARACTERIZATION
Mineral composition

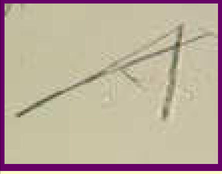

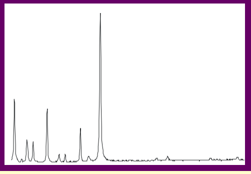

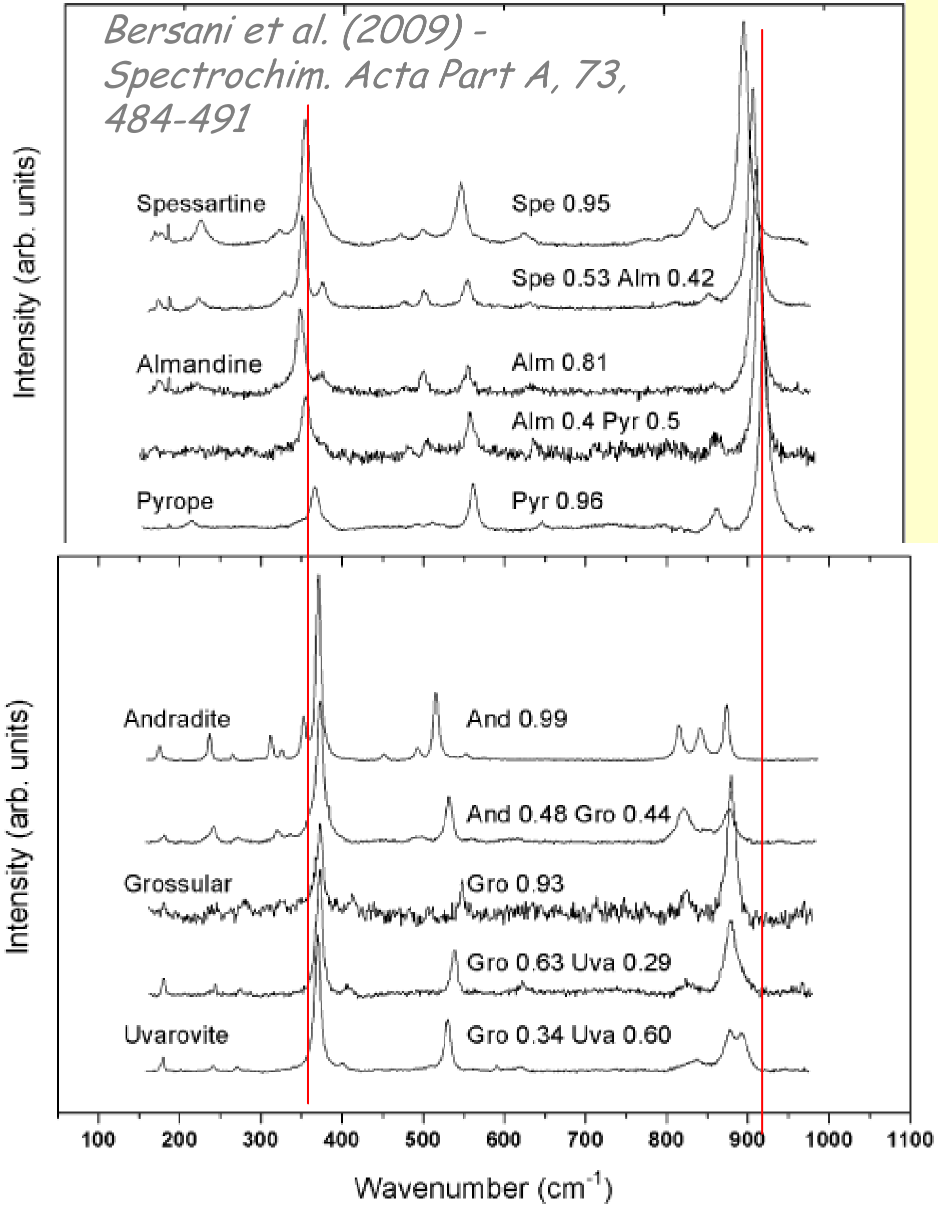

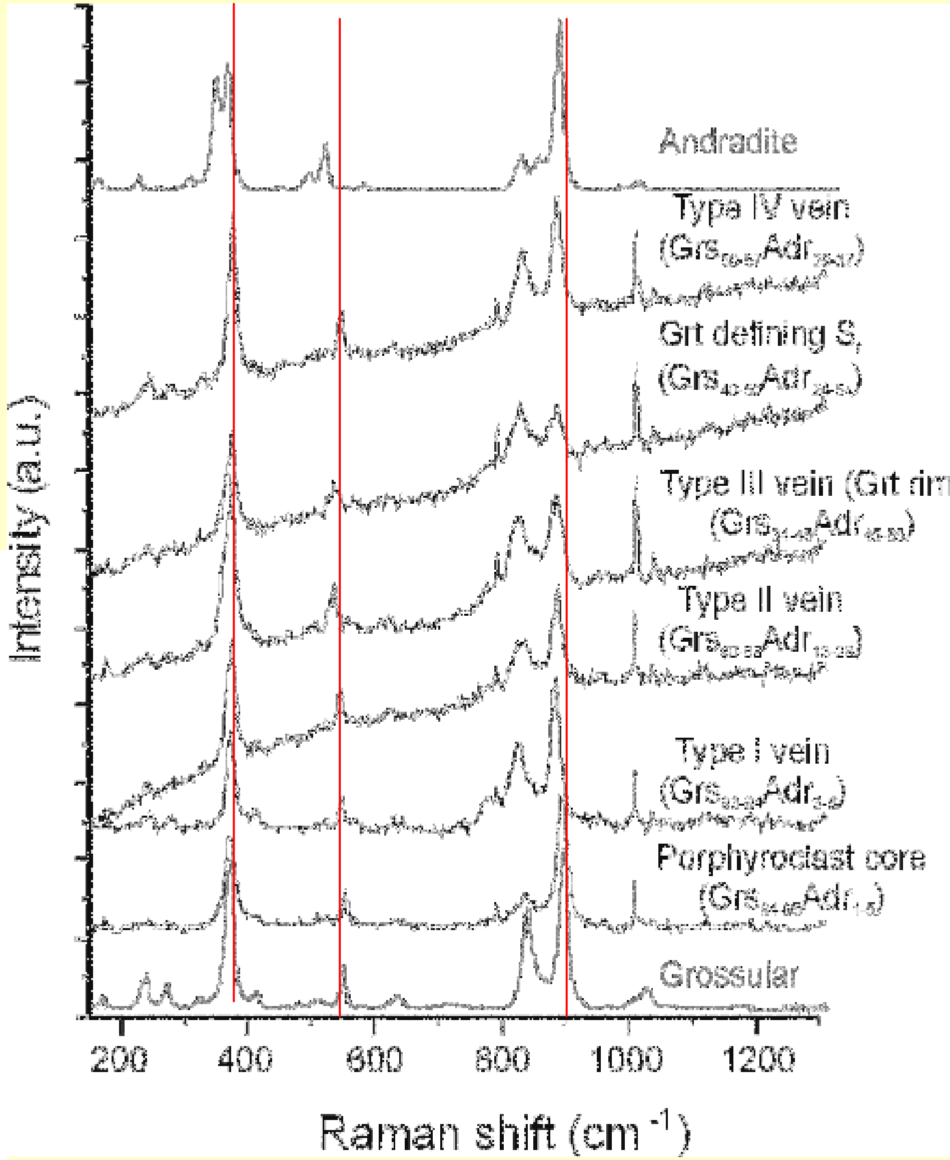

Ferrando et al. (2010) - Int. Geol. Rev., 52, 1220-1243

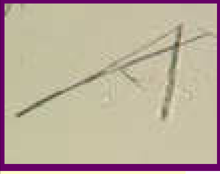

MINERAL CARACTERIZATION
Characterization of new minerals

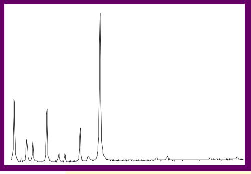

Mineralogical Magazine, April 2017, Vol. 81(2), pp. 305–317

As-bearing new mineral species from Valletta mine, Maira Valley, Piedmont, Italy: III. Canosioite, $Ba_2Fe^{3+}(AsO_4)_2(OH)$, description and crystal structure

F. Cámara[1,2], E. Bittarello[1,2], M. E. Ciriotti[3], F. Nestola[4], F. Radica[5], F. Massimi[6], C. Balestra[7] and R. Bracco[8]

Fig. 1. Reddish-brown granules or subhedral crystals of canosioite on calcite (Field of view = 5 mm)

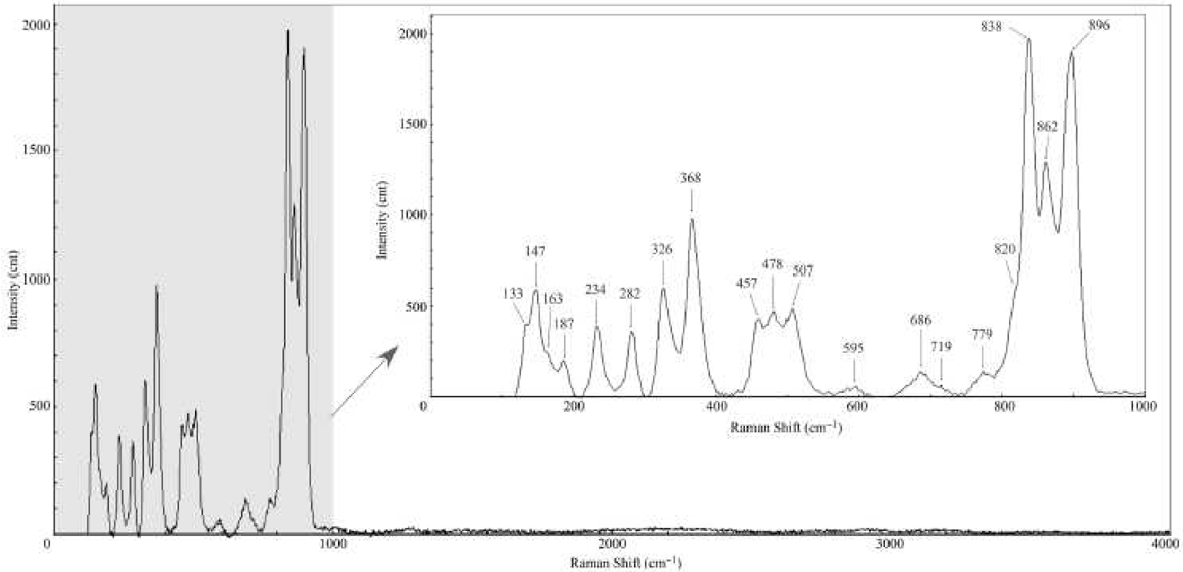

Fig. 3. Raman spectra of canosioite showing the 100–4000 cm^{-1} range and the region between 100 and 1200 cm^{-1} enlarged.

Fluid inclusions characterization

FLUID INCLUSIONS

Fluid inclusions (FI): small cavities (1-50 micron) containing tiny volumes of mobile volatile-rich phases trapped in minerals during, or after their growth → represent remnants of palaeo-fluids present in the system.

The fluid phase may be liquid or vapor, and may include aqueous solutions, volatiles, minerals precipitated, liquid hydrocarbons.

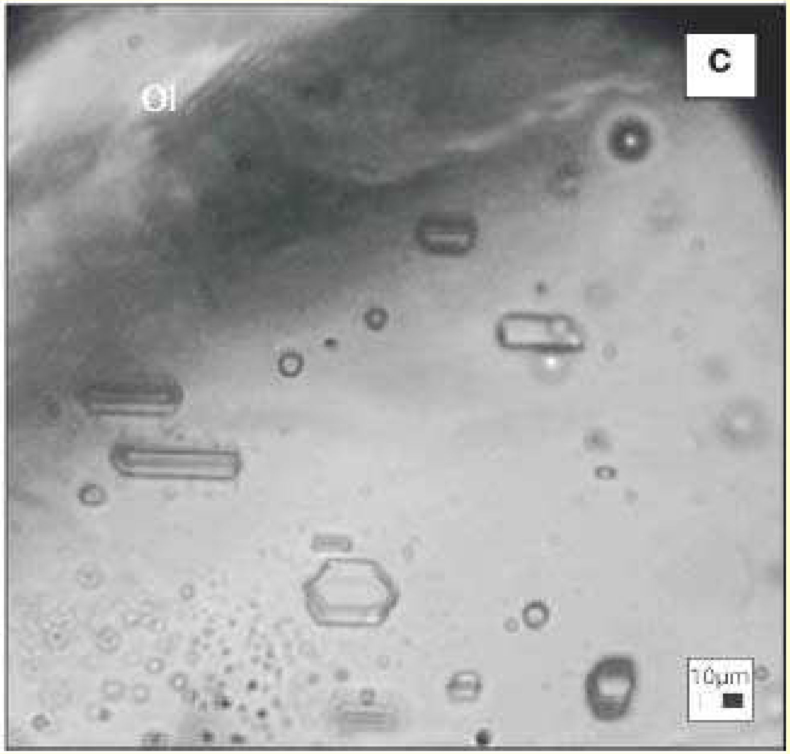

*Oglialoro et al. (2017)–Bull. Volcanol., **79**, 70*

Raman microspectroscopy is a highly suitable method:
- performing in situ spot analyses of ca. 1 µm
- data on the liquid, vapor and solid phases

FLUID INCLUSIONS

Main vibrational regions in fluid inclusions

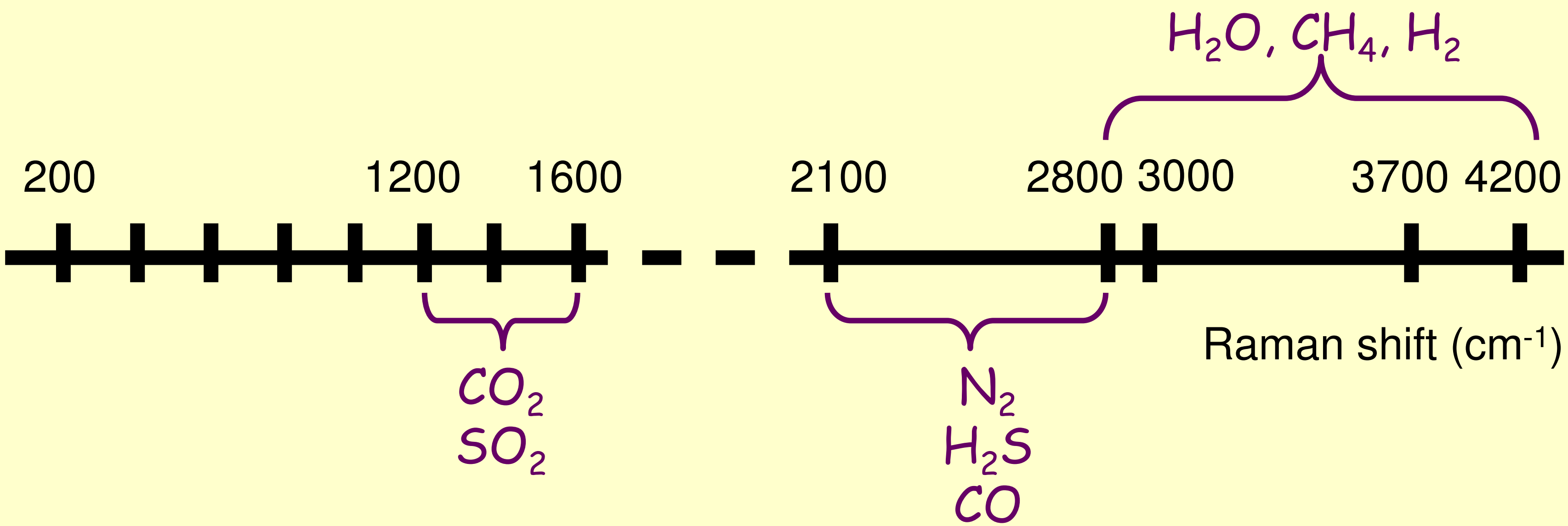

FLUID INCLUSIONS
Daughter or incidentally trapped minerals

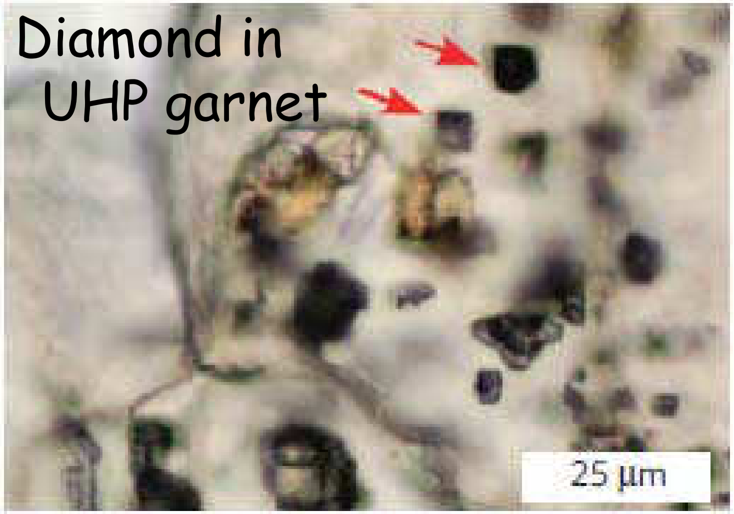

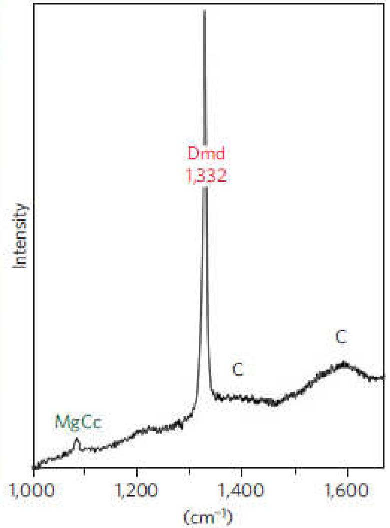

Frezzotti et al. (2012) - Nature Geoscience

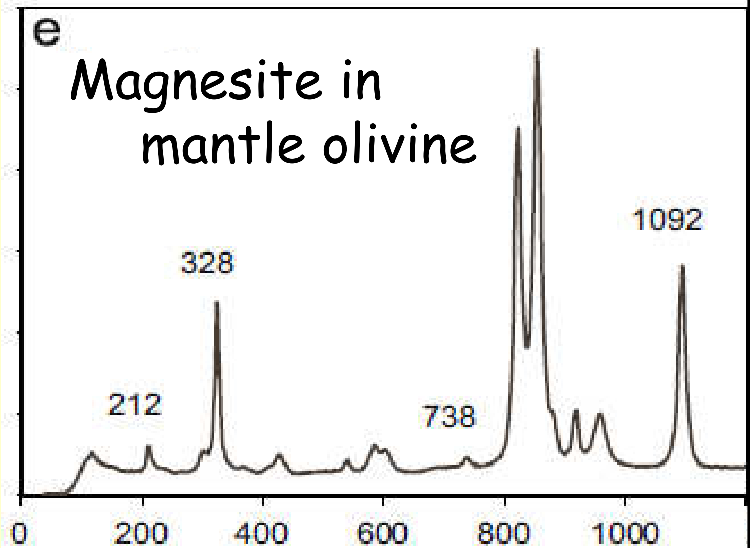

Frezzotti et al. (2012)- EPSL, 351-352, 70-83

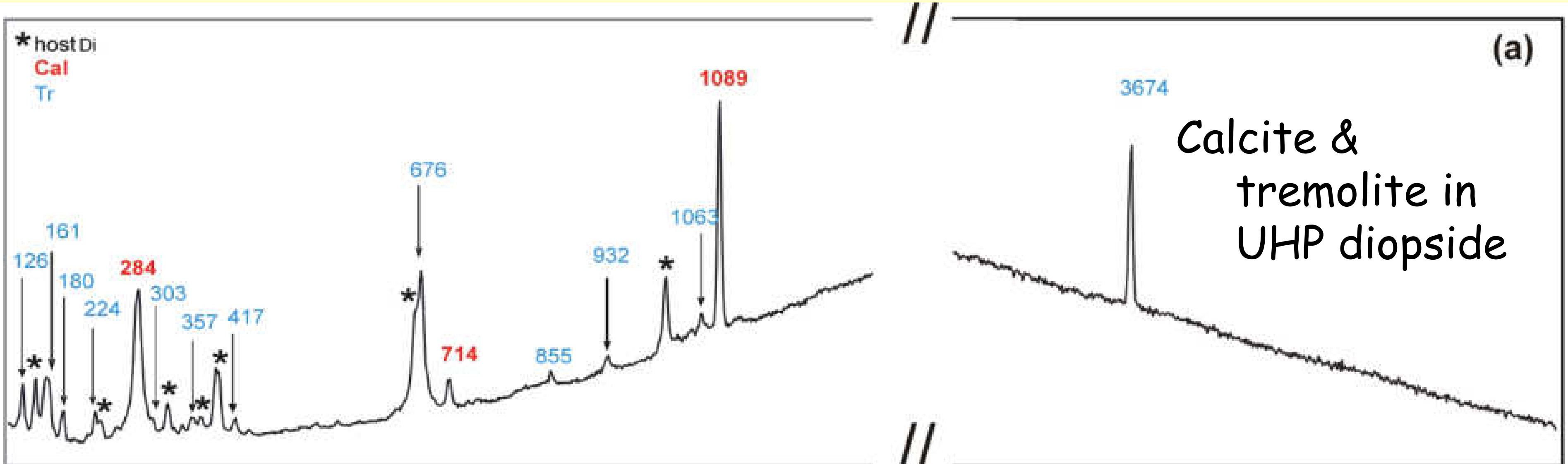

Ferrando et al. (2017) - Am. Mineral, 102, 42-60

FLUID INCLUSIONS
Daughter or incidentally trapped minerals

Raman maps

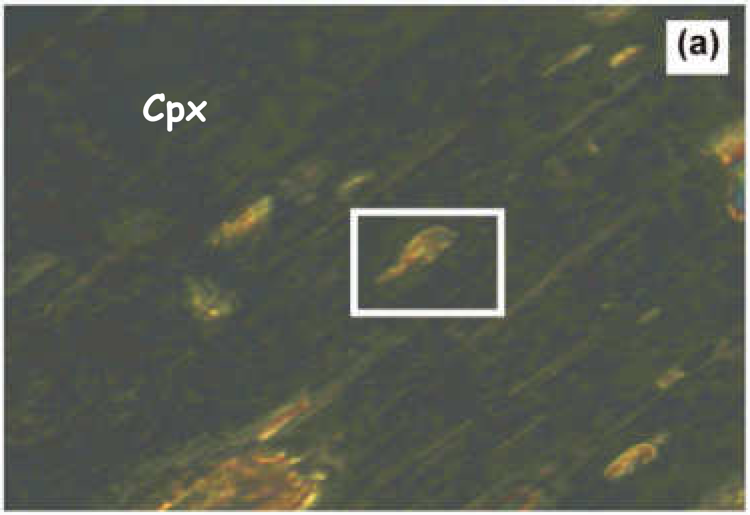

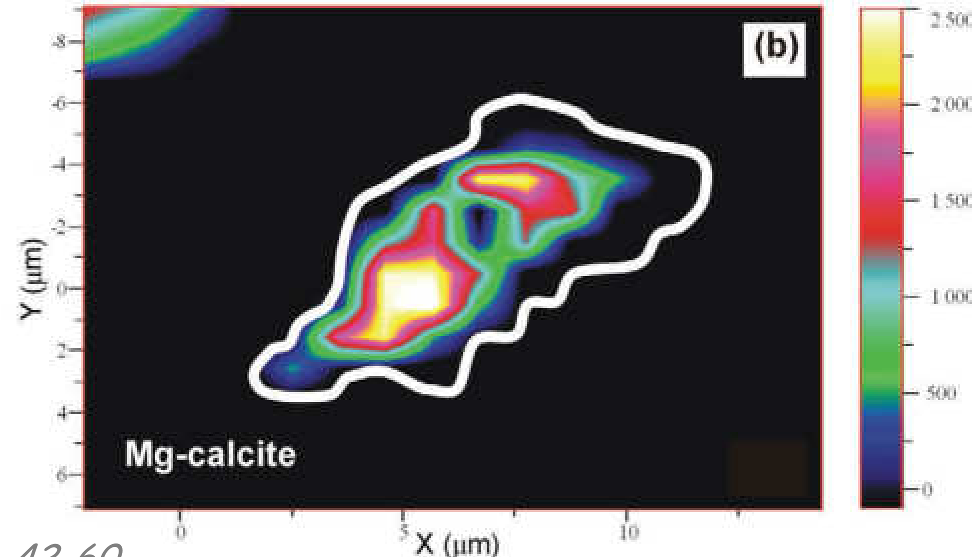

*Ferrando et al. (2017) - Am. Mineralogist, **102**, 42-60*

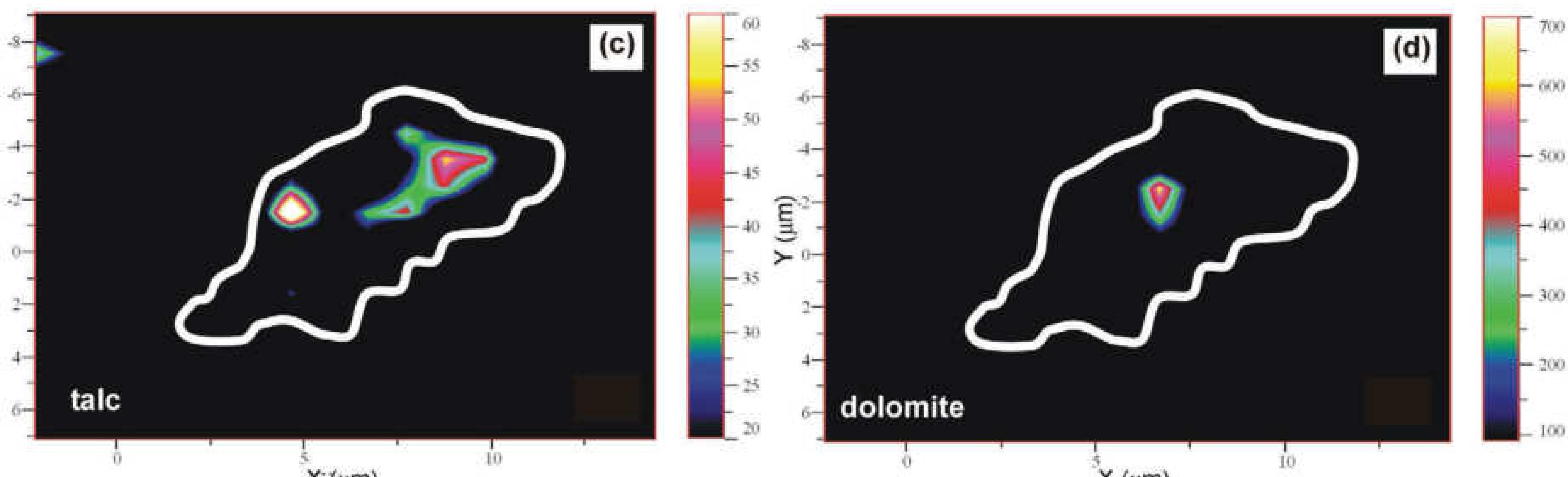

FLUID INCLUSIONS
Gaseous fluids

Gaseous species: identification

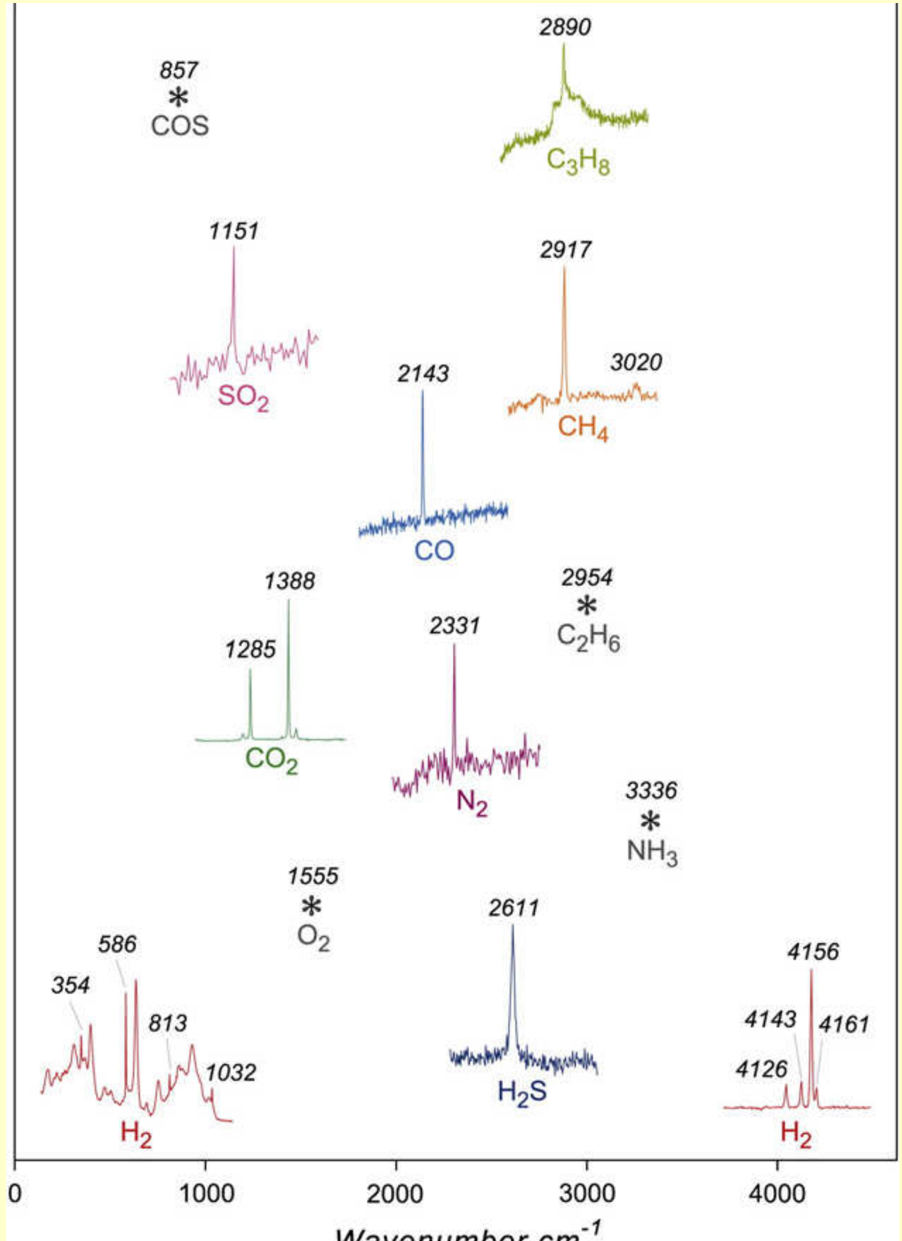

Frezzotti et al. (2012) - J. Geochem. Explor., 112, 1-20

FLUID INCLUSIONS
Gaseous fluids

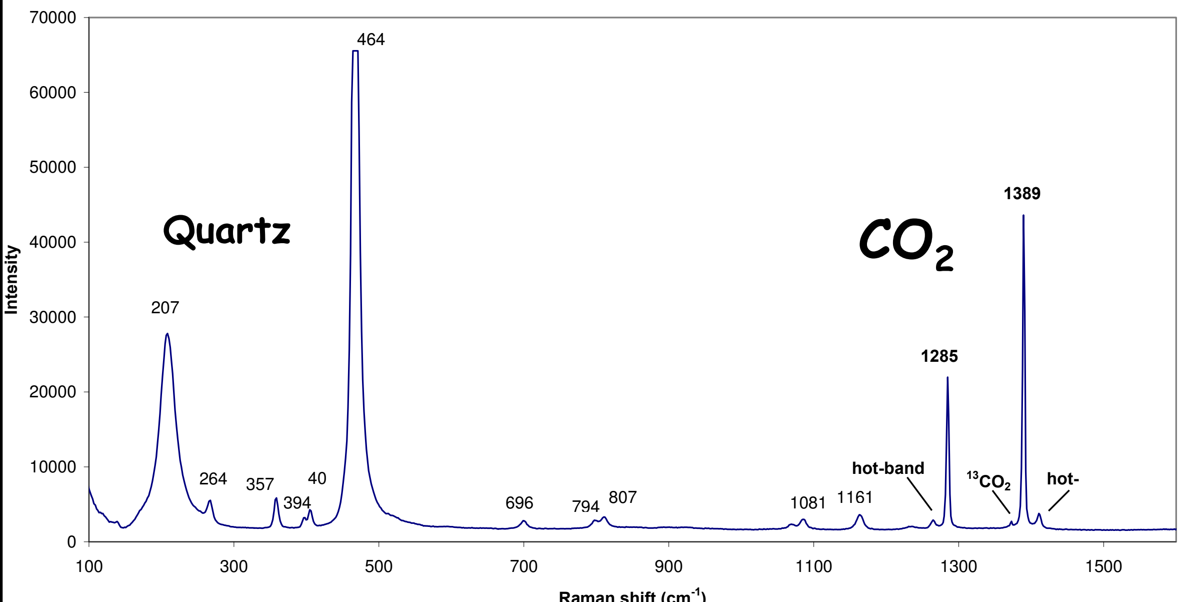

Ferrando, Frezzotti

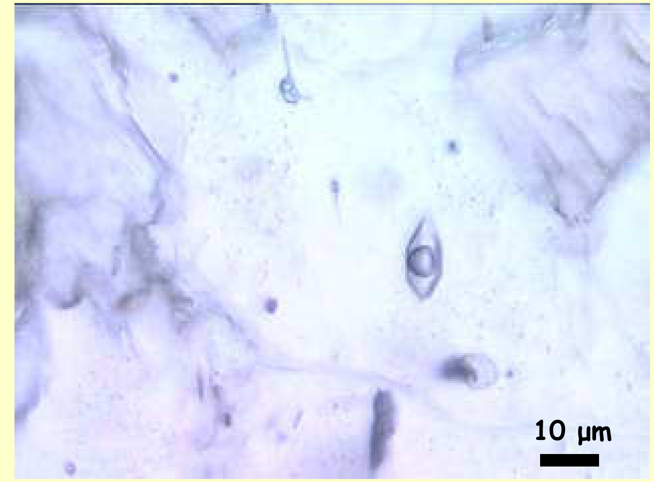

Fermi doublet (diad): two strong bands at 1285 and 1388 cm^{-1} → splitting of the admixed symmetric stretching ν^1 and bending ν^2 modes (Fermi resonance)

Hot bands: transitions due the thermal energy of the molecules.

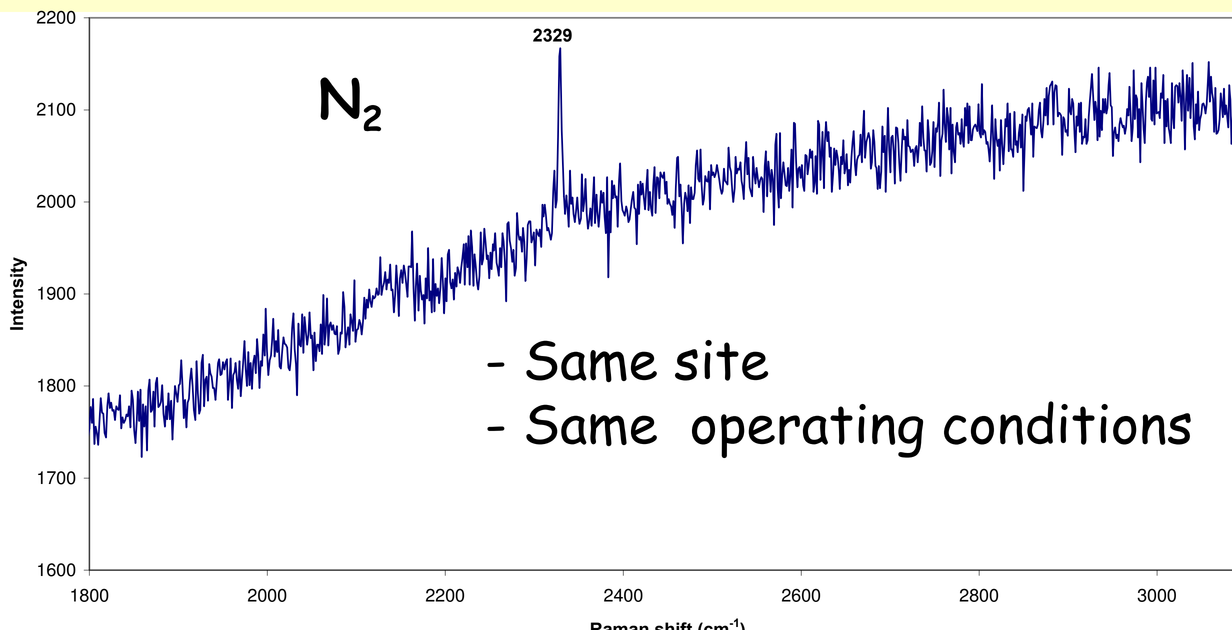

- Same site
- Same operating conditions

FLUID INCLUSIONS
Gaseous fluids

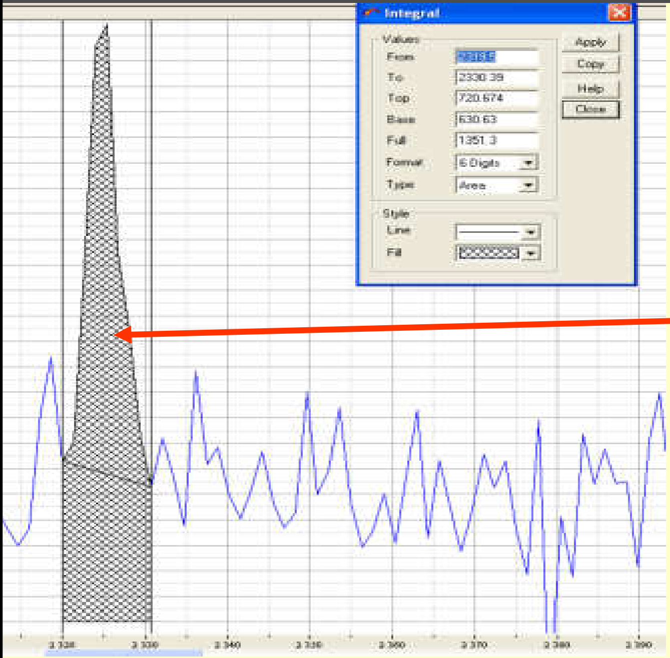

Gaseous species: quantification

Equation to calculate the molar fraction (X) of end-member components in a gas mixture

A = band area
σ = Raman cross-section
ζ = instrumental efficiency

$$X_\alpha = \frac{\dfrac{A_\alpha}{\sigma_\alpha \zeta_\alpha}}{\sum \dfrac{A_i}{\sigma_i \zeta_i}}$$

- Same site
- Same operating conditions for all the components (e.g.: objective, acquisition time and accumulations, hole, laser power, ect.)

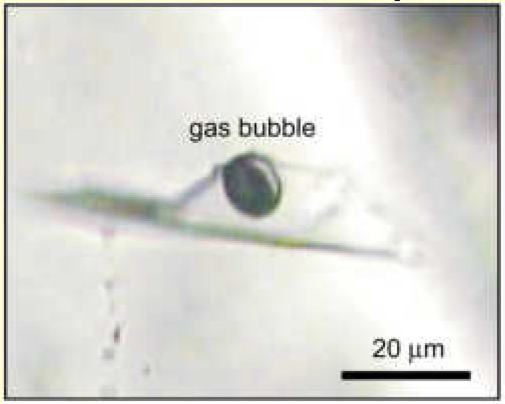

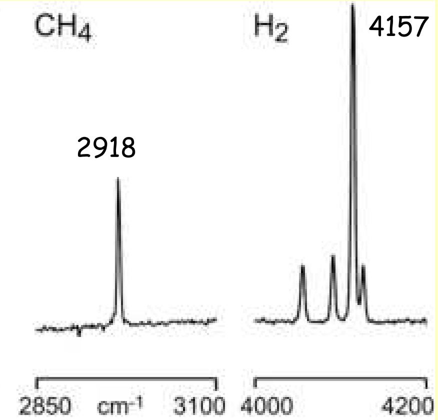

COMPONENT	σ 514.5 nm	MEASUREMENT CONDITIONS: Integral time (sec)	Accum. (Nr.)	ζ	Laser power (mW)	BAND AREA		COMPOSITION (mole %)
CH_4	7.5	60	2	1.16	300	ν_1	1,144	18
H_2	2.3	60	2	1.47	300	ν_1	2,065	82

Data from Ferrando et al. (2010)

FLUID INCLUSIONS
Gaseous fluids

Gaseous species: density → CO_2 Raman "densimeter"

Microthermometry: high precision technique to obtain CO_2 density from fluid inclusions → Limit: fluid inclusion size > 3 μm.

↓

Raman microspectroscopy spatial resolution: 1 μm.

The distance between the Fermi doublet (Δ) is proportional to fluid density. The shift of the lower band is more density dependent.

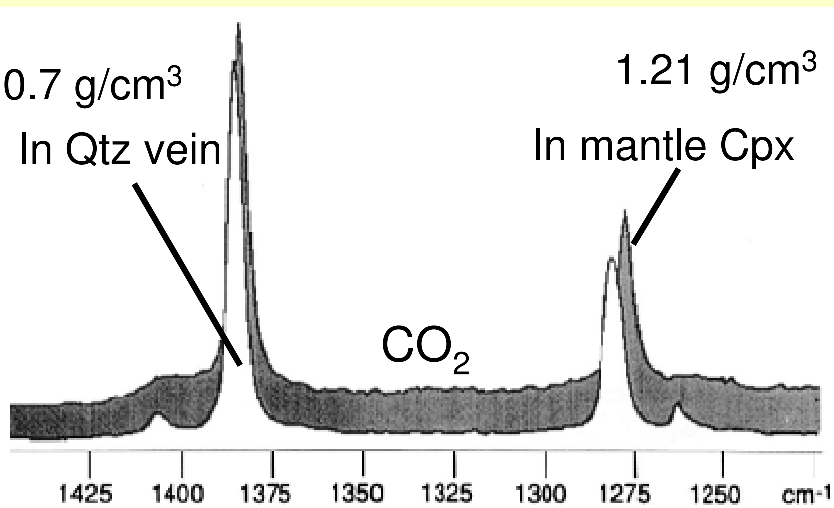

Frezzotti et al (1992)-Eur. J. Mineral., 4, 1137-1153

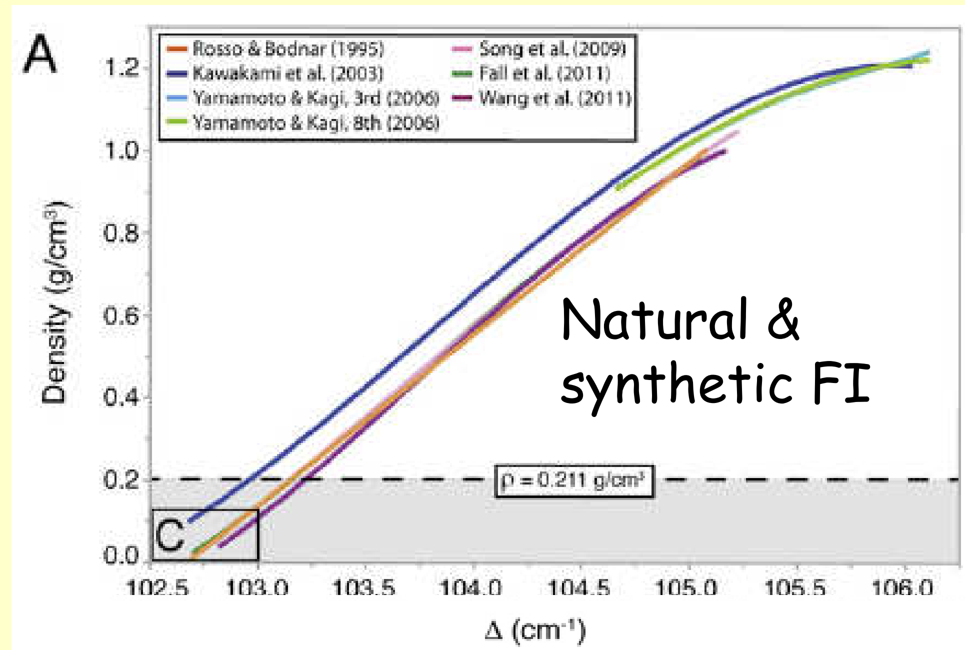

Lamadrid et al. (2017)-Chem. Geol., 450, 210-222

FLUID INCLUSIONS
Aqueous fluids

Low polarizability of H_2O molecule

H_2O is poorly Raman active

Use IR spectroscopy
for detailed investigations

With a suitable setting
(e.g., laser source),
some information can be obtained

Identification of water in apparently pure gaseous FI

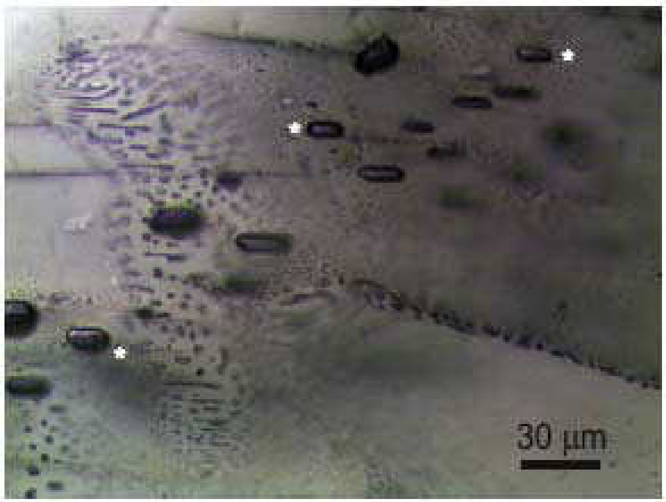

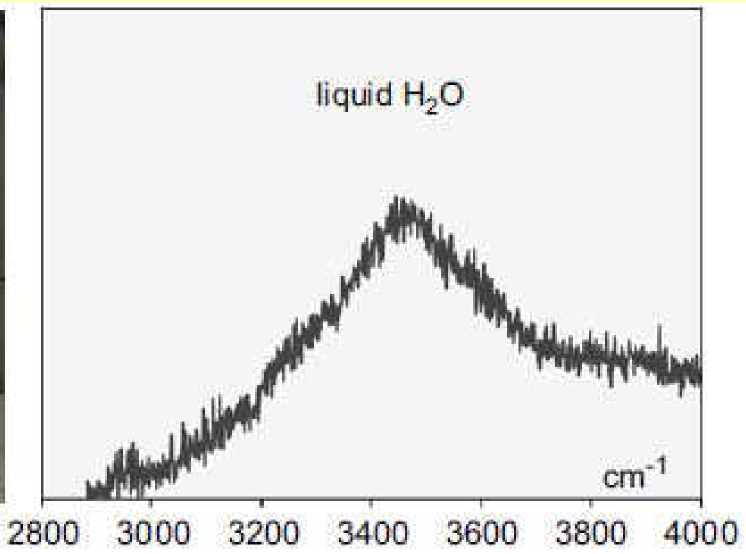

Frezzotti et al. (2010) - GCA, 74, 3023-3039.

FLUID INCLUSIONS
Aqueous fluids

Monoatomic ions dissolved

Na^+, K^+, Ca^{2+}, & Mg^{2+} have very weak Raman spectra between 350-600 cm^{-1}

freeze the inclusions and analyze the solids below T_e

A rough identification between low salinity and high salinity aqueous fluid is possible

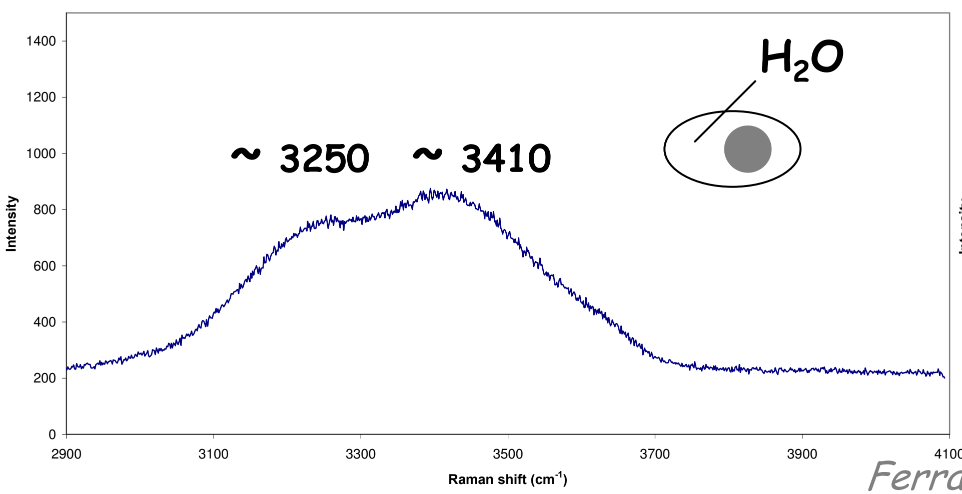

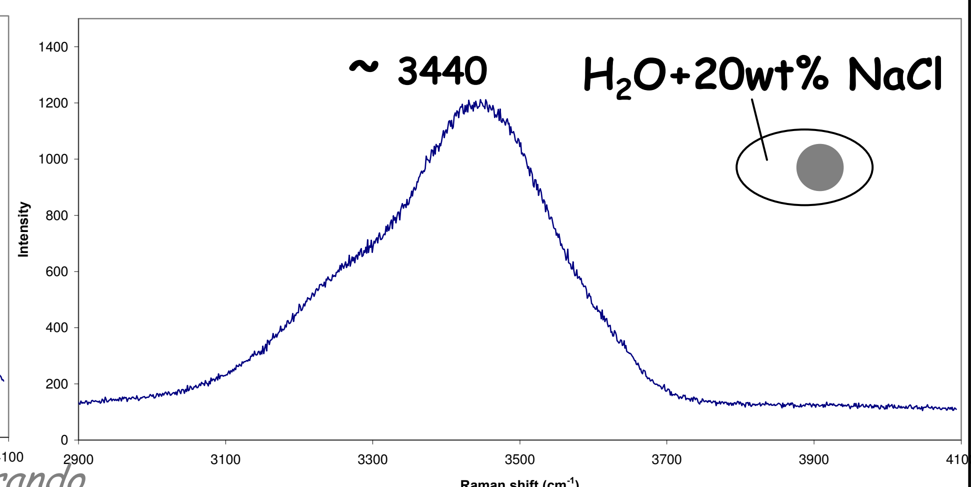

Ferrando

Semiquantitative estimation of the salt content, complementary to data from microthermometry, requires a specific calibration for each spectrometer

FLUID INCLUSIONS
Aqueous fluids

Poliatomic ions & molecules dissolved

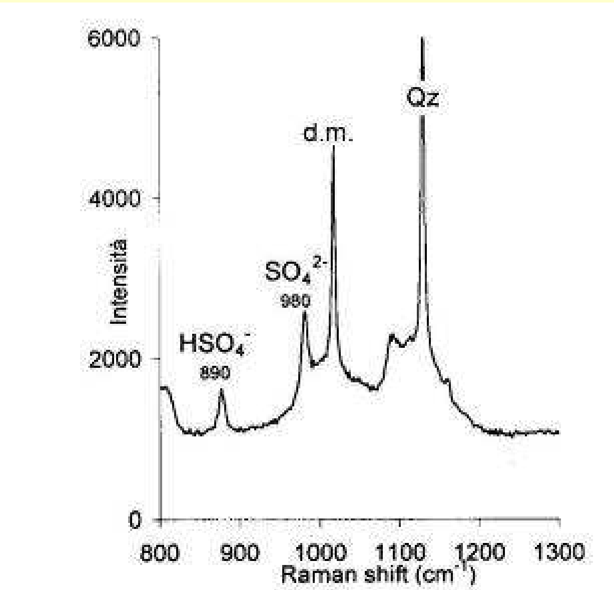

Frezzotti et al. (1992) – Eur. J. Mineral., 4, 1137-1153

Frezzotti et al. (2012) - Nature Geoscience

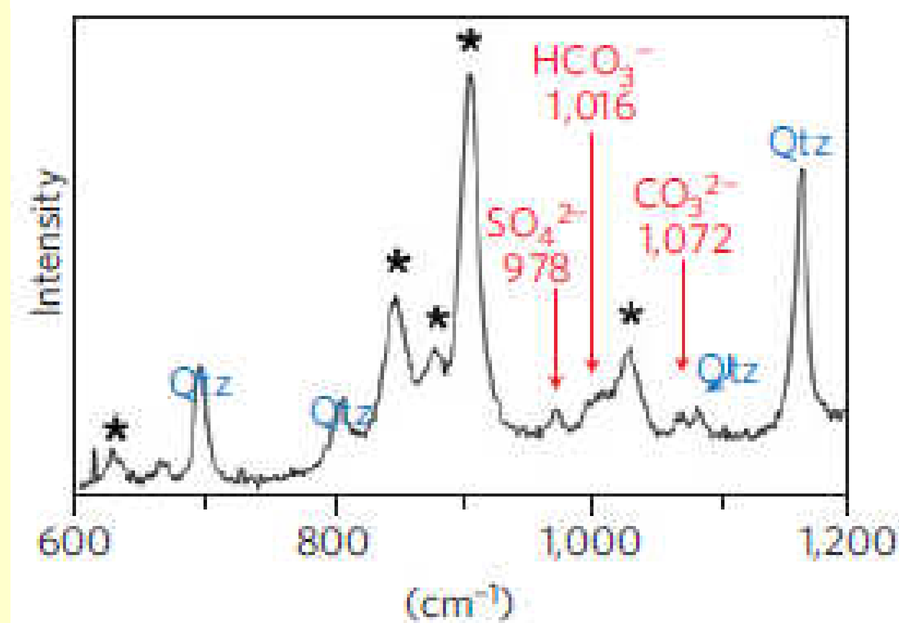

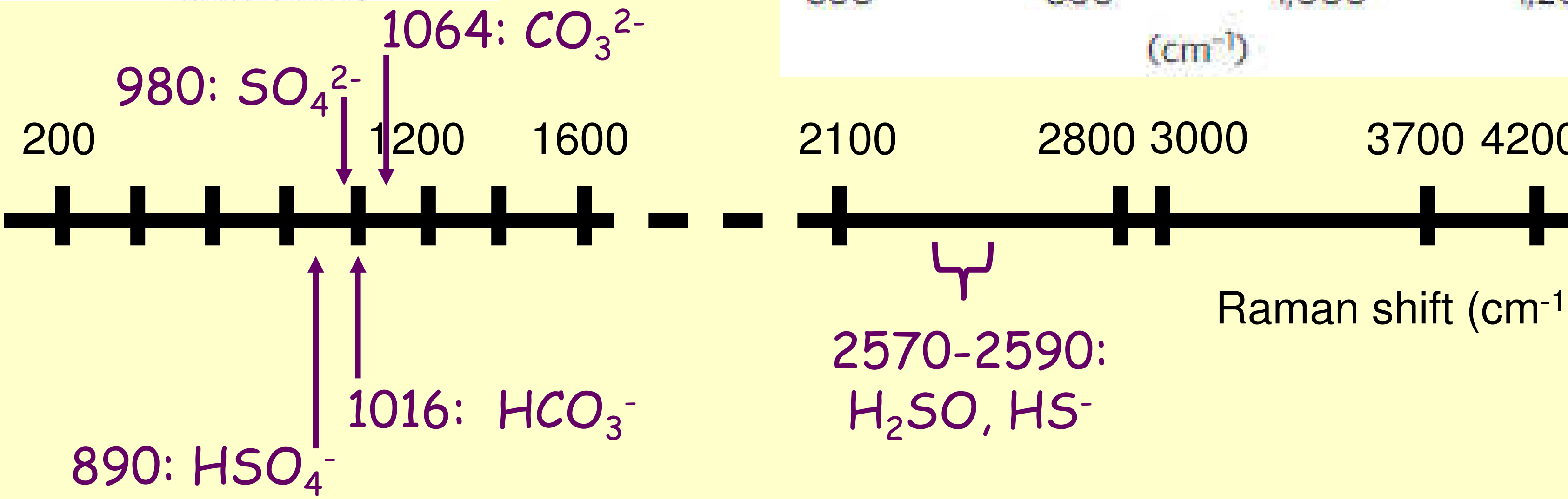

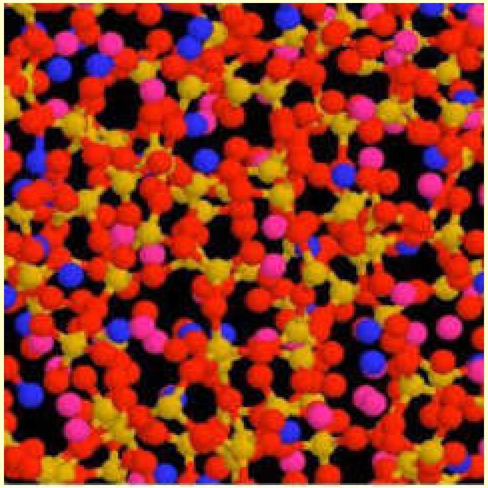

Glass &
Melt inclusions characterization

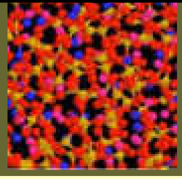

GLASS - MELT INCLUSIONS

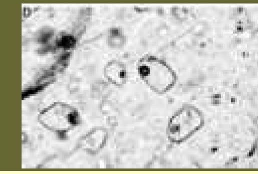

Crystal vs Glass

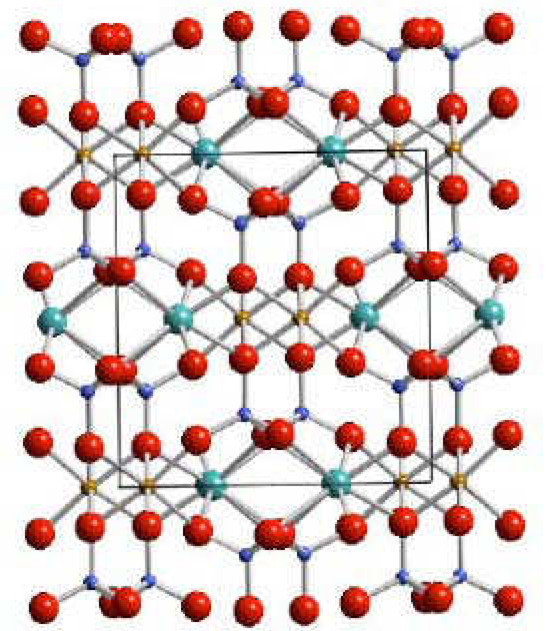

Crystalline $CaFeSi_2O_6$

Fe, Ca, Si, O

Rossano & Mysen, 2012

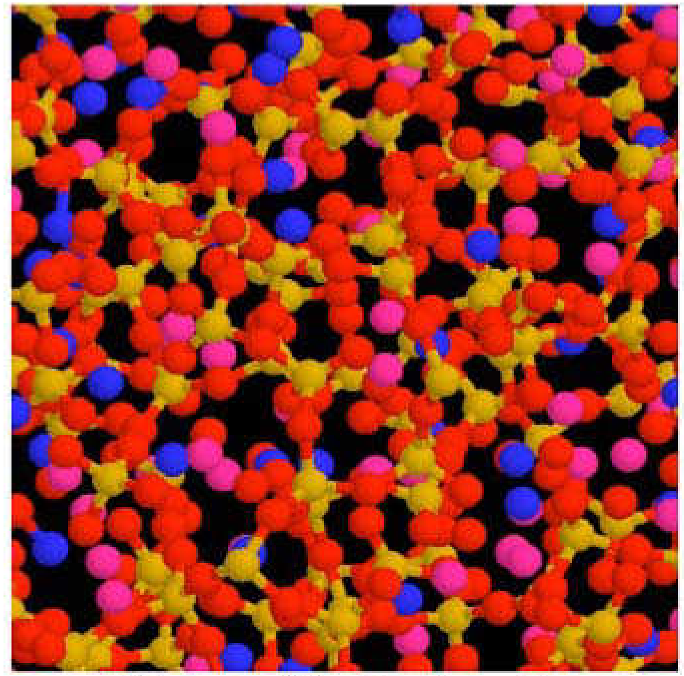

Glass of hedenbergite composition

Fe, Ca, O, Si

no periodicity

no special atomic planes/directions

increase of disorder

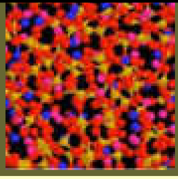

GLASS - MELT INCLUSIONS

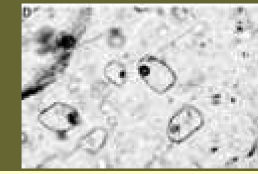

Main vibrational regions in glasses

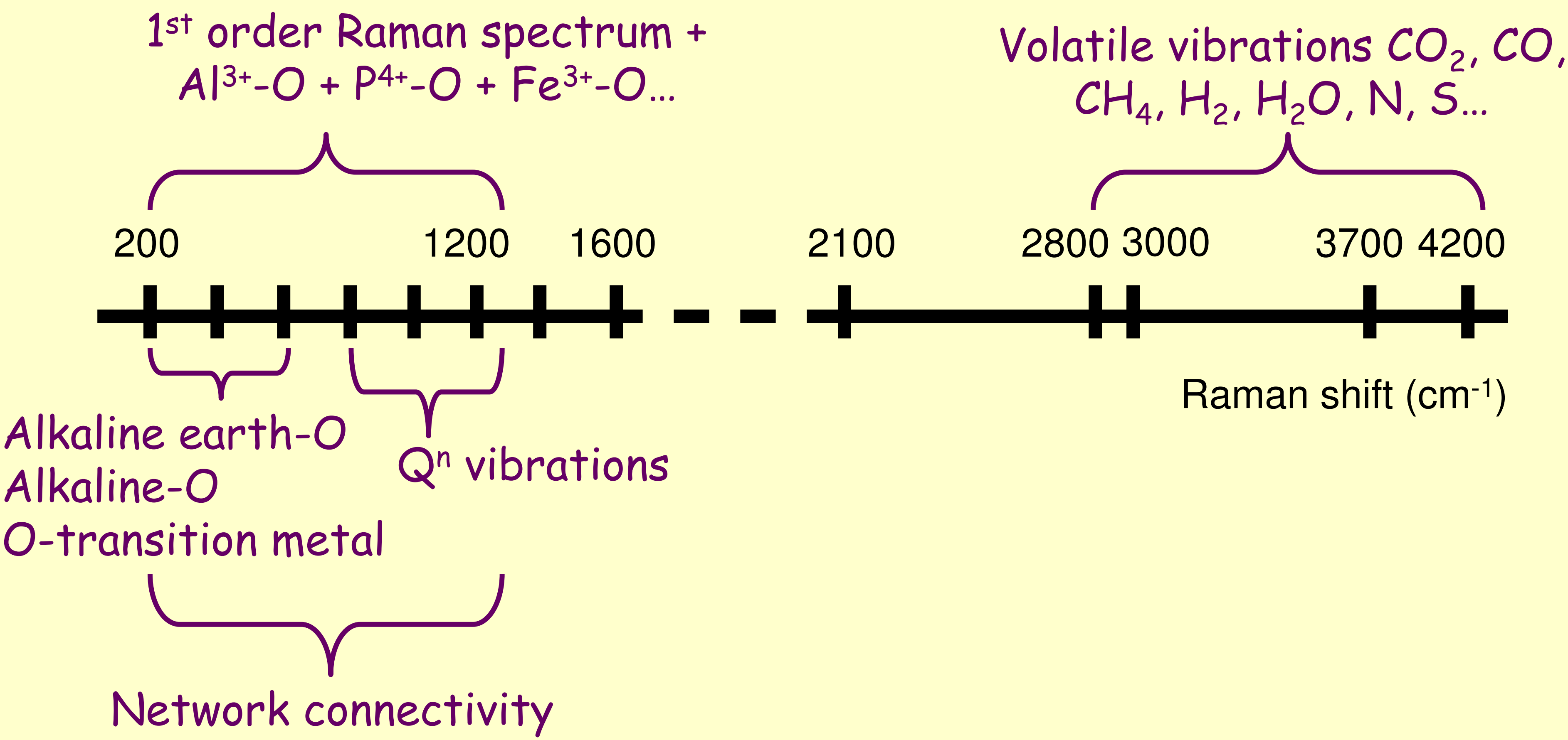

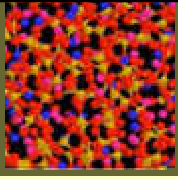

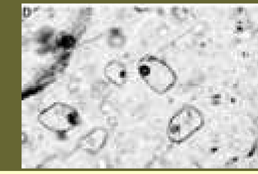

Q^n species

n = number of bridging oxygens

Tetrahedra entities centred on Si^{4+} or Al^{3+}

Connectivity of the glass network (polymerization)

Raman spectroscopy gives information on:

- **composition**
- **polymerization**

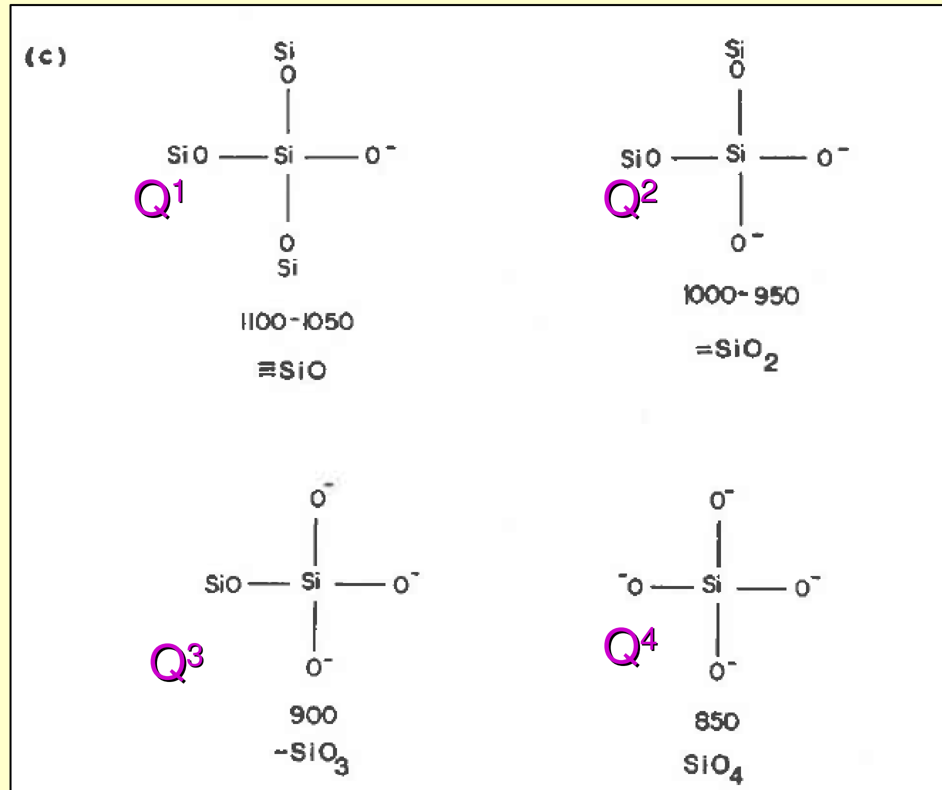

McMillan (1984) - Am. Mineral., 69, 622-644

GLASS – MELT INCLUSIONS
Chemical composition of silicate glass

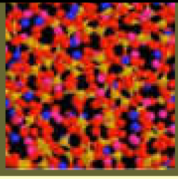

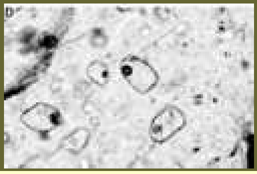

Martian glass analogues

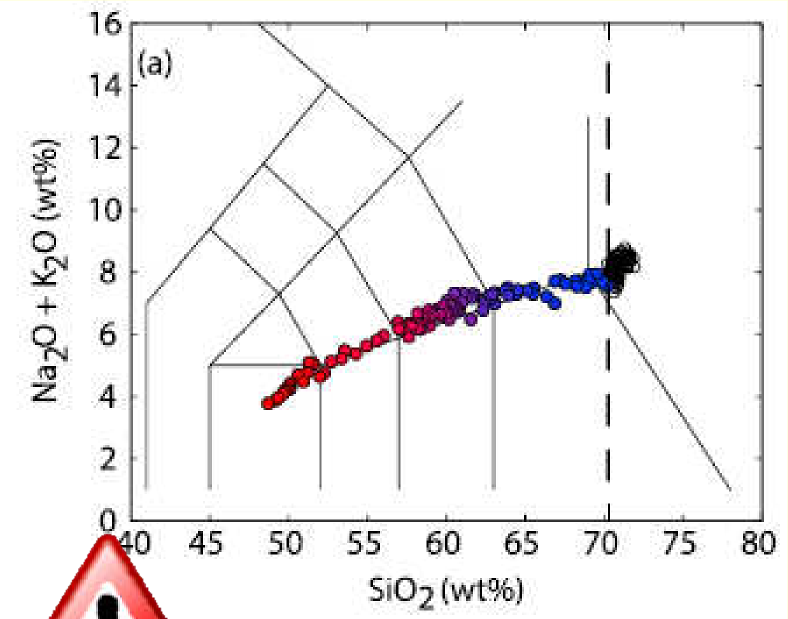

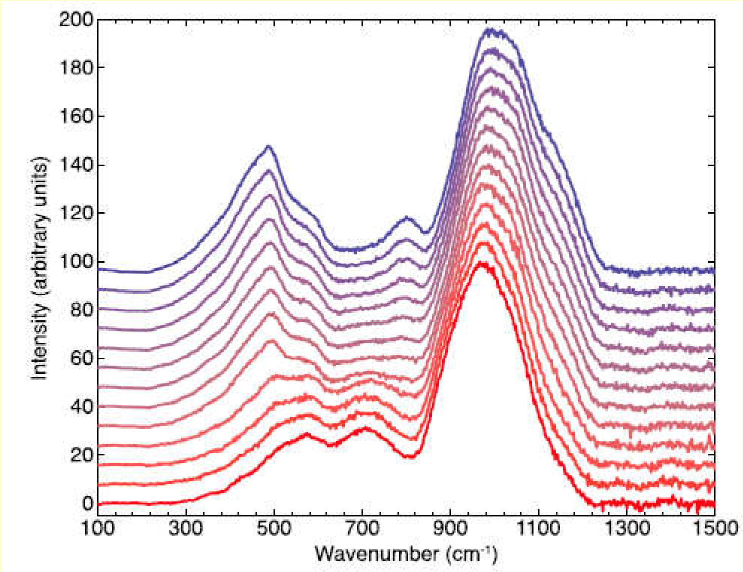

Di Genova et al. (2016) – J. Geophys. Res. Plan., ***121****, 740-752*

$$I_n = E_B \cdot \boxed{R_p} + E_R \cdot (1 - \boxed{R_p})$$

Spectra processing!!!

CAUTION

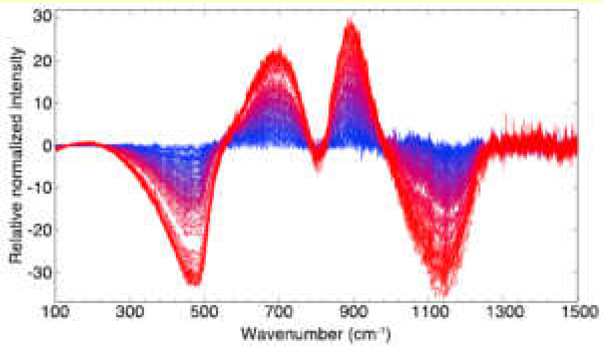

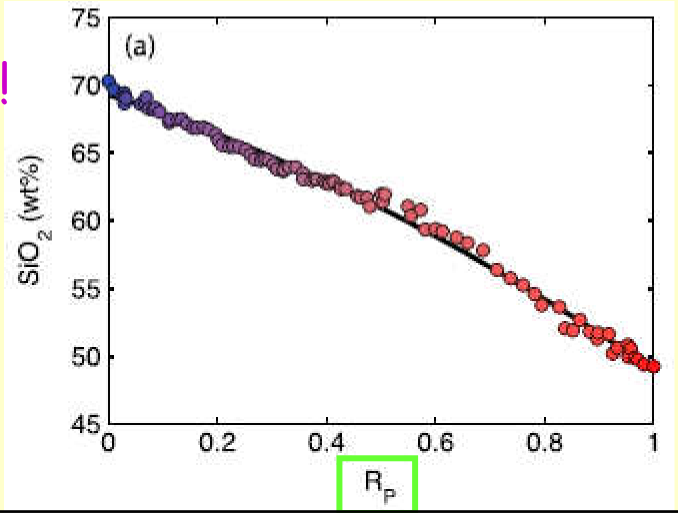

R_P=Raman parameter

I_n=normalized intensity

E_B=normalized intensity of the basalt end-member

E_R=normalized intensity of the rhyolite end-member

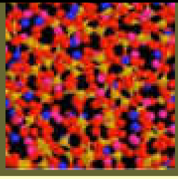

GLASS – MELT INCLUSIONS
Water content in silicate glass

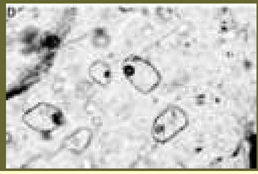

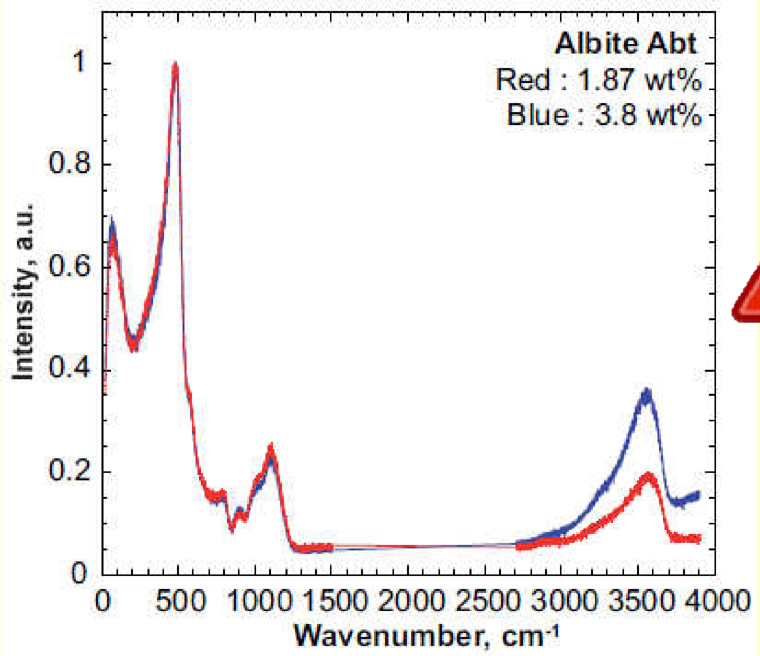

*Thomas et al. (2006) – Am. Mineral., **91**, 467-470*

CAUTION
Spectra processing!!!

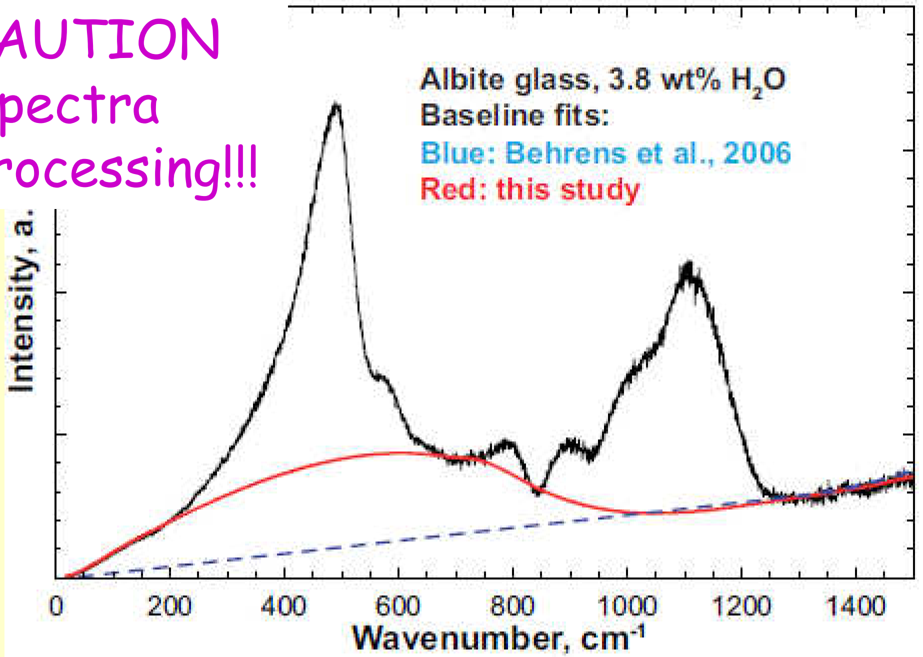

*Le Losq et al. (2012) – Am. Mineral., **97**, 779-790*

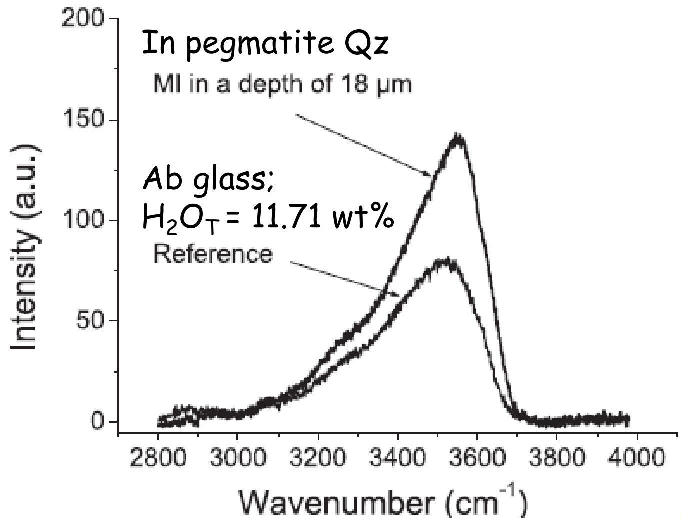

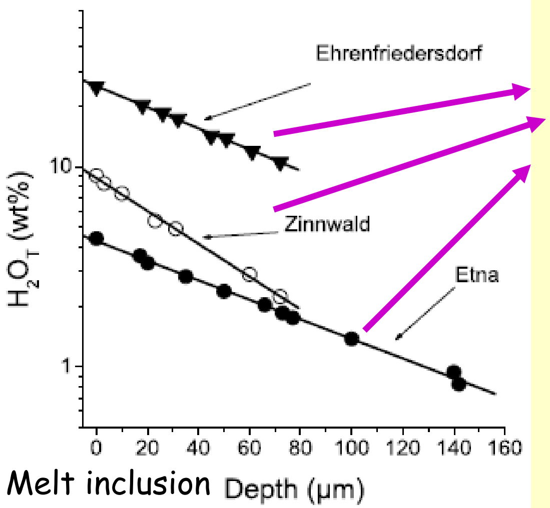

Same homogenized melt inclusions progressively brought to the surface

Inclusions analyzed under the surface avoid effect of preparation and water adsorption/diffusion

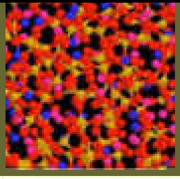

GLASS – MELT INCLUSIONS
Water content in melts inclusions

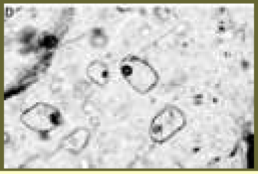

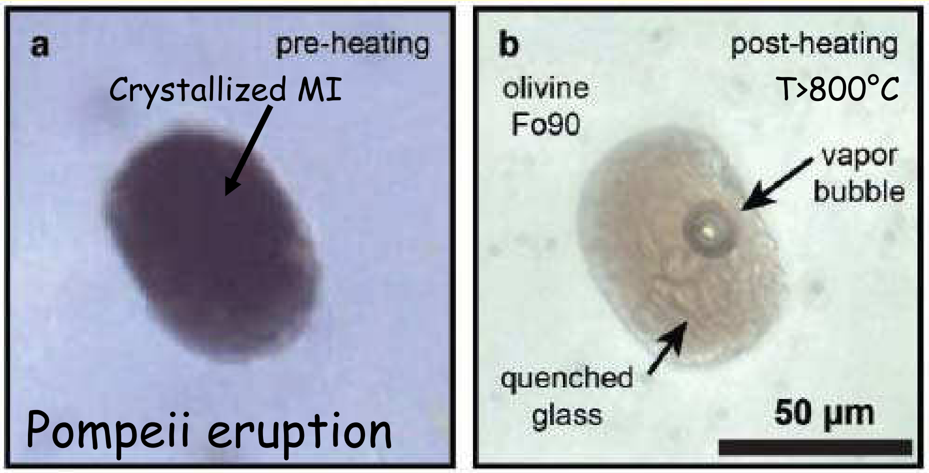

Melt inclusions may contain liquid H_2O as a <0.5 μm film, optically undetectable, at the glass/bubble interface

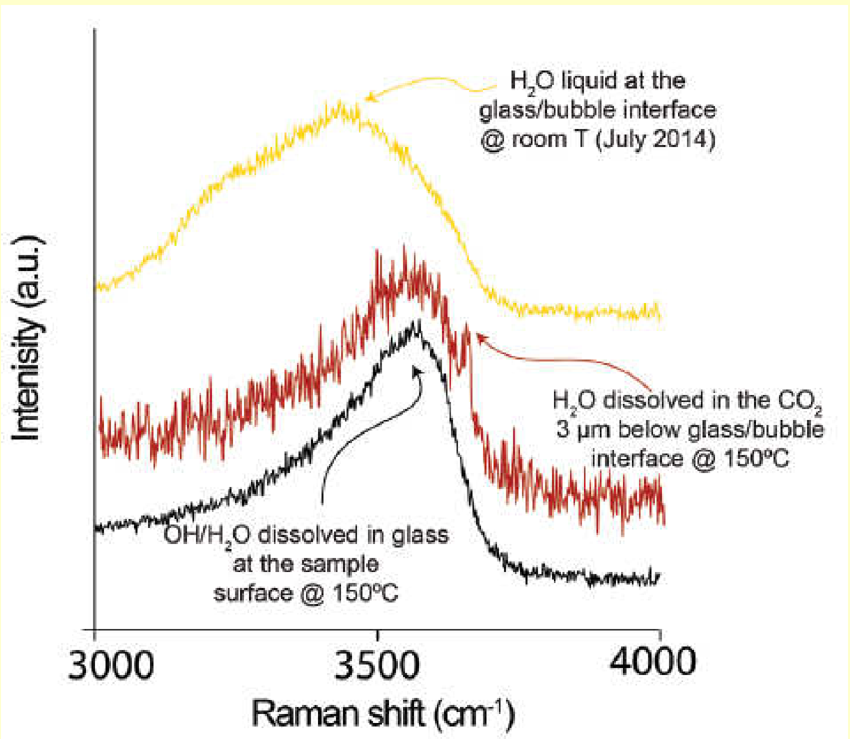

The composition of magmatic fluids exsolving from melts may contain higher H_2O content than previously reported

Esposito et al. (2016) – Am. Mineral., ***101****, 1691-1695*

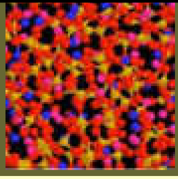

GLASS – MELT INCLUSIONS
Volatile content in melts inclusions

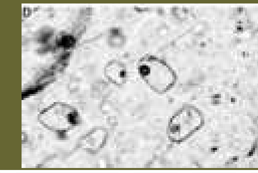

Moore et al. (2015) – Am. Mineral., 100, 806-823

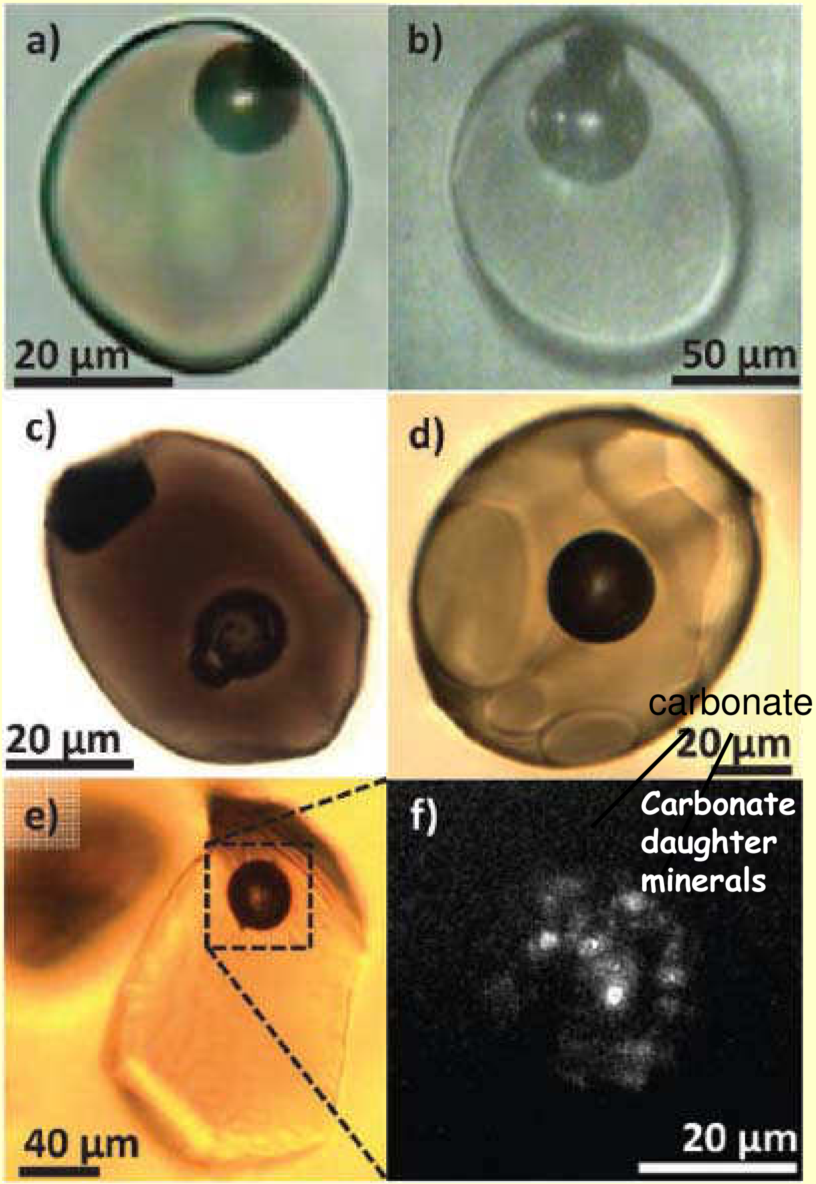

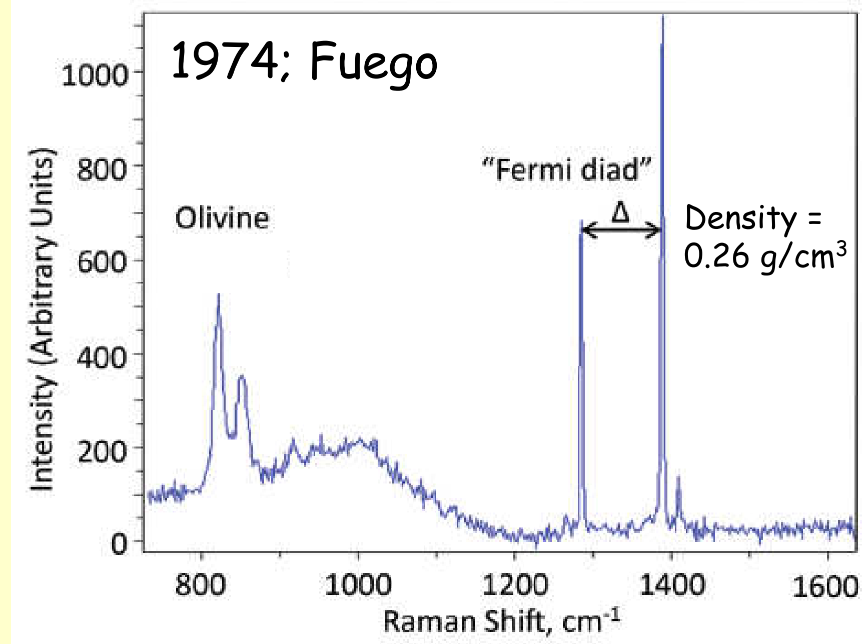

Determination of pre-eruptive volatile content of melts based on melt inclusion data must consider volatiles in the bubble and daughter carbonates

1) The CO_2 budget is higher than previously calculated by measurements in the glass alone.
2) Trapping pressures are significantly greater than previously predicted.

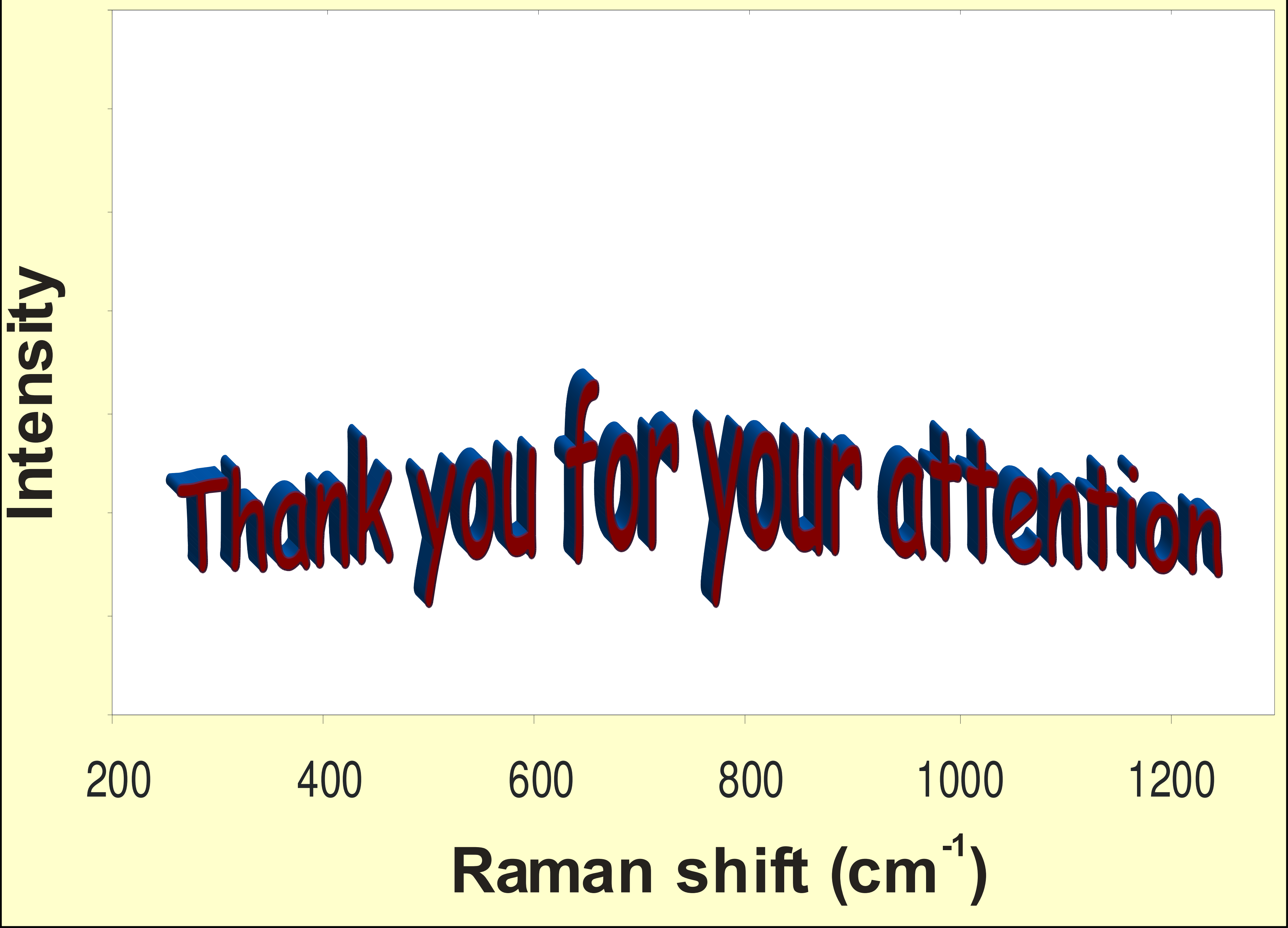
Thank you for your attention
Intensity
200
400
600
800
1000
1200
Raman shift (cm-1)